



Universidade do Estado do Rio de Janeiro

Centro de Tecnologia e Ciências

Faculdade de Geologia

Gabriella de Oliveira Amaral Quaresma

**Alternative volcanism-model related to small-scale convection: applied case
for the Vitória-Trindade Ridge volcanism investigated in the Davis Bank -
geodynamics implications**

Rio de Janeiro

2022

Gabriella de Oliveira Amaral Quaresma

**Alternative volcanism-model related to small-scale convection: applied case for the
Vitória-Trindade Ridge volcanism investigated in the Davis Bank - geodynamics
implications**

Dissertação apresentada, como requisito parcial para obtenção do título de Mestre, ao Programa de Pós-Graduação em Geociências, da Universidade do Estado do Rio de Janeiro. Área de concentração: *Geologia e Geofísica de Margens tipo Atlântico*.

Orientador: Prof. Dr. Anderson Costa dos Santos

Coorientador: Prof. Dr. Eduardo Reis Viana Rocha-Júnior

Rio de Janeiro

2022

CATALOGAÇÃO NA FONTE
UERJ/REDE SIRIUS / BIBLIOTECA CTC/C

Q1 Quaresma, Gabriella de Oliveira Amaral.

Alternative volcanism-model related to small-scale convection:
applied case for the Vitória-Trindade Ridge volcanism
investigated in the Davis Bank - geodynamics implications /
Gabriella de Oliveira Amaral Quaresma. – 2022.
132 f.: il.

Orientador: Anderson Costa dos Santos
Coorientador: Eduardo Reis Viana Rocha Júnior
Dissertação (Mestrado) – Universidade do Estado do Rio de
Janeiro, Centro de Tecnologia e Ciências.

1. Vulcanismo – Espírito Santo – Teses. 2. Geologia – Vitória (ES) –
Teses. 3. Magmatismo – Teses. I. Santos, Anderson Costa dos. II
Rocha Júnior, Eduardo Reis Viana. III. Universidade do Estado do Rio
de Janeiro, Centro de Tecnologia e Ciências. IV. Título.

551.21(815.2)

Bibliotecária responsável: Ingrid Pinheiro / CRB-7: 7048

Autorizo, apenas para fins acadêmicos e científicos, a reprodução total ou parcial desta Dissertação,
desde que citada a fonte.

Assinatura

Data

Gabriella de Oliveira Amaral Quaresma

**Alternative volcanism-model related to small-scale convection: applied case for the
Vitória-Trindade Ridge volcanism investigated in the Davis Bank - geodynamics
implications**

Dissertação apresentada, como requisito parcial para
obtenção do título de Mestre, ao Programa de Pós-
Graduação em Geociências, da Universidade do Estado do
Rio de Janeiro. Área de concentração: *Geologia e
Geofísica de Margens tipo Atlântico*.

Aprovada em 12 de Julho de 2022.

Orientador: Prof. Dr. Anderson Costa dos Santos

Faculdade de Geologia - UERJ

Coorientador: Prof. Dr. Eduardo Reis Viana Rocha-Júnior

Instituto de Física - UFBA

Banca Examinadora: _____

Prof. Dr. Claudio de Morrison Valeriano

Faculdade de Geologia - UERJ

Prof. Dr. Joao Mata

Faculdade de Ciências - Universidade de Lisboa (UA)

Prof. Dr. Artur Corval

Universidade Federal Rural do Rio de Janeiro - UFRRJ

Rio de Janeiro

2022

AGRADECIMENTOS

Sou profundamente grata ao meu orientador, Prof. Dr. Anderson Costa dos Santos, que tem sido um exemplo extraordinário de dedicação e paixão tanto pelo ensino quanto pela pesquisa. Seu entusiasmo inabalável pela ciência e sua orientação ao longo dos anos foram uma fonte constante de inspiração. Obrigada por me incentivar continuamente a dar o meu melhor. Gostaria também de expressar minha sincera gratidão ao meu coorientador, Prof. Dr. Eduardo Reis Viana Rocha-Júnior, pelos conselhos inestimáveis, apoio contínuo e paciência durante todo o desenvolvimento deste projeto. Sem sua orientação, este trabalho não teria sido possível. Agradecimentos especiais também ao Prof. Dr. João Mata, cujo conhecimento profundo e *insights* enriqueceram esta jornada.

Estendo meu apreço aos membros da minha banca de defesa, Prof. Dr. Claudio de Morrison Valeriano, Prof. Dr. Artur Corval e, mais uma vez, ao Prof. Dr. João Mata, pelo tempo dedicado, feedback construtivo e comprometimento em ajudar a moldar a versão final deste trabalho.

Gostaria de agradecer aos técnicos do laboratório LGPA (UERJ) pelo apoio no processamento das amostras. Sou também profundamente grato ao Prof. Dr. Claudio Valeriano e à equipe técnica do Laboratório de Geocronologia e Isótopos Radiogênicos (LAGIR), assim como ao Prof. Dr. João Mata, pela assistência nas análises isotópicas. Agradeço ainda à equipe do Programa LEPLAC da Marinha do Brasil, especialmente à Capitã Izabel King Jack e à Capitã Ana Angélica Ligiero Alberoni, por generosamente compartilharem as amostras de rochas dragadas do Programa LEPLAC com nossa equipe da Faculdade de Geologia, bem como por permitirem o uso do conjunto de dados batimétricos.

Às professoras e professores e ao corpo técnico do Programa de Pós-Graduação em Geociências (PPGG) da Universidade do Estado do Rio de Janeiro (UERJ), agradeço por oferecerem uma base sólida e pelo encorajamento ao longo desta jornada acadêmica.

Por fim, à Universidade do Estado do Rio de Janeiro (UERJ), foi uma honra concluir esta fase da minha carreira acadêmica sob a sua bandeira. Aos meus colegas e amigos da área de geociências, vocês tornaram este caminho menos solitário e muito mais agradável. Agradecimentos especiais a Thais Mothé Maia pelo apoio constante e por compartilhar generosamente seus *insights*, ideias, dados e por engajar-se em discussões valiosas. Suas contribuições foram essenciais para a conclusão bem-sucedida desta dissertação.

ABSTRACT

QUARESMA, Gabriella de Oliveira Amaral. **Alternative volcanism-model related to small-scale convection: applied case for the Vitória-Trindade Ridge volcanism investigated in the Davis Bank - geodynamics implications**. 2022. 132 f. Dissertação (Mestrado em Geociências) – Faculdade de Geologia, Universidade do Estado do Rio de Janeiro, Rio de Janeiro, 2022.

Davis Bank is the largest and most voluminous volcanic building in the Vitória-Trindade Ridge (VTR), which comprehends a notable alignment of volcanic features on the South Atlantic Ocean, located parallel to Vitória City along the *ca.* 20°S. The VTR has been interpreted by some authors as a symptomatic of the passage of the Trindade hotspot underneath the South American Plate, although the importance of structural control on the ridge formation is evident. This study presents the first integrated analysis of Sr-Nd-Pb-Hf isotopic compositions of Davis Bank, where scarce data have been published so far, to provide new constraints on the magmatism nature. We also present new whole-rock geochemistry data of Davis Bank samples. Sr-Nd-Pb-Hf isotopic signature Davis Bank rocks, along with isotopic signatures observed on the Vitória Seamount, are more enriched than the other magmatic manifestations of the VTR. This precludes the fact that Davis Bank was generated via the exclusive melting of a depleted mantle source, requiring the involvement of one or several enriched components homogenized before eruption. We posit that one of these components is related to the recycled subducted oceanic crust and evolved in an environment with low Sm/Nd and slightly high Rb/Sr, U/Pb, and Th/Pb ratios. The enriched component is probably represented by a HIMU-type pyroxenite (hybrid component). Our modeling of the isotopic data indicates that Davis Bank isotopic composition is achieved by a dominant asthenospheric component (DMM) hybridized by the addition of EMI (< 24% in the mixing) and HIMU (up to 20% in the mixture) melts. The behavior of major, minor and trace elements suggest that fractional crystallization may have played an important role in the evolution of these rocks, although it cannot solely explain chemical differences observed, given that Nd and Hf isotopic variation between Davis samples analyzed in this work and those from literature. We believe that the Vitória-Trindade Ridge is the surface manifestation of upwelling flow attributed to anomalous fertile shallow sources within a depleted mantle matrix with ubiquitous heterogeneities. Important contributions of detached SCLM fragments and subducted slabs from the Brasiliano Orogeny contaminating the mantle underneath the South Atlantic Ocean are suggested.

Keywords: Sr-Nd-Pb isotopic ratios; mantle heterogeneity; hybrid mantle; brasiliano orogeny heritage; vitória-trindade ridge.

RESUMO

QUARESMA, Gabriella de Oliveira Amaral. **Modelo alternativo de vulcanismo relacionado à convecção em pequena escala: caso aplicado ao vulcanismo da Serra Vitória-Trindade investigado no Banco Davis - implicações geodinâmicas**. 2022. 132 f. Dissertação (Mestrado em Geociências) – Faculdade de Geologia, Universidade do Estado do Rio de Janeiro, Rio de Janeiro, 2022.

O Banco Davis é o maior e mais volumoso edifício vulcânico da Cadeia Vitória-Trindade (VTR), que compreende um notável alinhamento de feições vulcânicas no Oceano Atlântico Sul, localizado paralelo à cidade de Vitória, aproximadamente na latitude 20°S. A VTR tem sido interpretada por alguns autores como sintomática da passagem do ponto quente de Trindade sob a Placa Sul-Americana, embora a importância do controle estrutural na formação da cadeia seja evidente. Este estudo apresenta a primeira análise integrada das composições isotópicas de Sr-Nd-Pb-Hf do Banco Davis, onde até o momento existem dados escassos publicados, com o objetivo de fornecer novas restrições sobre a natureza do magmatismo. Apresentamos também novos dados de geoquímica de rocha total de amostras do Banco Davis. A assinatura isotópica de Sr-Nd-Pb-Hf das rochas do Banco Davis, juntamente com as assinaturas isotópicas observadas no Monte Submarino Vitória, são mais enriquecidas do que as outras manifestações magmáticas da VTR. Isso exclui a hipótese de que o Banco Davis tenha sido gerado exclusivamente pelo derretimento de uma fonte de manto empobrecido, exigindo o envolvimento de um ou vários componentes enriquecidos homogeneizados antes da erupção. Propomos que um desses componentes está relacionado à crosta oceânica subductada reciclada, que evoluiu em um ambiente com baixa razão Sm/Nd e razões Rb/Sr, U/Pb e Th/Pb ligeiramente elevadas. O componente enriquecido é provavelmente representado por uma piroxenita do tipo HIMU (componente híbrido). Nosso modelo com base nos dados isotópicos indica que a composição isotópica do Banco Davis é atingida por um componente astenosférico dominante (DMM), hibridizado pela adição de fusões EMI (< 24% na mistura) e HIMU (até 20% na mistura). O comportamento dos elementos maiores, menores e traços sugere que a cristalização fracionada pode ter desempenhado um papel importante na evolução dessas rochas, embora não possa, por si só, explicar as diferenças químicas observadas, dado que há variação isotópica de Nd e Hf entre as amostras do Banco Davis analisadas neste trabalho e aqueles presentes na literatura. Acreditamos que a Cadeia Vitória-Trindade seja a manifestação superficial de um fluxo ascendente atribuído a fontes rasas férteis anômalas dentro de uma matriz de manto empobrecido com heterogeneidades ubíquas. Sugere-se uma importante contribuição de fragmentos destacados da SCLM e de placas subductadas da Orogênese Brasileira, contaminando o manto sob o Oceano Atlântico Sul.

Palavras-chave: razões isotópicas Sr-Nd-Pb; heterogeneidade do manto; manto híbrido; herança da orogênese brasileira; cadeia vitória-trindade.

FIGURAS

Figure 1 – Small scale convection developed at the base of mature oceanic plates in cylindrical geometries ("Richter Rolls") and aligned to the plate movement, forming linear ridges.....	21
Figure 2 – Schematic profile of the Earth's interior according to the mantle plume model on the left and the "plates" model on the right.....	23
Figure 3 – Schematic model of heterogeneous convective mantle in which slabs have a variety of destinations in the mantle.....	25
Figure 4 – Scheme suggested by Mallik and Dasgupta (2012) for the formation of OIB by partial melting reaction of MORB-eclogite with peridotite subsolidus.....	27
Figure 5 – Schematic of tectonic crustal delamination.....	28
Figure 6 – Bathymetric map and 3D profile of the Vitória-Trindade Ridge with the published geochronological ages.....	32
Figure 7 – 3D bathymetry of the central portion of the VTR.....	33
Figure 8 – Seismic tomography showing a low velocity anomaly in the mantle below the Trindade Island region.....	36
Figure 9 – South Atlantic tectonic map.....	38
Figure 10 – Schematic model of the transtensional stresses related to the VTFZ that affected the intrusion of the alkaline rocks in Trindade Island.....	39
Figure 11 – Location of Davis Bank samples.....	43
Figure 12 – Photomicrographs of Davis Bank basanite samples under polarized microscope, displaying the trachytic groundmass, clinopyroxene with hourglass twinning and opaque minerals.....	48
Figure 13 – Photomicrographs of plagioclase minerals in Davis Bank basanite samples under polarized microscope.....	49
Figure 14 – Photomicrographs of opaque microphenocrysts in Davis Bank tephrite samples under polarized microscope.....	50
Figure 15 – Classification diagram based on Total Alkali vs. Silica (TAS) plot after Le Maitre (1989).....	51
Figure 16 – Fenner Variation Diagram for MgO vs. SiO ₂ contents.....	55
Figure 17 – Fenner variation diagrams for Davis Seamount samples including major elements content.....	56
Figure 18 – Variation diagram between MgO (wt. %) and K ₂ O, V and Sc for Davis	

Seamount sample.....	58
Figure 19 – Binary variation diagram between trace elements (ppm) and K ₂ O (wt.%) vs. Th (ppm) for the different alkaline rocks of Vitória-Trindade Ridge.....	59
Figure 20 – Trace-element spider diagram normalized to primitive mantle (Sun and McDonough, 1989) for Davis Bank and other Vitória-Trindade Ridge seamounts.....	61
Figure 21 – Chondrite-normalized REE diagrams (values from Boynton, 1984) for the different alkaline rocks of Vitória-Trindade Ridge.....	62
Figure 22 – Plot of ternary mixing calculations between DMM, EMI and HIMU-type pyroxenite to describe ⁸⁷ Sr/ ⁸⁶ Sr and ¹⁴³ Nd/ ¹⁴⁴ Nd isotopic variability of Davis bank and other VTR rocks.....	67
Figure 23 – Plot of ternary mixing calculations between DMM, EMI and HIMU-type pyroxenite to describe measured (m) ²⁰⁶ Pb/ ²⁰⁴ Pb, ²⁰⁷ Pb/ ²⁰⁴ Pb and ²⁰⁸ Pb/ ²⁰⁴ Pb isotopic variability of Davis bank and other VTR rocks.....	69
Figure 24 – VTR plots in ²⁰⁶ Pb/ ²⁰⁴ Pb versus ⁸⁷ Sr/ ⁸⁶ Sr and ²⁰⁶ Pb/ ²⁰⁴ Pb versus ¹⁴³ Nd/ ¹⁴⁴ Nd correlation diagram.....	71
Figure 25 – Three-dimensional isotopic plot for Vitória-Trindade Ridge (VTR) samples and mantle end members.....	72
Figure 26 – ¹⁴³ Nd/ ¹⁴⁴ Nd versus ¹⁷⁶ Hf/ ¹⁷⁷ Hf correlation diagram for Davis Bank samples.....	73
Figure 27 – ¹⁷⁶ Hf/ ¹⁷⁷ Hf versus ²⁰⁶ Pb/ ²⁰⁴ Pb for VTR magmatic rocks.....	74
Figure 28 – Variations in selected incompatible trace element ratios in lavas from the Vitória- Trindade Ridge.....	77
Figure 29 – Variation between Ba and Ba/Nb versus LOI in lavas from the VTR.....	78
Figure 30 – Variation between Ba and Nb in lavas from the VTR.....	79
Figure 31 – Ce/Nb versus Ba/Nb in lavas from VTR.....	80
Figure 32 – Variations in Ba/Th versus Zr/Nb in lavas from the Vitória-Trindade Ridge (VTR).....	81
Figure 33 – Plot of ternary mixing calculations between DMM, EMI and HIMU-type pyroxenite to describe ¹⁴³ Nd/ ¹⁴⁴ Nd and ²⁰⁶ Pb/ ²⁰⁴ Pb isotopic variability of Davis bank and other VTR rocks.....	83
Figure 34 – Nd isotopic signature along the seamounts from Vitória-Trindade Ridge.....	90
Figure 35 – Andean uplift and South American Plate tectonic events.....	94
Figure 36 – Schematic sketch depicting the envisioned model for the three-component mantle source of the VTR magmatism and the tectonic setting associated....	97

TABELAS

Table 1 –	Sampling localization by dredging with Vessel Prof. Logachev (2010) carried out by the Brazilian Navy under LEPLAC project of Brazilian Margin Extension.....	44
Table 2 –	Summary of the petrographic characteristics.....	47
Table 3 –	VTR Seamounts Whole Rock Composition.....	53
Table 4 –	Sr-Nd -Pb isotope ratios of the Vitória-Trindade Ridge.....	64

SUMÁRIO

	INTRODUCTION	14
1	OBJECTIVES	18
1.1	General	18
1.2	Specifics	18
2	THEORETICAL CONCEPTUALIZATION	19
2.1	Plume hypothesis versus plate hypothesis	19
2.2	Sources of mantle heterogeneity	25
2.3	Mantle reservoirs	29
3	CONTEXT OF THE STUDY AREA	32
3.1	Tectonic and geodynamic context	34
3.2	Geologic background	40
4	METHODS	42
4.1	Bibliography	43
4.2	Samples	43
4.3	Petrography	45
4.4	Whole-rock chemistry	46
4.5	Sr and Nd isotopes	46
4.6	Pb and Hf isotopes	47
5	RESULTS	48
5.1	Petrography	48
5.2	Major and trace elements compositions for Davis Bank	52
5.3	Sr-Nd-Pb-Hf isotopes	65
6	DISCUSSIONS	78
6.1	Magma genesis	78
6.2	Identification and quantification of source components involved in the Davis Bank magmatism	86
6.3	A genetic model for the Davis Bank source components	88
6.4	On the heterogeneity of the VTR magmatism	95
6.5	Davis Bank distinct characteristics and similarities with the Vitória Seamount	96
6.6	On the origin of the Vitória-Trindade Ridge	97
6.7	A model for the Vitória-Trindade Ridge magmatism	102
	FINAL CONCLUSIONS	106
	REFERENCES	108

INTRODUCTION

Oceanic island basalts (OIB) are important objects of study to help better understand the compositions of the Earth's convective mantle. The petrogenetic study of OIB and the vast chemical spectrum of these rocks are the key to understanding mantle heterogeneities (*e.g.* LOUBET *et al.*, 1988; HOFMANN, 2003; WEAVER, 1991; WHITE, 2015). Several studies recognize the existence of intrinsic chemical heterogeneities of shallower portions of the mantle (NIU *et al.*, 2002; KORENAGA; KELEMEN, 2000; LASSITER; HAURI, 1998; JANNEY *et al.*, 2000) and their contribution to the isotopic diversity of OIB. This diversity in isotopic compositions is interpreted as a reflection of the presence in the mantle of distinct end-members proposed based on the isotopic compositions of Sr, Nd and Pb, through which the isotopic spectrum of all oceanic basalts can be explained by variable mixing ratios, being the four most commonly invoked: DMM (depleted-MORB mantle), HIMU (high- μ ; $\mu = {}^{238}\text{U}/{}^{204}\text{Pb}$), EMI (enriched mantle I), EMII (enriched mantle II) (ALLÈGRE; TURCOTTE, 1986; WEAVER, 1991; WHITE, 1985; ZINDLER; HART, 1986; HOFMANN, 1997, 2003).

On the other hand, the origin and petrological nature of the sources of these end-members is still somewhat enigmatic and the concept behind such end-members is a subject of debate (*e.g.* ARMIENTI; GASPERINI, 2007). Some authors suggest that in addition to isotopic heterogeneity, the source regions of oceanic island basalts may also be heterogeneous in terms of lithology and mineralogy (*e.g.* DASGUPTA *et al.*, 2010; GURENKO *et al.*, 2009; JACKSON; DASGUPTA, 2008). As pointed out by Gurenko *et al.* (2009), the identification of mantle components and their varied mixing ratios that contribute to the generation of mafic magmas is one of the great challenges in understanding the dynamics of the mantle.

The supposed lithological heterogeneities (major elements) in the terrestrial mantle are extremely important for the understanding of the mechanical behavior of regions of the mantle and for discussion about the geodynamic mechanisms that can lead to the generation of OIB magmas. For instance, Anderson (2006 and 2007) and Foulger and Anderson (2005) assume that it is precisely these heterogeneities in the mantle lithology that are the main cause of melting anomalies, being more important than thermal variations in mantle dynamics. The recycling of subducted oceanic crust slabs and continental lithosphere fragments are widely invoked as sources of mantle heterogeneity (LUSTRINO, 2005; HOFMANN, 1997; HIRSCHMANN; STOLPER, 1996; JACKSON; DASGUPTA, 2008; KOGISO;

HIRSCHMANN, 2006, MALLIK; DASGUPTA, 2012, SOBOLEV *et al.*, 2000, SOBOLEV *et al.*, 2005, SOBOLEV *et al.*, 2007, SOBOLEV *et al.*, 2011) and commonly attributed to the generation of magmas with signatures of enriched components HIMU and EMI, respectively. Several studies (YAXLEY; GREEN, 1998; YAXLEY, 2000; DAY *et al.*, 2010; KOGISO *et al.*, 1997; MALLIK; DASGUPTA; 2012, SOBOLEV, 2005, 2007; DASGUPTA *et al.*, 2010; JACKSON; DASGUPTA, 2008; GURENKO *et al.*, 2009; ROCHA-JÚNIOR *et al.*, 2013; JIANG *et al.*, 2021), including studies using experimental petrology, suggest the participation of olivine-poor mafic lithologies, such as pyroxenites and eclogites, in the generation of alkaline OIB-types magmas.

The nature of mantle sources and the geodynamic mechanisms related to the occurrence of intraplate volcanism, more specifically of oceanic islands related to hotspots, are still very controversial and debated topics. Different models have been invoked to explain the origin of these igneous manifestations, the main ones being: (1) hotspot/mantle plume (originally proposed by Wilson, 1963 and Morgan, 1971) and (2) shallow processes inherent to plate tectonics itself and the convective dynamics of the mantle with its intrinsic heterogeneities (*e.g.* ANDERSON, 2001, 2007; FOULGER, 2007; FOULGER; NATLAND, 2003; FOULGER; ANDERSON, 2005).

The hotspot/mantle plume model was originally proposed to explain the age progression in volcanic island chains, specifically the Emperor-Hawaii Chain, that extend across oceanic basins and therefore evoke a stationary origin in the mantle that has been attributed to the core- mantle boundary layer. However, this classic model underwent several adaptations by authors over the years in order to justify data that violated the original predictions of this model or that were not sufficiently explained by it. For example, Tarduno (2008), Foulger and Natland (2003) and Konrad *et al.* (2018) proposed non-stationary hotspot models, which can undergo lateral displacements. Another example, Courtillot *et al.* (2003) proposed that not all hotspots are attributed to a deep mantle plume as initially envisioned by Morgan (1971). Alternatively, these authors suggested the existence of three types of hotspots, which may come from different layers in the mantle, namely: (1) “primary”, which meet the criteria of very deep mantle origin coming from the D layer”; (2) "secondary", which would possibly come from the top of the domes of the so-called "superplumes" near the depth of the transition zone; (3) “tertiary”, which may have a surface origin, linked to the asthenosphere, as a passive response to tension stresses in the lithosphere and decompression melting.

Despite the widespread use of the mantle plume model to explain the origin of intraplate magmatism occurrences such as LIPs and linear volcanic chains, this model has been questioned, especially in recent years, with more alternative proposals being formulated by authors. An example of an alternative model is the "plate" model (FOULGER, 2007) in which the generation of significant volumes of magma and enriched signatures can be explained by the melting of a fertile shallow mantle (*e.g.* containing eclogitic/pyroxenitic material from recycled crust) without the need for a thermal anomaly, just processes explained by plate tectonics.

The Vitória-Trindade Ridge (VTR) is an interesting example to investigate the formation of linear chains of volcanic edifices, since it presents both tectonic control characteristics and a supposed temporal progression generally attributed to mantle plume activity. On the one hand, there is evidence of a distensive regime controlling the intrusion of alkaline rocks into the VTR (BARÃO *et al.*, 2020), and the role of the Vitória-Trindade fracture zone (VTFZ) on magma ascent has been well discussed previously (ALVES *et al.*, 2006; MOHRIAK, 2020). The absence of an expressive igneous body of size related to the VTC, attributed to the initial impact of a mantle plume of deep origin in the lithosphere (COURTILLOT *et al.*, 2003), is another feature that raises discussions about the existence of the Trindade Plume or the magnitude of this anomaly (VANDECAR; JAMES; ASSUMPÇÃO, 1995). On the other hand, some evidence would be consistent with the plume hypothesis, such as: (1) The remarkable thickness of the lithosphere (*ca.* 120 km; MÜLLER *et al.*, 2008; ELLAM, 1992) in which these igneous bodies had their emplacement; (2) supposed progression of ages along the ridge (SKOLOTNEV *et al.*, 2011; SANTOS, 2016; PIRES *et al.*, 2016; SKOLOTNEV; PEIVE, 2017; SANTOS *et al.*, 2015; 2021); (3) the previous reported homogeneity of the chemical and isotopic compositions of the VTC rocks that occur along *ca.* 1200 km and the enriched origin of these rocks, which suggest recycling of enriched materials introduced into the mantle (*e.g.* subducted oceanic crust, subcontinental lithospheric mantle) (SIEBEL *et al.*, 2000; FODOR; HANAN, 2000; BONGIOLO *et al.*, 2015; PEYVE; SKOLOTNEV *et al.*, 2014; SANTOS, 2016; SKOLOTNEV; PEIVE, 2017) common in OIB associated with deep mantle plumes; (4) mantle tomography study showing occurrence of low velocity anomaly below Trindade Island between 100-250 km, current location of the hotspot (Celli *et al.*, 2020). However, some of this evidence is still debated, such as the correlation between low velocity anomaly and thermal anomaly, and the lack of reliable geochronological

data that attest to the progression of ages in the VTC, which will be discussed in more detail in this work.

In this context, the nature of the source regions of the Vitória-Trindade Ridge (VTR) magmatism and the geodynamic mechanisms that caused the melting of these source regions are still open topics and based mainly on speculations about the Trindade Plume hypothesis, being that few authors have proposed alternative models. This reflects, in part, the difficulty of sampling in this region of the South Atlantic, with most of the published geochemical and geochronological data referring to the islands of Trindade and the Martin Vaz Archipelago (*e.g.* MARQUES *et al* 1999; HALLIDAY, 1992; SIEBEL *et al.*, 2000; BONGIOLO *et al.*, 2015; PIRES *et al.*, 2016; SANTOS *et al.*, 2020) and scarce data on submarine volcanic buildings (PEYVE; SKOLOTNEV, 2014; SANTOS, 2016; SKOLOTNEV; PEIVE, 2017; JESUS *et al.*, 2019; MAIA *et al.*, 2021). Thus, this work aims to contribute with new whole-rock chemistry and Sr-Nd-Pb-Hf isotope data, as well as a petrographic description of the rocks and comparison with previously published data in the literature to help understand the nature of the magmatism of the ridge and raise possible suggestions about the geodynamic and tectonic processes that gave rise to this magmatism, whether or not they are related to the supposed Trindade Plume.

Furthermore, the results presented here were used to develop a new model of origin of the distinctive isotopic signature of Banco Davis and Monte Vitória (MAIA *et al.*, 2021), assuming source heterogeneity.

1 OBJECTIVES

The primary objective of this dissertation is to enhance the understanding of magmatic enrichment in the VTR, focusing specifically on Davis Bank. The study aims to identify the mantle sources involved, considering the tectonic context and geodynamic processes.

1.1 General

In general, the present dissertation aims to help elucidate the origin of the VTR magmatism enrichment, specifically from the Davis Bank, and identify the mantle sources involved, taking into account tectonic background and geodynamic processes.

1.2 Specifics

The specific objectives are:

- a) Petrographic, whole-rock chemistry and isotopic characterization of the Davis Bank;
- b) Modeling of Sr-Nd-Pb isotopic chemistry data in order to quantify the mixing percentage of mantle end-members;
- c) Discuss the possible models that best explain the evolution of these bodies, as well as the tectonic implications of these models.

2 THEORETICAL CONCEPTUALIZATION

This section presents theoretical frameworks that form the basis of this study, examining different hypotheses regarding mantle dynamics and magmatic processes. The main models discussed include the Mantle Plume hypothesis and the Plate Tectonics hypothesis, each offering distinct perspectives on the sources and characteristics of intraplate magmatism. Additionally, concepts of mantle heterogeneity and the identification of specific mantle reservoirs are introduced, emphasizing their relevance in understanding the geochemical diversity observed in oceanic and continental volcanic formations.

2.1 Plume hypothesis *versus* plate hypothesis

The Mantle Plume model (Figure 2) is widely used to explain the occurrence of intraplate magmatism in linear and age-progressing chains. The concept of hotspot was originally proposed by Wilson (1963) as an anomalously hot and fixed source in the mantle over which the passage of the lithosphere occurs, explaining the decrease in ages found in the volcanoes of the Emperor-Hawaii chain. Years later, Morgan (1971) proposed the mantle plume hypothesis to explain the occurrence of about 20 hot spots on Earth and the relative fixity between them. For Morgan (1971), this relative fixity of hotspots is explained through a source deep in the mantle. The compositional difference between hotspot lavas and ridge lavas was predicted in the model proposed by Morgan (1971). Experiments with fluids in tanks carried out in the laboratory showed the formation of a "mushroom-shaped" plume (CAMPBELL; GRIFFITHS, 1990; GRIFFITHS; CAMPBELL, 1990) characterized by a larger section comprising the "head" of the plume followed by a narrow conduit comprising the "tail" of the plume. With the initial impact of the plume head on the lithosphere, the occurrence of generalized uplift and the generation of flood basalts by adiabatic decompression is predicted (*e.g.* CROUGH, 1983; COURTILOT *et al.*, 2003), which is attributed to the mechanism of formation of LIPs. These flood basalts would, then, be related to the formation of linear volcanic chains (hotspot tracks) attributed to the phase in which the plume's tail reaches the lithosphere, which, when migrating above this reference, forms progressively younger volcanoes (*e.g.* COURTILOT *et al.*, 2003). One of the initial

assumptions of the mantle plume model is that its rise in the mantle would be due to a thermal origin of a boundary layer of thermal instability within the mantle, generally attributed to the D" layer.

According to Foulger (2010), some of the most convincing arguments that support the Mantle Plumes hypothesis are: (1) high magma temperature; (2) lithospheric uplift; (3) crustal thickness; (4) lithospheric thermal erosion; and (5) deep mantle tomography signal. The mantle plume hypothesis gained a lot of popularity for its elegance and over the decades after its formation, several authors invoked this model to explain the occurrence of intraplate volcanism, mainly LIPs and linear ridges, even in the absence of the necessary evidence such as those stated before (from number 1-5). Due to the aforementioned and other reasons, such as the difficulty in obtaining reliable data that confirm this model, such as seismic tomography and absolute dating of samples in deep ocean locations, there has been several debates about which locations are most convincingly attributed to a deep origin of thermal anomaly. For this, Courtillot *et al.* (2003) used some observations as criteria to assess a deep mantle origin: (1) presence of linear volcanic ridge with reliable age progression; (2) the presence of basaltic flow at the origin of this track; (3) high "buoyancy" flow; (4) high He isotopic ratios in basalts; and (6) significant low velocity signal (V_s) in the underlying mantle (*ca.* 500 km). Using these criteria, Courtillot *et al.* (2003) made a subjective analysis, assigning scores according to which characteristics each investigated site had. The sites with the highest score were attributed to a deep origin of the D" layer, called primary plumes (1); those with moderate scores were attributed to the layer of transition of the mantle, called secondary plumes that rise from the top of superplumes of D" origin (2); and the tertiary hotspots would have a shallow origin related to distensive stresses of the lithosphere (3). This shallow origin consequence of processes inherent to plate tectonics had been previously proposed by Anderson (2000).

The Mantle Plume model has gained so much popularity in the Earth geodynamics literature that attempts have been made to correlate most, if not all, igneous provinces at some point with this model. As previously mentioned, the classical mantle plume model has undergone several adaptations by authors over the years in order to justify data that violated the original predictions of this model or that were not sufficiently explained by it. For example, in regions where the supposed location of the plume does not match the location of the igneous province, a displacement of the plume is suggested (DUNCAN; RICHARDS, 1991). This occurs in publications on the Trindade Plume, in an attempt to attribute the

activity of this plume to the Serra do Mar Igneous Province, even assuming a migration of hundreds of kilometers (GIBSON *et al.*, 1995; THOMPSON *et al.*, 1998; THOMAZ FILHO; RODRIGUES, 1999).

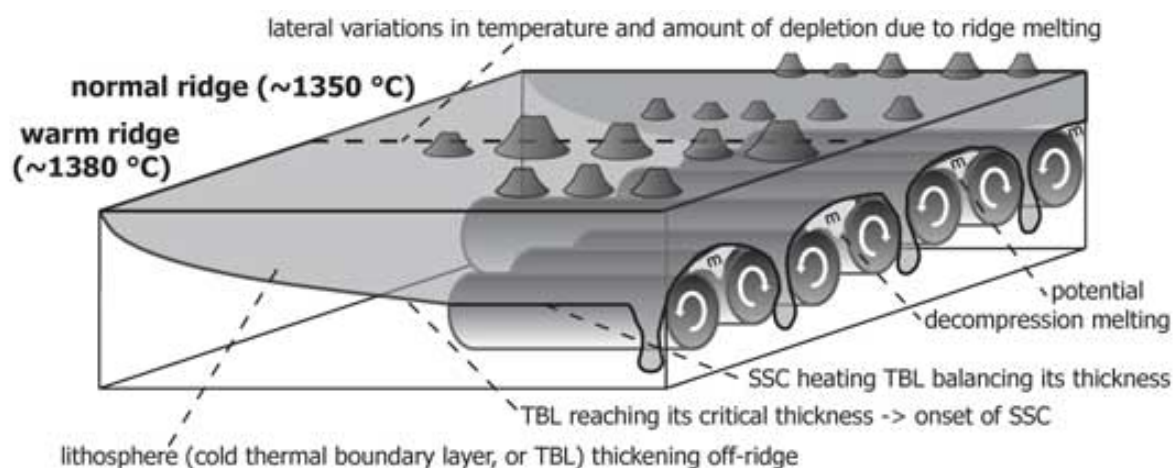
Another example, to explain very close or even possibly synchronous ages in the magmatism of the Vitória-Trindade Ridge, Skolotnev and Peive (2017) suggested lateral migration of plume material as a consequence of tectonic processes related to the fracture zone present in the region, a phenomenon which these authors call "hot lines". For this and other reasons, many criticisms of the Mantle Plume model have been raised in recent decades.

The "plate" model (Figure 2) was formulated as an alternative to explain intraplate magmatism without the need to invoke a model independent of the theory of plate tectonics, taking into account the methodological principle of Occam's razor (*i.e.*, to seek the simplest hypothesis to explain a phenomenon that can be explained in different ways). Supporters of this model argue that if the theory of Plate Tectonics itself can explain such volcanisms, there is no need for a model completely independent of it (ANDERSON, 2002). This model assumes that melting can occur where the lithosphere locally undergoes extension and that the volume of magma is related to the fertility (*e.g.* presence of eclogite/pyroxenite) of the source (FOULGER, 2010), in an asthenosphere that is close to the *solidus* (ANDERSON, 2007).

Another way of melting the mantle is the Edge-Driven Convection (EDC - *e.g.* ANDERSON, 1994; KING; RITSEMA, 2000) at the continental-oceanic lithospheric boundaries can also facilitate the occurrence of partial melting and the rise of magma through lithospheric discontinuities. The edge-driven convection model is mainly based on these discontinuities in the thickness of the lithosphere that can occur at the edges of the plate, as well as at the edges of thick cratons, which would generate small-scale convective instabilities in the upper mantle, commonly called the convective mantle, and would facilitate partial melting in the sublithospheric mantle (KING; ANDERSON, 1998). According to Anderson (2002), small-scale convection (SSC), such as edge-driven convection (EDC) and Richter rolls, and variations in stress and cracks in the lithosphere are consequences of plate tectonics and offer alternative explanations for the formation of "melting anomalies" (*e.g.* volcanic chains and intraplate volcanism; ANDERSON, 2002, JACKSON; SHAW, 1975, JANNEY *et al.* 2000). In addition, the EDC mechanism can contribute to the erosion processes of the subcontinental lithosphere (KING; ANDERSON, 1998). SSC (Figure 1) can spontaneously occur at the base of mature oceanic plates when the thermal boundary layer below the lithosphere exceeds a threshold thickness, and low effective asthenosphere viscosity and the amount of pre-existing lateral density heterogeneity can also generate these convections in

younger oceanic plates (BALLMER *et al.*, 2007). According to Ballmer *et al.* (2007), SSC can generate fusion by interrupting the thermal and compositional stratification of the upper mantle, forming linear volcanic ridges.

Figure 1 - Small scale convection developed at the base of mature oceanic plates in cylindrical geometries ("Richter Rolls") and aligned to the plate movement, forming linear ridges



Source: Ballmer *et al.*, 2007

The plate model is also able to explain the observations made through seismic tomography studies, on the occurrence of some seismic wave velocity anomalies in the mantle underlying the hotspots. The model predicts the presence of recycled materials in the convective mantle as a source of fertility, and that seismic waves vary not only with temperature, but also with the composition and presence of partial melting (FOULGER, 2010). According to Foulger (2010), even a minimal partial melting can radically decrease wave velocity, in addition to the fact that lithologies such as eclogite in the mantle have a low melting point and may have low wave velocity anomalies equivalent to peridotite with temperature anomalies of *ca.* 200° C.

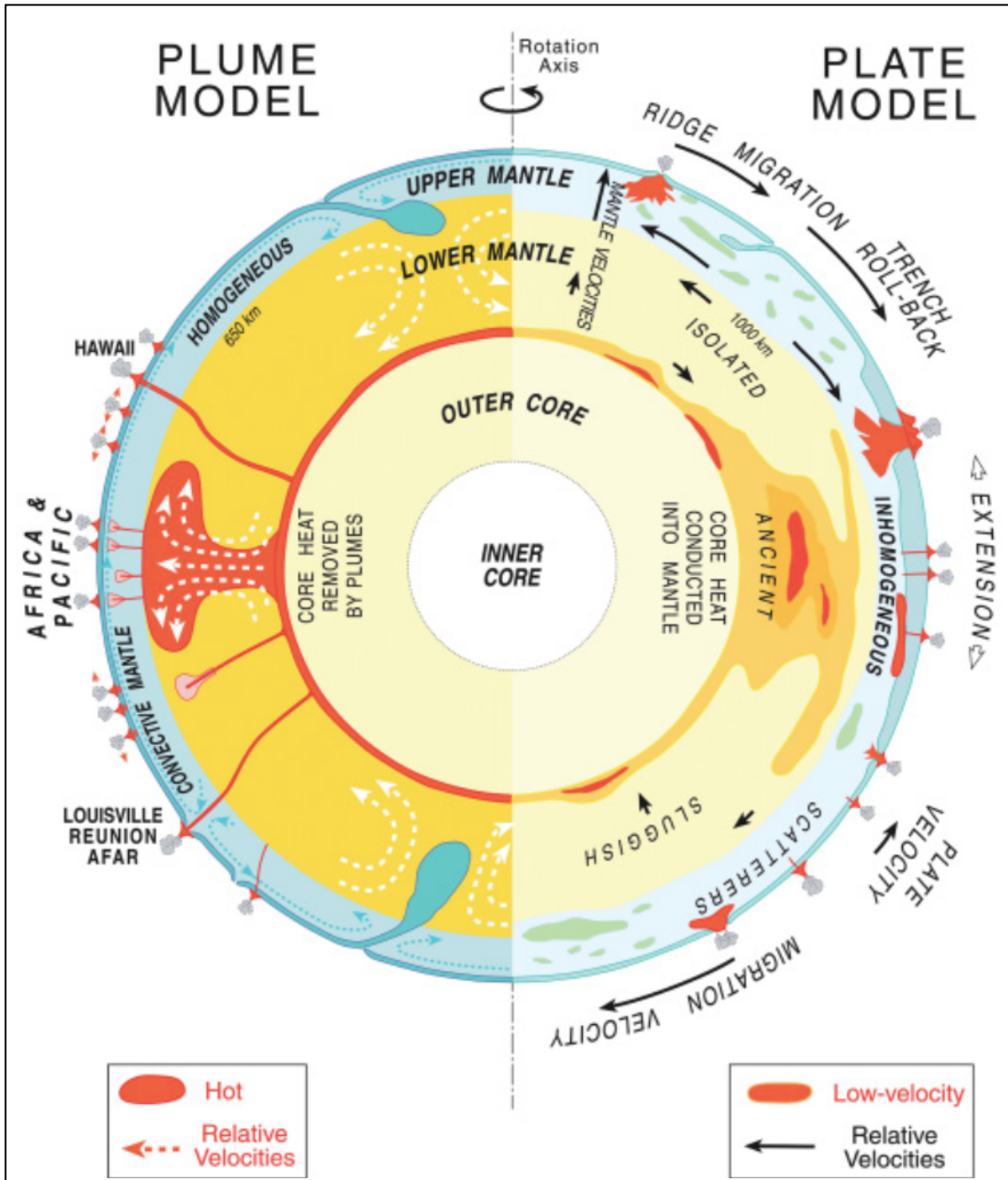
According to Rocha *et al.* (2011), correlations made between V_p and V_s anomalies and volcanic features on the surface may represent chemical variations and not elevated temperatures. Compositional variations and the occurrence of partial melting have the greatest effect on decreasing the speed of seismic waves, more than temperature (FOULGER, 2010).

Perhaps one of the weakest explanations that the "plate" model offers is concerned with the apparent fixity of some hotspots and the age progression in some volcanic ridges. The model assumes that mid-ocean ridges, for example, migrate relative to the underlying mantle and that, therefore, the mantle-localized melting anomaly, even if restricted to the asthenosphere, will move significantly slower than the overlying lithospheric plate, which

may, as a consequence, give the illusion of fixed hotspots (ANDERSON, 2005). According to Anderson (2005), melting anomalies appear to be relatively fixed not because they are deep or surrounded by a high-viscosity or stationary mantle, but because the return convective flow associated with plate tectonics occupies a greater volume than the plates.

Furthermore, inconsistencies regarding the fixity of hotspots are discussed even in the Emperor-Hawaii ridge, considered a classic hotspot track, which gave rise to the concept originally conceived by Wilson in 1963 of hotspot as a fixed hot spot in the mantle over which the Pacific plate migrated generating volcanisms with progression in ages. Some authors have suggested the occurrence of migration of the Hawaii hotspot (which may be around 2000 km), raising discussions about a non-stationary model for this volcanic chain (*e.g.* TARDUNO; COTTRELL, 1997; TARDUNO *et al.*, 2009; SAGER, 2007).

Figure 2 - Schematic profile of the Earth's interior according to the mantle plume model on the left and the "plates" model on the right



Source: Anderson, 2005.

2.2 Sources of mantle heterogeneity

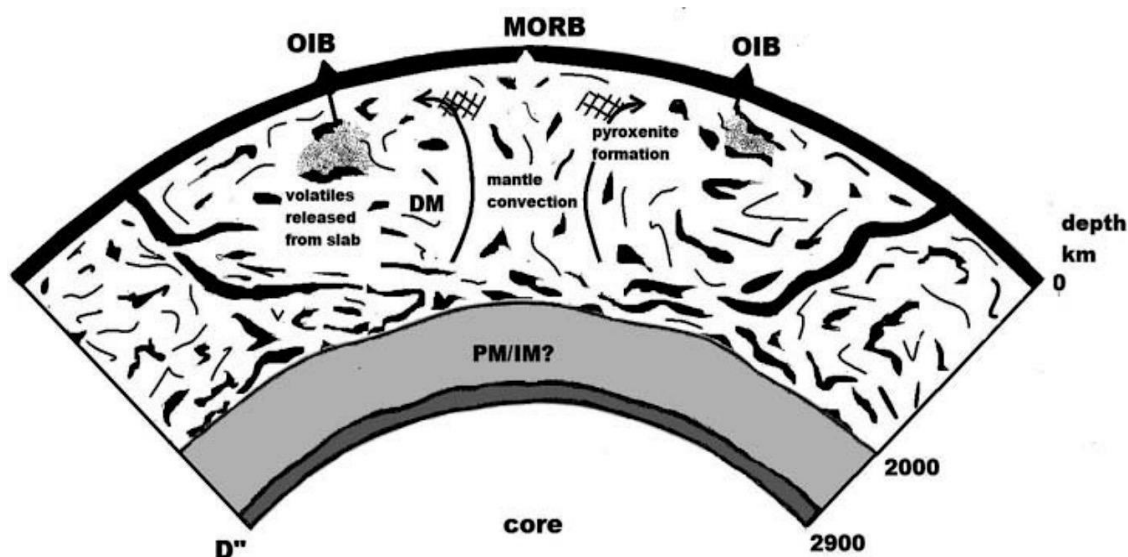
Several studies invoke Earth's mantle heterogeneity as a way of providing sources to explain the vast chemical and isotopic diversity of OIB and MORB (*e.g.* HOFMANN; WHITE, 1982; ALLÈGRE; TURCOTTE, 1986; SOBOLEV *et al.*, 2005). These authors argued that the compositional variability of these lavas cannot be generated solely by different degrees of peridotite melting. Indeed, very low degrees of partial melting of the mantle peridotite at high pressure, especially when generated in the presence of carbonate, can be strongly alkaline and, therefore, has the potential to be a source of OIB magmas (HIROSE, 1997). However, according to Hirschmann *et al.* (2003), experimentally produced partial melts of peridotite are generally too aluminous at a given MgO concentration to be a parent of typical OIB suites.

Alternatively, some authors suggest that the presence in the peridotite mantle of olivine-poor lithologies such as pyroxenites and eclogites significantly contribute to the generation of oceanic basaltic magmas (*e.g.* HOFMANN; WHITE, 1982; SOBOLEV *et al.*, 2005; MALLIK; DASGUPTA, 2012). Therefore, mixtures of eclogite or pyroxenite with peridotite, or amphibole veins in the oceanic lithosphere formed by mantle metamorphism, as well as metasomatic processes, have been proposed as candidates for the mantle source of OIB (SOBOLEV *et al.*, 2005, 2007; PILET *et al.*, 2008; GURENKO *et al.*, 2009; DAY *et al.*, 2009, 2010). Pilet *et al.* (2008), proposes the metasomatism of amphibolic and/or pyroxenitic veins present in the lithosphere, which melts would produce liquids with compositions close to the alkaline extremes (Nephelinites). According to these authors, when these nephelinitic liquids interact with the host rock (Peridotites), they produce modified melts forming alkaline lavas of basanitic composition. These veins are basically constituted by amphiboles, which is a stable mineral group in the lithosphere, but not in the Low Velocity Zone (LVZ), being a convincing argument for the lithospheric origin of basic alkaline magmas (PILET *et al.*, 2008).

In this sense, as highlighted by Rocha-Júnior (2013), the OIB source would be conceived as a model of heterogeneous convective mantle (*e.g.* 'marble cake' mantle; ALLÈGRE; TURCOTTE, 1986) that underwent several enrichment events of recycled materials from the oceanic crust and lithosphere, comprising a range of lithological varieties,

especially pyroxenites, introduced into peridotites by various geodynamic and magmatic processes (Figure 3).

Figure 3 - Schematic model of heterogeneous convective mantle in which slabs have a variety of destinations in the mantle



Source: Smith (2013).

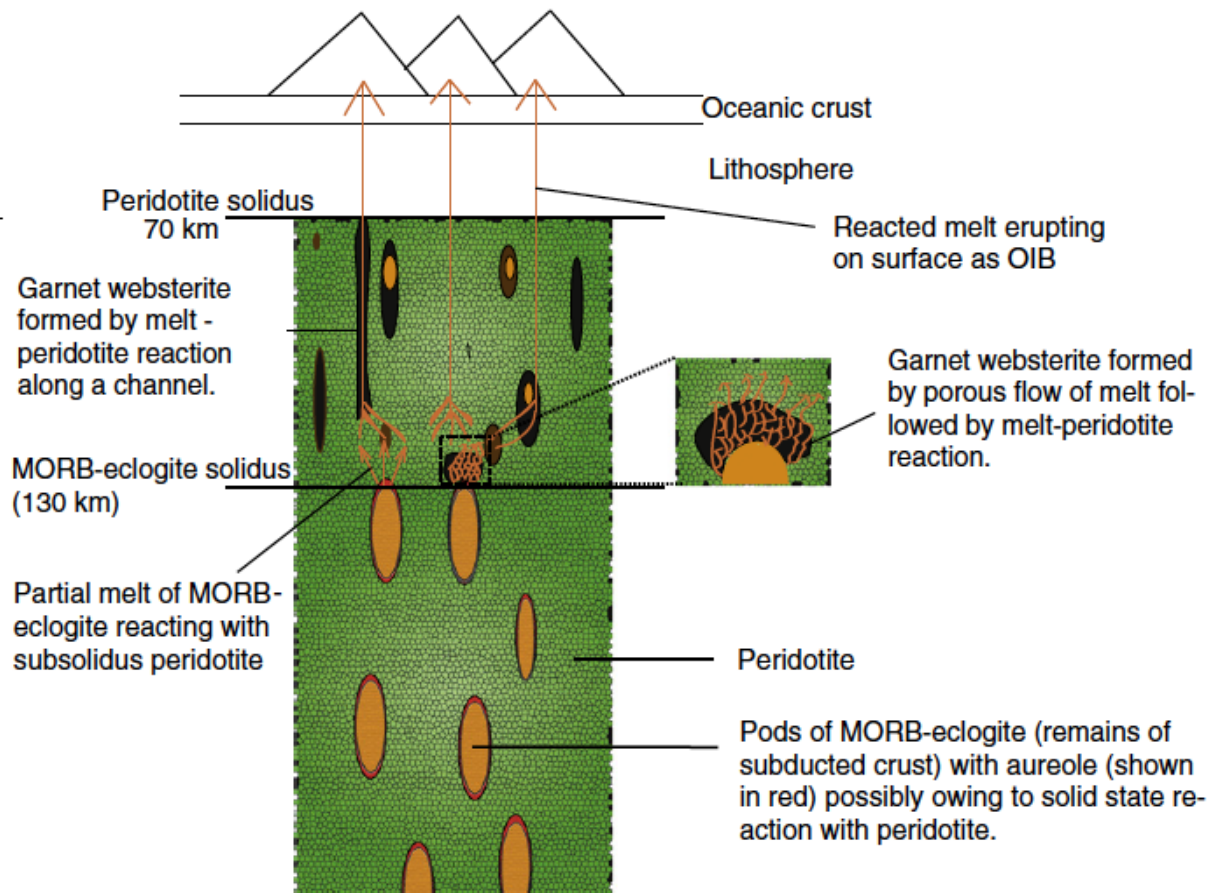
The origin of heterogeneous material in the mantle is commonly attributed to the recycling of oceanic crust and sediments (*e.g.* REHKÄMPER; HOFMANN, 1997), lower continental crust (*e.g.* KAMENETSKY *et al.*, 2001) or delaminated subcontinental lithospheric mantle (SCLM - subcontinental lithospheric mantle; GOLDSTEIN *et al.*, 2008). There are three main mechanisms for introducing recycled materials into the mantle: (1) subduction; (2) delamination and (3) thermal erosion by a thermal anomaly. As a result, Anderson (2005) envisioned the upper mantle as a significantly heterogeneous set of enriched and depleted lithologies that represent a wide range of chemical composition, melting point and fertility and, as a result of different ages of these lithologies, widely different isotopic compositions.

It is widely accepted that much of the observed convective mantle heterogeneity in the composition of mantle-derived magmas is due to subduction and recycling of oceanic crust into the mantle (HOFMANN; WHITE, 1982), either in the convective or deep mantle. One hypothesis is that the crust returns to the mantle and becomes hydrostatically unstable (buoyant) in thermal boundary layers, mainly core-mantle (HOFMANN; WHITE, 1982), and due to the thermal anomaly, they emerge in the form of diapirs (mantle plumes). On the other

hand, Anderson (2005) speculates that new oceanic plates or plate fragments (slabs) with thick oceanic crust do not have a very deep destination into the mantle and are likely to reside in the shallow mantle after subduction, whereas slabs formed from very old and cold lithospheric plates are more likely to sink deeper, where they will reside for longer timespan, before they can contribute to partial melts generated in the shallow upper mantle. However, Anderson (2005) believes that even the thickest slabs contribute to the heterogeneity of the shallow mantle with some of its sediments and fluids, and possibly its crusts, during subduction. Other authors have suggested that the subducted oceanic crust would be predominantly recycled into the depleted mantle (SAUNDERS *et al.*, 1988; CHRISTENSEN; HOFMANN, 1994).

Direct melting of recycled oceanic crust (in the form of eclogite) generates a silica-saturated liquid (GREEN *et al.*, 1967) which, therefore, does not explain the OIB compositions. Instead, mixtures of eclogite or pyroxenite with peridotite in varying proportions as a source of OIB have been proposed as an alternative. Experimental studies (*e.g.*, YAXLEY; GREEN, 1998; YAXLEY, 2000; MALLIK; DASGUPTA, 2012) show that the reaction of this silica-saturated liquid, generated from the partial melting of eclogite, with peridotite produces a hybrid pyroxenite, without the presence of olivine. This process of hybridization of the peridotitic mantle (Figure 4) has been studied by some authors (*e.g.* YAXLEY *et al.*, 2000; SOBOLEV *et al.*, 2005, 2007; GURENKO *et al.*, 2009; DAY *et al.*, 2009, 2010) and shows a good potential for the source of the silica-unsaturated alkaline lavas of OIBs that depict isotopic signatures of recycled materials associated, for example, with EMI-type signatures and, mainly, HIMU. Thus, larger volumes of magma are generated from pyroxenite compared to peridotite due to the lower *solidus* temperature of the former, as well as low-degree partial melts will preferentially show such a component (YAXLEY; GREEN, 1998). According to Day *et al.* (2009), metasomatic processes can generate a hybrid pyroxenite with an almost uniform chemical and isotopic composition, which can represent a single mixing end-member, as proposed by Rocha-Júnior *et al.* (2013) for the northeast portion of the Paraná basalt flow.

Figure 4 - Scheme suggested by Mallik and Dasgupta (2012) for the formation of OIB by partial melting reaction of MORB-eclogite with peridotite subsolidus



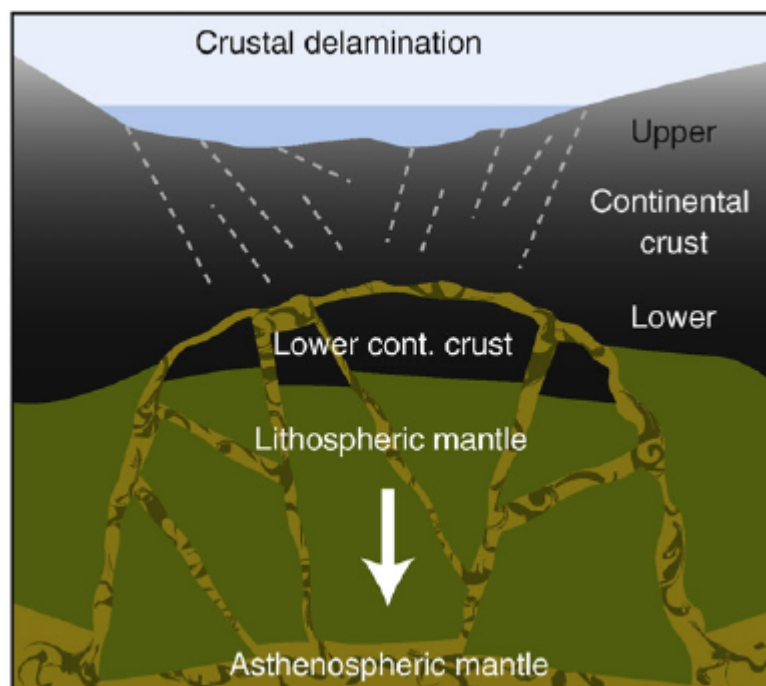
Source: Mallik and Dasgupta (2012).

The subcontinental lithospheric mantle (SCLM) and lower crust may also play an important role in mantle heterogeneity for the generation of EMI-type signature sources. Mechanisms that introduce these materials into the mantle can be, for example, delamination or tectonic 'detachment' during continental breakup (*e.g.*, HAWKESWORTH *et al.*, 1986) (Figure 5), delamination due to excess density of overlying thick continental regions (*e.g.* LUSTRINO, 2005), or thermal erosion by a thermal anomaly (*e.g.*, CLASS; ROEX, 2006). Some authors, for example, have suggested the presence of fragments of delaminated continental lithosphere dispersed in the asthenosphere underlying the South Atlantic after the breakup of the Gondwana supercontinent (HAWKESWORTH *et al.*, 1986; PEATE *et al.*, 1999; MARQUES *et al.*, 1999; MAIA *et al.*, 2021). According to Hawkesworth *et al.* (1986), the lithospheric mantle under Gondwana was significantly heated and remobilized before the continental breakup. Remobilization of such material separates it from lithospheric plates and therefore allows it to contribute to oceanic volcanism as continents move apart and the

ocean basin develops (HAWKESWORTH *et al.*, 1986).

According to Lustrino (2005), the insertion of fertile materials into the mantle, either by subduction or delamination, promotes melting in normal (rather than anomalous) thermal regimes.

Figure 5 - Schematic of tectonic crustal delamination



Source: Willbold and Stracke (2010).

2.3 Mantle reservoirs

As previously mentioned, OIB and MORB have a wide range of geochemical compositions, which led authors to define different mantle reservoirs based on the isotopic parameters Sr, Nd and Pb (*e.g.* WHITE, 1985; ZINDLER; HART, 1986). When describing the isotopic heterogeneities that comprise OIBs, four end-members (ZINDLER; JAGOUTZ; GOLDSTEIN, 1982) are most commonly invoked: DMM, EMI, EMII and HIMU; which are typical components of alkali basalts, basanites and nephelinites, and are present in varying

mixing ratios in most OIBs. In addition to these, other components have been proposed, from which all oceanic basalts can be produced by varying mixing proportions, namely: DMM (depleted MORB mantle), FOZO (focal zone), C (common mantle), PREMA (prevalent mantle), EMI (enriched mantle I), EMII (enriched mantle II), HIMU (High- μ) and PHEM (primitive helium mantle) (*e.g.* ALLÈGRE; TURCOTTE, 1986; WHITE, 1985; ZINDLER; HART, 1986; HART *et al.*, 1992; HAURI *et al.*, 1994; HOFMANN, 1997, 2003; FARLEY *et al.*, 1992). In recent years the term ‘PREMA’ has fallen into disuse, being replaced more commonly by ‘FOZO’, ‘C’ and ‘PHEM’ (HOFMANN, 2014). According to Hofmann (2014), these isotopic components are probably not well-defined end-members as entities that occupy a specific volume in the mantle and reflect distinct reservoirs, but instead encompass a continuum of isotopic compositions of mantle rocks.

Several authors attribute the origin of the EMI component to the subcontinental lithospheric mantle (SCLM) (*e.g.* LE ROEX; LANYON, 1998; MARQUES, 1999). According to Schaefer (2016), the subcontinental lithospheric mantle in this context is considered an SCLM that has separated from its continent and is now a discrete entity within the convective mantle. SCLM is generally referred to as being heterogeneous, particularly with respect to its isotopic chemistry, and variably metasomatized (EWART *et al.*, 2004).

Zindler and Hart (1986) pointed to the need for two enriched mantle components based on Sr and Nd isotopic data. In this perspective, EMI and EMII contain radiogenic Sr and non- radiogenic Nd isotopic ratios. Both features are typical of the continental lithosphere due to the relative enrichment of Rb and Nd in the contents because of mantle melting during continental formation. However, EMI has less radiogenic $^{87}\text{Sr}/^{86}\text{Sr}$ than EMII, implying a source that has a lower Rb/Sr ratio. According to Schaefer (2016), SCLM contains such features attributed to EMI, while continental crust and terrigenous sediments, in particular, have very high Rb/Sr being attributed to EMII.

The HIMU mantle component exhibits isotopic characteristics consistent with a source that has been enriched in U and Th relative to Pb, without an associated increase in the Rb/Sr ratio, in a time order equivalent to 1.5-2 Ga (HOFMANN, 2014). This can be observed, for example, in the very high $^{206}\text{Pb}/^{204}\text{Pb}$ ratio found in St. Helena and Tubuaii, associated with a low $^{87}\text{Sr}/^{86}\text{Sr}$ ratio and the intermediate ratio of $^{143}\text{Nd}/^{144}\text{Nd}$ (ZINDLER; HART, 1986). The most accepted hypothesis, suggested by Hofmann and White (1982) and Chase (1981), for the high values of the $^{238}\text{U}/^{204}\text{Pb}$ ratio in the HIMU component is that these rocks are examples of dehydrated subducted oceanic crust resulting in the preferential depletion of Pb in the fluids released during subduction of the oceanic plate. Many authors (*e.g.* ALLÈGRE;

TURCOTTE, 1986; HART, 1998; HOFFMAN, 1991; WHITE; HOFMANN, 1982) believe that the HIMU component characterizes material from the deep mantle of ascending plumes mainly from the mantle-core boundary. However, some authors (*e.g.*, SUN; MCDONOUGH, 1989; HALLIDAY *et al.*, 1995) suggest a shallow origin for HIMU attributed to metasomatic enrichment of the oceanic lithospheric mantle by infiltration of melts of low degree of partial melting with high U/Pb and Th/Pb. As aforementioned, HIMU is generally thought to result from enrichment of $^{238}\text{U}/^{204}\text{Pb}$ over a time period of above 1.5 Ga (ZINDLER; HART, 1986; CHAUVEL *et al.*, 1992). However, Thirlwall (1997) suggested, as an alternative, that if high U/Pb ratios were generated in the mantle throughout Earth's history, then it would be possible for basalts with $^{206}\text{Pb}/^{204}\text{Pb} > ca. 19.2$ to be derived from a 'young' HIMU and that this would be a significant mantle reservoir. According to this author, the main evidence, originally proposed by Vidal (1992), Chauvel *et al.* (1992) and Thirlwall (1995), which would allow identifying the young HIMU is the low ratio $^{207}\text{Pb}/^{204}\text{Pb}$ for a given $^{206}\text{Pb}/^{204}\text{Pb}$ and $^{208}\text{Pb}/^{204}\text{Pb}$, best expressed by the parameter $\Delta 7/4\text{Pb}$ (HART, 1984). This parameter is the percentage of vertical deviation of $^{207}\text{Pb}/^{204}\text{Pb}$ from the NHRL line (Northern Hemisphere Reference Line; HART, 1984) in the $^{207}\text{Pb}/^{204}\text{Pb}$ vs. $^{206}\text{Pb}/^{204}\text{Pb}$ chart. In contrast, Stracke *et al.* (2005) highlights uncertainties about $\Delta 7/4$ values, arguing that some of the islands that were originally used to define the NHRL by Hart (1984) are precisely the majority of those that define OIB with negative $\Delta 7/4$ values (*e.g.*, Azores, Canaries, Hawaii and Iceland). According to these authors, the meaning of small NHRL deviations ($\Delta 7/4$ up to $\pm ca. 3$) is still not entirely clear and that only similarities in the values of $\Delta 7/4$ are not enough to define the mantle components with chemical evolution integrated in the NHRL similar time (*e.g.*, the so-called "young HIMU").

The mantle component DMM has a depleted isotopic character (high $^{143}\text{Nd}/^{144}\text{Nd}$ and low $^{87}\text{Sr}/^{86}\text{Sr}$ and $^{206}\text{Pb}/^{204}\text{Pb}$), clearly identified along the Mid-Oceanic ridges (ZINDLER; HART, 1986). The existence of the component referred to as the "predominant mantle", from the English prevalent mantle (PREMA), characterized by the high frequency of the isotopic composition of Nd and Sr around 0.5130 and 0.7033, respectively, is suggested by Zindler and Hart (1986) as more likely than a constant mixture of spatially distant mantle end-members.

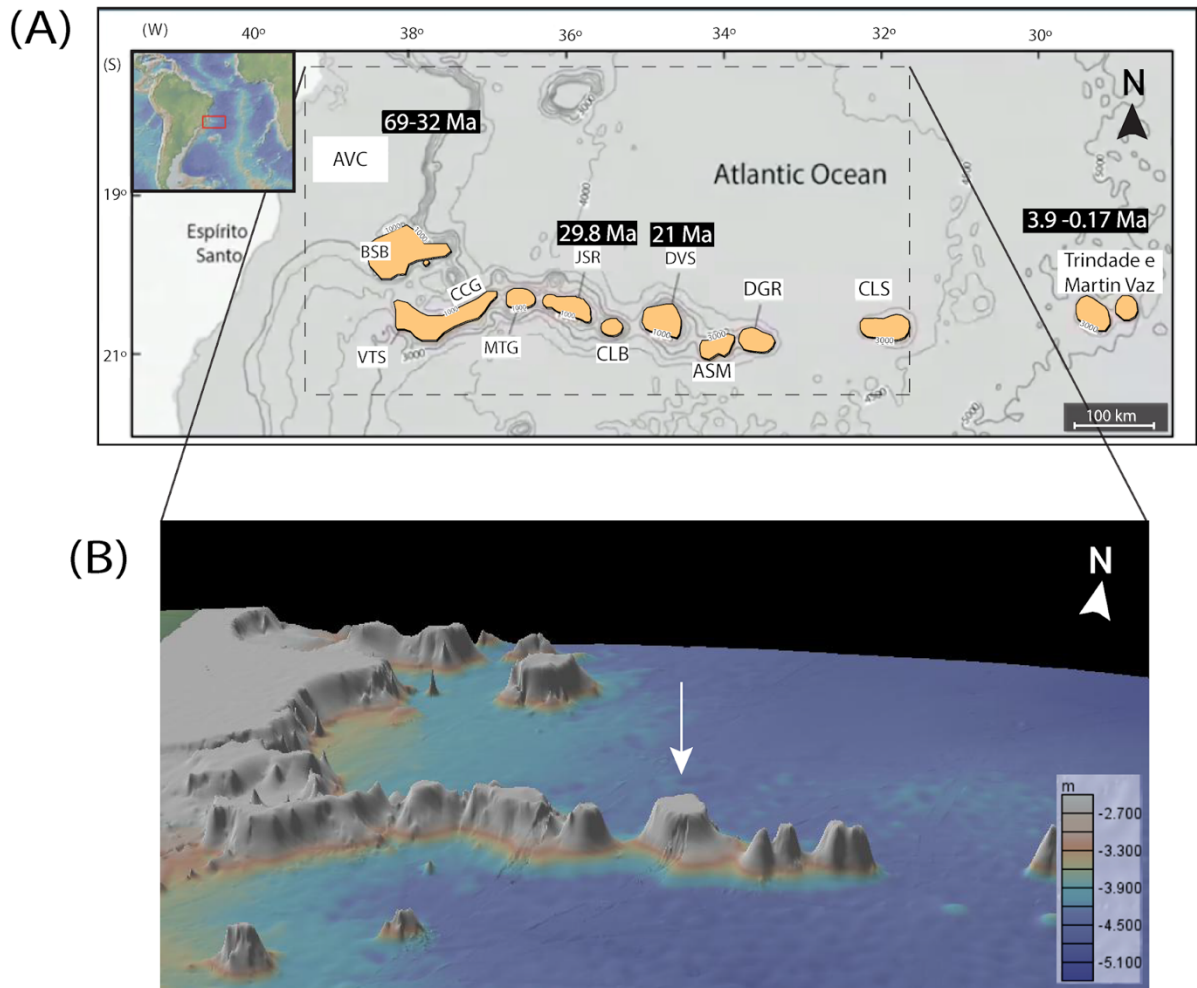
3 CONTEXT OF THE STUDY AREA

The Vitória-Trindade Ridge (VTR) comprises a remarkable alignment of volcanic structures of alkaline character with a E-W trend which extends for about 1200 km along the 20th parallel in the offshore portion of southeastern Brazil, state of Espírito Santo. The VTR is composed of several banks and seamounts, the main ones being, from West to East, (Figure 6): Besnard Bank, Vitória Seamount, Congress Seamount, Montague Seamount, Jaseur Seamount, Columbia Bank, Davis Bank, Dogaressa Bank and Colúmbia Seamount, as well as the islands of Trindade and Martin Vaz.

The Davis Submarine Bank (20°51'S and 34°47'W) is a conical volcanic structure of expressive size (Figure 7), with a flat top, which is submerged about 50 m deep. According to Motoki and Melo (2012), the Davis Bank has an area of about 872 km² and a height of 4000 m, being much larger than the other volcanic structures that make up the ridge. This voluminous volcanic structure (7.2 km³) has a base of approximately 60 km in diameter and a planar top of 35 km in diameter, with a moderate slope angle of 20° to 25° and in some locations the slope can reach 30° (MOTOKI; MELO, 2012; ALBERONI *et al.*, 2020).

At the western end of the Vitória-Trindade Ridge, adjacent to the Besnard Bank, is the Abrolhos Volcanic Complex (AVC - *ca.* 37.8° W), also called Abrolhos Magmatic Province (AMP), located on both continental and oceanic lithosphere (STANTON *et al.*, 2021; STANTON *et al.*, 2022). The Abrolhos Volcanic Complex is compositionally bimodal and is formed by volcanic rocks with transitional to alkaline affinity (STANTON *et al.*, 2021), dating from the Paleocene-Eocene (69-32 Ma; CORDANI, 1970; CORDANI; BLAZEKOVIC, 1970; FODOR *et al.*, 1983; SOBREIRA; SZATMARI, 2003; SOBREIRA *et al.*, 2004; MOHRIAK, 2005; FRANÇA *et al.*, 2007).

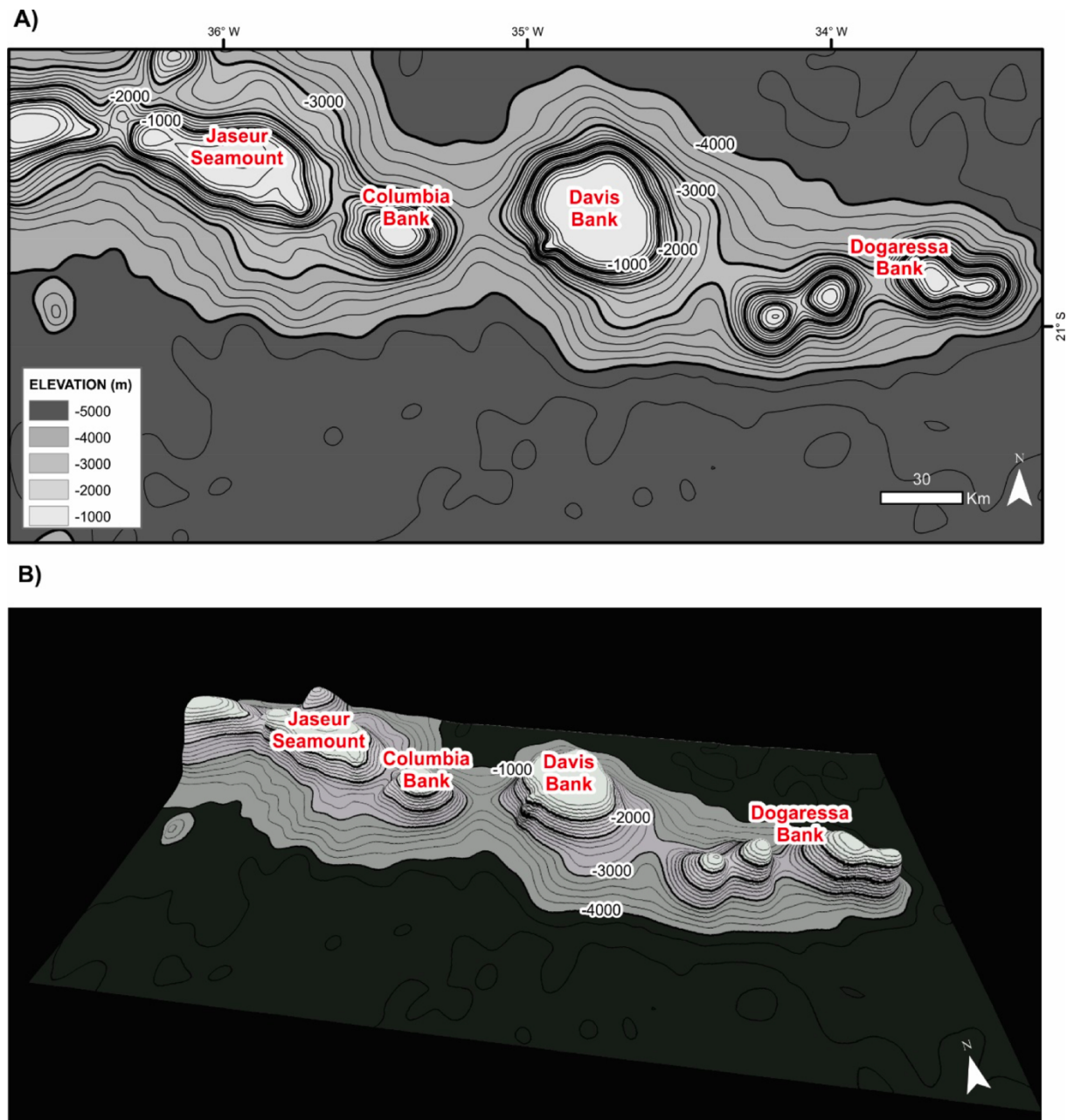
Figure 6 - Bathymetric map and 3D profile of the Vitória-Trindade Ridge with the published geochronological ages



Source: (A) AVC – Abrolhos Volcanic Complex (idades de Cordani, 1970; Cordani e Blazekovic, 1970; Fodor *et al.*, 1983; Mizusaki *et al.*, 1994; Sobreira *et al.*, 2004; França *et al.*, 2007); BSB –Besnard Bank; VTS – Vitória Seamount; CCG – Congress Seamount; MTG –Montague Seamount; JSR – Jaseur Seamount (age from Skolotnev *et al.*, 2011); CLB –Colúmbia Bank; DVS –Davis Bank (ages from Santos, 2016; Skolotnev e Peive, 2017, Quaresma, submitted); ASM –Asmus Bank; DGR –Dogaresa Bank; CLM – Colúmbia Seamount; Trindade and Martin Vaz (ages from Cordani, 1970; Pires *et al.*, 2016; Santos *et al.*, 2015; 2021). (B) 3D bathymetric profile, not to scale, depicting the West and central portion of the VTR. Davis Bank is highlighted by the white arrow. The 3D profile was made with georock app.

Source: The author, 2022.

Figure 7 - 3D bathymetry of the central portion of the VTR



Source: Rego *et al.* (2021)

3.1 Tectonic and geodynamic context

Many authors attribute the origin of both the VTR and the Abrolhos Volcanic Complex to the effect of the South American Plate passing above the Trindade hotspot (CROUGH *et al.*, 1980; DUNCAN, 1981; GIBSON *et al.*, 1995, 1997; HERZ, 1977; O'CONNOR AND DUNCAN, 1990; TOYODA *et al.*, 1994; VANDECAR *et al.*, 1995). The

existence of the Trindade Plume and the magnitude of this anomaly are still controversial. Authors who suggest the participation of a mantle plume in the VTR magmatism (e.g. FODOR; HANAN, 2000; SIEBEL *et al.* 2000; SKOLOTNEV; PEIVE, 2017; SANTOS *et al.*, 2020) mainly highlight the previously reported homogeneity, even though considering a previous heterogeneous source homogenized prior to eruption, of the mantle source in view of the very close values of isotopic compositions of the volcanic rocks found along about 1,200 km of the VTR, either in some seamounts, such as the ankaramite of Columbia Seamount and melanephelinite of Jaseur Seamount, or in the rocks from Trindade Island and Martin Vaz Archipelago, like basanites and nephelinites. According to Fodor and Hanan (2000), the similarity of isotopic signatures both along the VTR and in the Abrolhos Volcanic Complex points to a common mantle plume source for both provinces. On the other hand, Marques *et al.* (1999) identified two groups of ultrabasic rocks on Trindade Island, a more primitive one composed of melanephelinites and a more evolved one composed of basanites and tephrites, which present chemical differences in major, minor and trace elements that these authors interpreted as being the result of participation of different mantle sources.

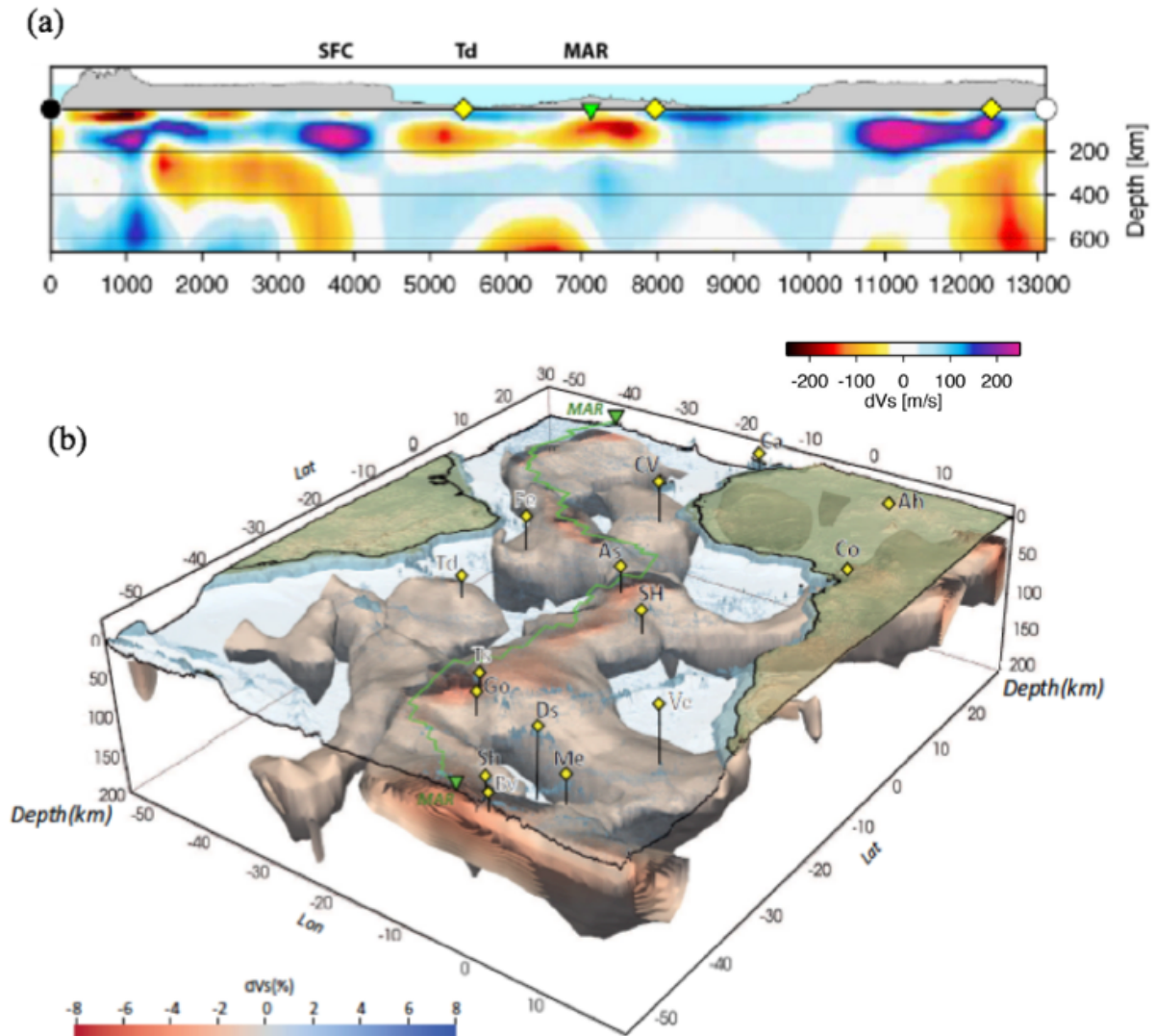
The apparent age progression (Figure 6) related to these two provinces is also evidence used to corroborate the mantle plume generation hypothesis (e.g. SKOLOTNEV *et al.*, 2011; SKOLOTNEV; PEIVE, 2017; SANTOS *et al.*, 2015; 2021). However, few geochronological data have been published in the literature to confirm this assumption, especially in relation to the submarine volcanic structures. Only the Davis Bank, among the seamounts and banks, has robust published geochronological data: a whole rock $^{40}\text{Ar}/^{39}\text{Ar}$ age (21.57 ± 0.1 Ma; SANTOS, 2016) and two $^{40}\text{Ar}/^{39}\text{Ar}$ ages in plagioclase and clinopyroxene (19.2 ± 0.7 Ma and 21.1 ± 1.6 Ma, respectively; SKOLOTNEV; PEIVE, 2017). Skolotnev *et al.* (2011) published U-Pb ages of 30 zircons collected from Jaseur Seamount, however, a wide range of ages were found reaching 2 Ga, with only a recent age with a large analytical error (29.8 ± 6.6 Ma) being interpreted as the magma crystallization age. The islands of Trindade and Martin Vaz have well-established $^{40}\text{Ar}/^{39}\text{Ar}$ ages ranging from 6.4 ± 3.5 Ma to 0.17 Ma (CORDANI, 1970; VALENCIO; MENDÍA, 1974; GERALDES *et al.*, 2013; PIRES *et al.*, 2016;) and 0.49 ± 0.08 Ma to 0.64 ± 0.08 Ma (SANTOS, 2013; 2016; SANTOS *et al.*, 2015, 2021), respectively.

However, regarding the Abrolhos Volcanic Complex recently linked to the VTC, Stanton *et al.* (2021) interpreted, through seismic reflection investigation of the region and

magnetic anomaly data, the occurrence of magmatic activity from the Paleocene up to possibly the Miocene, *i.e.* contemporary with the Davis Bank magmatism, and perhaps despite the great uncertainty, from Dogaressa Bank where the age of the carbonates at the top containing fragments of volcanic rocks was speculated to be between 19 and 24 Ma by the micropaleontological investigation from Skolotnev *et al.* (2011). Thus, Stanton *et al.* (2021) suggests the presence of either an anomalous thermal structure or a convective structure responsible for the long-term magmatism along a large area from Abrolhos to the central portion (Davis and Dogaressa banks) of the VTR, given that this region also corresponds to a positive dynamic topography anomaly (COWIE; KUSZNIR, 2018). Stanton *et al.* (2021) conclude that Abrolhos and VTR volcanism is inconsistent with a fixed hotspot model, implying alternative geodynamic mechanisms such as convective processes related to plate tectonics. Similarly, Knesel *et al.* (2011) and Perlingeiro *et al.* (2013), through $^{40}\text{Ar}/^{39}\text{Ar}$ dating, had identified simultaneous volcanism in Fernando de Noronha Island (also commonly attributed to the activity of a mantle plume) and in Borborema Province, in the continental portion, and proposed the alternative edge-driven convection mechanism. Knesel *et al.* (2011) also mention that the edge-driven convection mechanism is plausible, given the geometry of the region, for the Vitória-Trindade Ridge.

Furthermore, in the mantle below the Trindade Island region, Celli *et al.* (2020) identified a wide zone of seismic wave attenuation between approximately 100-250 km (Figure 8). Due to the resolution of the model by Celli *et al.* (2020), the authors were unable to interpret whether this structure extended to greater depths, which could confirm the existence of a mantle plume below the current location of the hotspot. Some authors (ITO; VAN KEKEN, 2007; ROCHA; SCHIMMEL; ASSUMPÇÃO, 2011) point out that the fact that seismic tomography data showing low-velocity S-wave anomalies at depths of 150 to 250 km, coincident with the provinces of Lower Cretaceous alkaline intrusions in the continental portion, corroborate the hypothesis of generation by mantle plume of these rocks and ratify the existence of the Trindade Plume, correlating these continental alkaline provinces (Poxóreu, Iporá and Alto Parnaíba) to the beginning of the impact of the Trindade Plume (GIBSON *et al.*, 1995; THOMPSON *et al.*, 1998).

Figure 8 – Seismic Tomography showing a low velocity anomaly in the mantle below the Trindade Island region



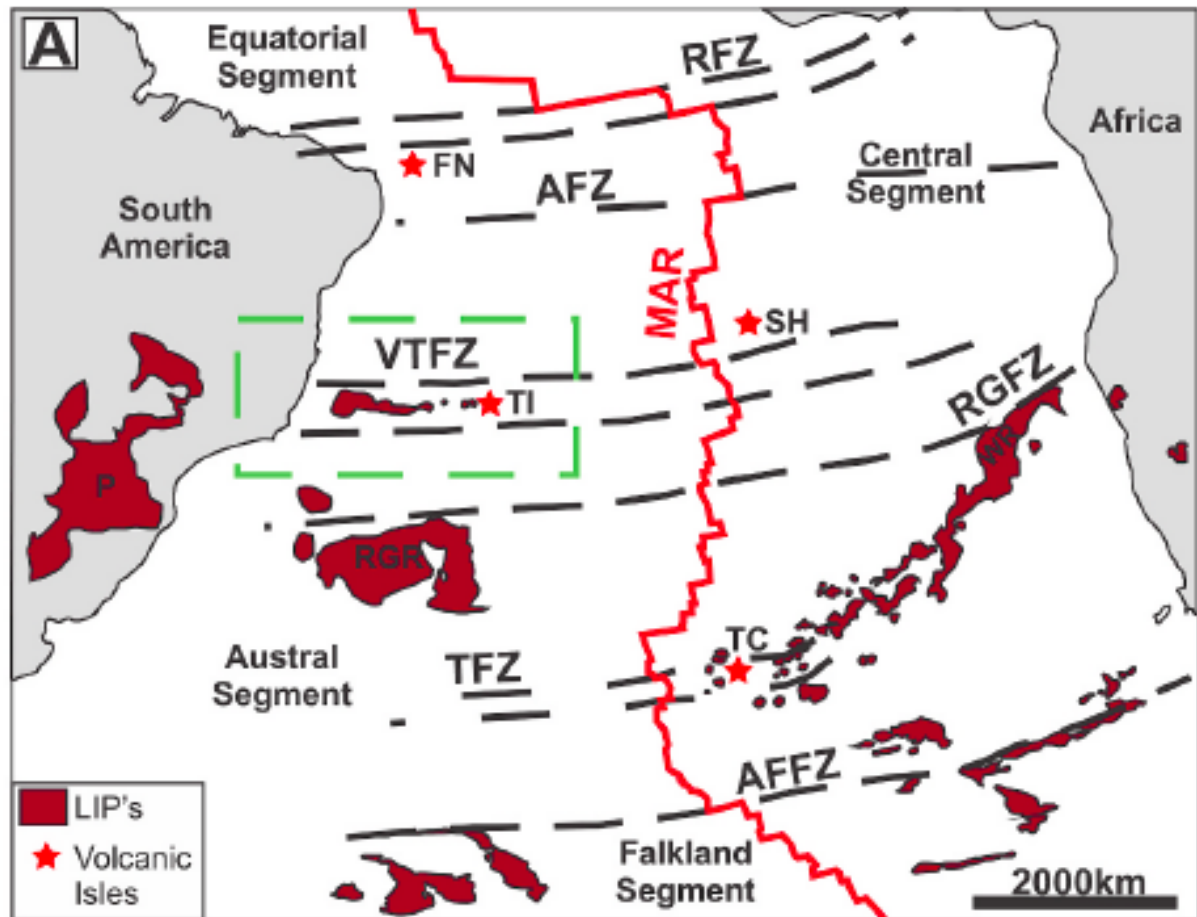
Subtitle: (a) E-W profile passing through the continental portion of the South American Plate through the South Atlantic Ocean and the VTR region to the continental portion of the African Plate. Td, Trindade hotspot; SFC, São Francisco Craton; MAR, Mid Atlantic Ridge. (b) 3D scheme of low velocity anomalies underneath the South Atlantic and the main hotspots plotted on the surface as yellow dots. Ca, Canary; CV, Cabo Verde; As, Ascension; SH, Saint Helena; Fe, Fernando de Noronha; Td, Trindade; Ve, Vema; Ts, Tristan da Cunha; Go, Gough; Ds, Discovery; Me, Meteor; Sh, Shona; Bv, Bouvet; Ah, Ahaggar; Co, Mount Cameroon.

Source: Modified from Celli *et al.* (2020).

Although most researchers associate these alkaline intrusions with a thermal anomaly in the mantle, the importance of structural control in the formation and evolution of the Vitória-Trindade Ridge should also be highlighted (MOHRIAK, 2003; ALVES *et al.*, 2006; BARÃO *et al.*, 2020; SKOLOTNEV; PEYVE; TURKO, 2010).

The tectonic framework of the South Atlantic Ocean (Figure 9) should be considered to discuss the origin and evolution of the Vitória-Trindade Ridge. This important sublatitudinal alignment of volcanic structures occurs parallel to the Vitória – Trindade Fracture Zone (VTFZ; MOHRIAK, 2003; ALVES *et al.*, 2006; Figure 10). Another point of view about the formation of the VTR considers the role of the fracture zone as a conduit for the ascent of magmas generated by a sub-lithospheric thermal anomaly (*e.g.*, ALVES *et al.*, 2006). Barão *et al.* (2020) identified important structural features of the extensional regime both on Trindade Island and throughout the entire VTR stratigraphy, suggesting that this extensional regime played a key role in the intrusion of the alkaline rocks. Skolotnev, Peyve and Turko (2010) interpreted, through results of acoustic profiles performed along the central part of the VTR, that tectonic movements that caused the uplift in steps of the seafloor (forming a linear elevation that would be the base of the volcanoes) preceded the volcanic activity and that tectonism continued to act synchronously along the entire central part of the ridge.

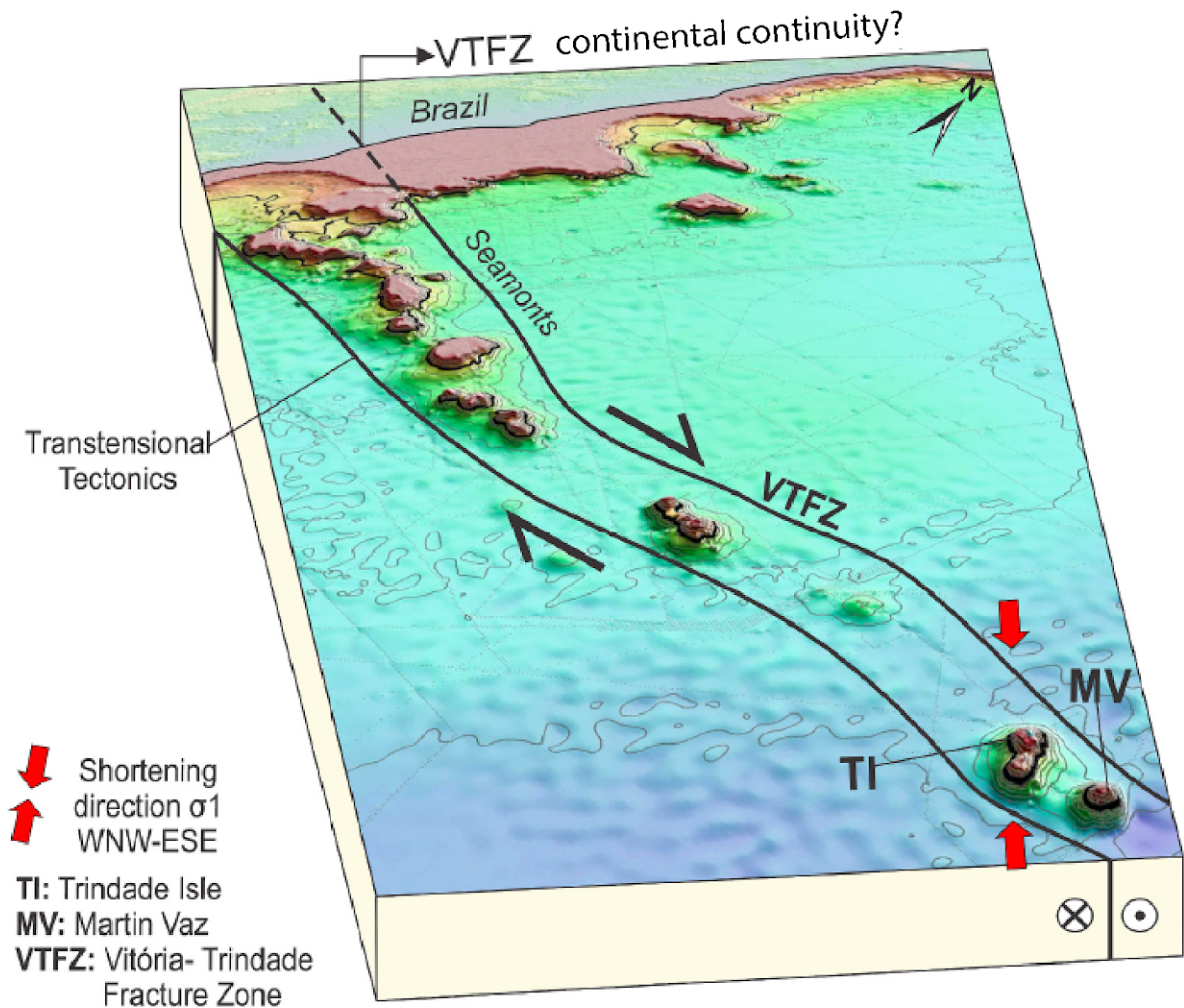
Figure 9 - South Atlantic tectonic map



Subtitle: FN: Fernando de Noronha, SH: Santa Helena, TI: Trindade, MV: Martin Vaz, TC: Tristão da Cunha, RGFZ: Romanche Fracture Zone; AFZ: Ascension Fracture Zone, VTFZ: Vitória-Trindade Fracture Zone, TFZ: Tristão da Cunha Fracture Zone, AFFZ: Agulhas Fracture Zone, P: Paraná, RGR: Rio Grande Rise, WR: Walvis Ridge.

Source: Barão *et al.*, 2020.

Figure 10 - Schematic model of the transtensional stresses related to the VTFZ that affected the intrusion of the alkaline rocks in Trindade Island



Subtitle: Tectonic stresses active from the middle Pleistocene until present, with a NW-SE main direction affecting the Trindade and Martin Vaz islands.

Source: Barão *et al.*, 2020.

3.2 Geologic background

The previously studies show that the submarine volcanic structures of the VTR are mostly composed of ultrabasic rocks of alkaline character, such as alkali basalt from the Vitória Seamount (MAIA *et al.*, 2021), ankaramites from the Colúmbia Seamount and Dogaressa Bank (FODOR; HANAN, 2000; SKOLOTNEV *et al.*, 2010), melanephelinites from the Montague and Jaseur seamounts (SANTOS, 2016), while the islands of Trindade and Martin Vaz are composed of nephelinitic-phonolitic successions (MARQUES *et al.*,

1999; SANTOS, 2013; 2016; BONGIOLO *et al.*, 2015; PIRES; BONGIOLO, 2016; SANTOS *et al.*, 2015; 2018a; 2018b; 2021; OLIVEIRA *et al.*, 2021). Some Davis Bank rocks contrast by their basic signature, being classified as basanites, tephrites and olivine-basalts (SKOLOTNEV *et al.*, 2010; SANTOS, 2016; JESUS *et al.*, 2019). According to Santos (2013; 2016), the VTR rocks are generally similar in terms of shape, color and general REE compositions, being described as vesiculated melanocratic rocks, usually filled with yellowish amorphous material and clay minerals.

Davis Bank is formed by ultrabasic to basic volcanic rocks, such as picro basalt, olivine basalts, basanites and tephrites (SKOLOTNEV; PEYVE; TURKO, 2010; PEYVE; SKOLOTNEV, 2014; JESUS *et al.*, 2019; SANTOS, 2016). These rocks range from aphyric to porphyritic and microglomeroporphyritic, with phenocrysts of olivine, clinopyroxene and plagioclase (PEYVE; SKOLOTNEV, 2014; JESUS *et al.*, 2019; SANTOS, 2016). The rocks matrix is formed by some apatite, oxides, clinopyroxene and olivine, and some ones have a large amount of plagioclase and k-feldspar microlites (PEYVE; SKOLOTNEV, 2014; JESUS *et al.*, 2019; SANTOS, 2016). According to Skolotnev, Peyve and Turko (2010) the more porphyritic rocks and those with olivine phenocrysts have the highest MgO (7–15.78 wt.%) and CaO (*ca.* 11 wt.%) contents and the lowest silica content (*ca.* 40–41 wt.%), in relation to the aphyric and less porphyritic rocks which, in turn, have higher Na₂O content (*ca.* 4 wt.%) (SiO₂ *ca.* 45 wt.%; MgO *ca.* 4 wt. %; CaO *ca.* 8 wt.%; PEYVE; SKOLOTNEV, 2014). The less porphyritic rocks also show greater enrichment in incompatible elements and REEs, being the most evolved compared to other submarine buildings and islands (SANTOS, 2016; JESUS *et al.*, 2019).

Geochemical studies carried out at the VTR previously point to a restricted variation of the isotopic compositions of the samples studied, mainly in relation to the rocks of Trindade and Martin Vaz. A common interpretation is that this restricted range of the Sr, Nd, and Pb isotopic compositions would attest to a homogeneity of these bodies' origin (FODOR; HANNAN, 2000; BONGIOLO *et al.*, 2015; SANTOS, 2016). Bongiolo *et al.* (2015) suggested a homogeneous source with asthenospheric heterogeneities inherent to the convective mantle processes, considering the Sr and Nd ratios from Trindade Island rocks.

Siebel *et al.* (2000), through Sr-Nd-Pb isotopic systematics, showed that Trindade and Martin Vaz rocks were derived from moderately depleted sources in relation to the bulk-earth. For these authors, the isotopic compositions of Sr, Nd and Pb present a restricted range, suggesting that the region of origin was homogeneous (similar to the mantle component FOZO), or originated by partial melting from three heterogeneous components (HIMU, EMI and DMM), well mixed before the eruption. On the other hand, Marques *et al.* (1999) highlighted the need for distinct mantle sources to explain two groups of ultrabasic rocks identified in Trindade and Martin Vaz islands that present significant chemical differences, of major, minor elements and traces, but mainly differences in Nd isotopic ratios, which, as known, could not be explained by fractional crystallization processes.

Marques *et al.* (1999) considered that the Nd model ages of rocks from Trindade Island coincide with the Brasiliano Cycle and suggest the involvement of the delaminated subcontinental lithospheric mantle in the source of magmatism. Peyve and Skolotnev (2014) highlighted that the VTR isotopic signature could be explained by a deep plume material related to the HIMU component, mixed with subcontinental lithospheric material related to the EMI component. Fodor and Hanan (2000) also considered the regional subduction history to suggest that small levels of isotopic variations in $^{207}\text{Pb}/^{204}\text{Pb}$ along the VTR may be due to small percentages of sediment introduced into the mantle source. Furthermore, Halliday *et al.* (1992) proposed, based on the Pb isotopic ratios of rocks from Trindade Island, some of which plot below the NHRL, that recent enrichments in U and Th relative to Pb occurred at the source of the Trindade mantle, suggesting participation of the component HIMU that these authors attributed as derived from metasomatism processes from the oceanic lithospheric mantle.

4 METHODS

In view of the aforementioned objectives, the methodology adopted for the preparation of this master's research comprised the following steps: bibliographic review and data compilation; analysis and selection of samples; and laboratory. The procedures adopted for sample preparation and laboratory analysis are described in detail below.

4.1 Bibliography

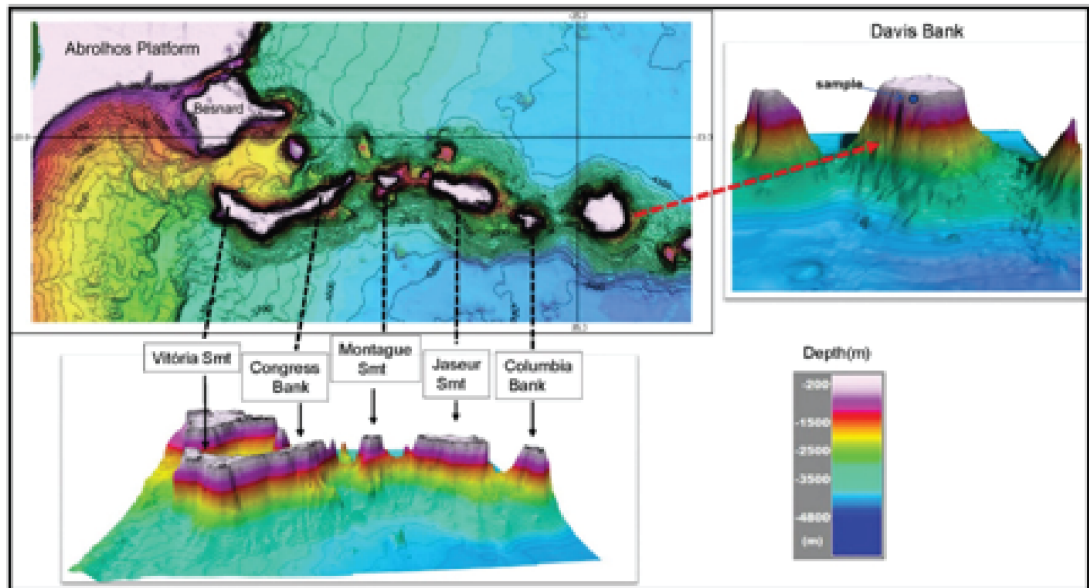
Initially, all the bibliography relevant to the research objectives was gathered to support the execution of this work. This step consisted in the compilation of geological data, mainly on the methodology of Sr, Nd, Pb and Hf isotopes, as well as on geochronological methods, petrography, chemistry of major elements and traces of OIB and the processes of generation of this type of magmatism available in the literature, mainly related to the alkaline magmatism of the Vitória-Trindade Ridge and other possibly analogous intrusions from the South Atlantic. It was also sought, through bibliographic reading, to better understand the different geodynamic hypotheses invoked to explain the generation of intraplate magmatism and possible mechanisms that explain the enrichment of the mantle source and the relationship with the tectonic context of the South Atlantic.

4.2 Samples

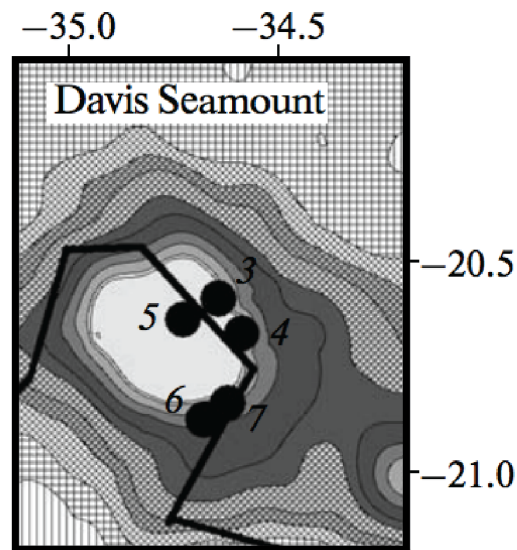
Samples obtained during a dredging campaign carried out in 2010 with the logistics of the Brazilian Navy. The dredging report available from the “Deep Sea Dredging, Offshore Brazil” project was analyzed in order to consult the sampling criteria used, which involved carrying out a preliminary geophysical survey of the site before concluding the position on which the sampling was carried out, followed by a local geological survey with the rock or sediment samples. The operations involved the collection of samples at thirteen points for the Vitória-Trindade Ridge, where fifteen samples related to the Davis Bank were obtained (Table 1). Twelve samples from the Davis Bank are used in this work. The results obtained by Skolotnev, Peyve and Turko (2010) and Peyve and Skolotnev (2014) were used for comparison purposes, considering that these authors collected samples from different positions on the flanks of the Davis Bank (*Figure 11*).

Figure 11 - Location of Davis Bank samples

(A)



(B)



Subtitle: (a) sample location at davis bank se flank (-1940 m) for new data presented herein; (b) only number 6 (from - 2380m to - 2200 m) represents the sample location of peyve and turko (2010) and peyve and skolotnev (2014).

Source: Modified from skolotnev, peyve and turko (2010) and Rego *et al.* (2021).

Table 1 - Sampling localization by dredging with Vessel Prof. Logachev (2010) carried out by the Brazilian Navy under LEPLAC project of Brazilian Margin Extension

Samples	Latitude	Longitude	Depth (m)	Lithology
VIT-TRIN-DR-4	20°51'38.40"S	34°47'52.20" W	- 1940 m	Basanite/ Tephrite

Source: The author, 2022.

Samples from this work were collected at the same site as samples from Santos (2016), Santos *et al.* (in progress) and Jesus *et al.* (2019). Rocks from Davis Bank from a different site were analyzed by Peyve and Skolotnev (2014). We compiled data from the aforementioned authors in order to have a wider picture of Davis Bank lavas and to better understand their evolution, from data from Santos (2016), Santos *et al.* (in progress) and Jesus *et al.* (2019) all plot very close to each other in diagrams possibly indicating being different fragments of the same rock collected at the same samples site assessed herein.

The preparation of samples was carried out systematically, following the petrographic, whole-rock chemistry and isotopic methods described below. Samples were powdered at the Universidade do Estado do Rio de Janeiro for geochemical purposes. The entire samples were crushed to a nominal minus 10 mesh using a steel mill to avoid contamination with metals such as Cr and Ni, mechanically split to get a representative aliquot and then pulverized in a ball mill to get a powder at least 150 mesh.

4.3 Petrography

Rock slices were made for description and petrographic studies carried out at the Laboratório Geológico de Preparação de Amostras (LGPA-UERJ). The methodology followed the standard specified in the technical procedures (Palermo & Coelho, 2009), taking place in the following steps: a) dredging sample and identification; b) cutting rock with diamond saw, obtaining slabs (slices of rock) with approximate dimensions of 47x30x25 mm; c) heating the slab in a hotplate, around 60 °C; d) impregnation of the slab with a mixture of resin (araldite® and hardener) and acetone; e) polishing the rock slice in the polisher using successively decreasing-grade abrasives (320, 600 and 800 microns); f) reheating the rock slice to about 60°C; g) bonding the still heated rock slice, on the side that does not identify it, to the glass slide using the resin; h) drying the slab in a light bath; (i) roughing the blade/rock

assembly with diamond pastes ($\frac{1}{4}$ and 3 microns) together with high viscosity lubricant; j) finally, washing the sample with detergent and water and drying with compressed air; (k) polishing the blade/sample assembly with a polishing cloth covered with polishing using diamond pastes of the following particle size: 6, 3, 1 and $\frac{1}{4}$ microns successively for 30 minutes; l) washing with detergent and alcohol, and drying with a tissue. Minerals were analyzed in parallel and crossed nicols in an Akioscop Zeiss® microscope at Rio de Janeiro State University (UERJ).

4.4 Whole-rock chemistry

Samples were analyzed at Actlabs Laboratories by a combination of fusion-inductively coupled plasma (FUS-ICP – major elements analyzed and some traces such as Sc, Be, V, Ba, Sr, Y, Zr) and fusion-inductively coupled plasma mass spectrometer (FUS-ICP-MS – trace elements analyzed). The samples fusion was obtained in an induction furnace by means of a flux of lithium metaborate and lithium tetraborate. The molten melt was immediately poured into a solution of 5% nitric acid containing an internal standard and mixed continuously until completely dissolved (~30 minutes). Major and trace elements were analyzed on a Perkin Elmer Sciex ELAN 6000, 6100 and 9000. Analytical procedures were those described by Hoffman (1992). Three blanks and five controls (three before sample group and two after) were analyzed per group of samples. Duplicates were fused and analyzed every 15 samples. The instrument was recalibrated every 40 samples.

4.5 Sr and Nd isotopes

Two samples (VIT-TRIN-DR-4M; VIT-TRIN-DR-4N) were analyzed for Sr-Nd isotopes at the Laboratório de Geocronologia e Isótopos Radiogênicos (LAGIR) from Universidade do Estado do Rio de Janeiro (UERJ). Analyses were performed using Thermal Ionization Mass Spectrometry (TIMS) on a TRITON instrument (for details on measurement procedures see Valeriano *et al.*, 2003). Wet chemical methods were identical to those described by Heilbron *et al.* (2013). The isotopic ratios were normalized to $^{146}\text{Nd}/^{144}\text{Nd} =$

0.7219; $^{147}\text{Sm}/^{152}\text{Sm} = 0.5608$ and $^{88}\text{Sr}/^{86}\text{Sr} = 8.3752$. Repeated analyses on NBS-987 (NIST) (n=140) and JNdi-1 (n = 214) (Tanaka *et al.*, 2000) standard reference materials yielded mean $^{87}\text{Sr}/^{86}\text{Sr}$ ratios of 0.710239 ± 0.000007 (2σ) and $^{143}\text{Nd}/^{144}\text{Nd} = 0.512100 \pm 0.000006$ (2σ) (Valeriano *et al.* 2008, 2009; Neto *et al.* 2009). Analytical total procedure blanks during this study were less than 200 pg for Nd and less than 70 pg for Sm. Sr value for blank was not obtained.

4.6 Pb and Hf isotopes

Isotopic analyses of Pb and Hf were performed at the Laboratoire G-Time of the Université Libre de Bruxelles (ULB, Belgium) on a Nu Plasma I Multi-Collector Inductively Coupled Plasma Mass Spectrometer (MC-ICP-MS) (@ Nu instruments).

Sr analyses were performed in wet mode. In routine, the raw data was normalized to $^{86}\text{Sr}/^{88}\text{Sr}=0.1194$, and corrected for mass bias by standard sample bracketing using the lab's in-house Sr standard solution. The in-house shelf Sr standard was calibrated and normalized to the certified value of NBS 987 Sr standard (0.710248) reported by Weis *et al.* (2006). During our analytical sessions, an in-house standard solution was run every two samples and gave an average value of 0.710287 ± 50 (2σ) for raw $^{87}\text{Sr}/^{86}\text{Sr}$ data (21 runs).

Nd and Hf were run in dry mode with an Aridus II desolvating system. To monitor the instrumental mass bias during the analysis sessions, the standard sample bracketing method was also applied. Standards were systematically run between every two samples, giving an average value in $^{143}\text{Nd}/^{144}\text{Nd}$ of 0.511921 ± 41 (2σ , 8 runs) for the Rennes Nd standard, and $^{176}\text{Hf}/^{177}\text{Hf}=0.282172 \pm 30$ (2σ , 10 runs) for the JMC 475 Hf standard. The Nd and Hf isotopic measurements were internally normalized to $^{146}\text{Nd}/^{144}\text{Nd}=0.7219$ and $^{179}\text{Hf}/^{177}\text{Hf}=0.7325$, respectively. For the Pb isotope analyses, a Tl dopant solution was added for every sample and standard, within a Pb-Tl concentration ratio of $\pm 5:1$ (for a minimum signal of 100 mV in the axial collector - ^{204}Pb). ^{202}Hg is routinely monitored to correct for the potential isobaric interference of ^{204}Hg on ^{204}Pb . Mass discrimination was monitored using $\ln - \ln$ plots and corrected by the external normalization and the standard sample bracketing technique using the recommended values of Galer & Abouchami (1998) (*i.e.* $^{206}\text{Pb}/^{204}\text{Pb} = 16.9405 \pm 15$; $^{207}\text{Pb}/^{204}\text{Pb} = 15.4963 \pm 16$; $^{208}\text{Pb}/^{204}\text{Pb} = 36.7219 \pm 44$). The repeated measurements of the NBS981 gave the following values: $^{206}\text{Pb}/^{204}\text{Pb} = 16.9403 \pm 8$,

$^{207}\text{Pb}/^{204}\text{Pb} = 15.4961 \pm 10$, $^{208}\text{Pb}/^{204}\text{Pb} = 36.7217 \pm 31$ (2σ) for the NBS981 Pb standard (5 runs).

5 RESULTS

In this section are presented the findings from the investigation of the volcanic rocks at Davis Bank, focusing on their petrographic characteristics, major and trace element compositions, and isotopic signatures. The analyses conducted provide insight into the geological processes that have shaped this region, contributing to a better understanding of the petrogenesis of these volcanic rocks. The following subsections detail the petrographic descriptions, geochemical data, and isotopic analyses of the samples collected from the Davis Bank flank, which collectively elucidate the compositional and evolutionary traits of these intriguing volcanic formations.

5.1 Petrography

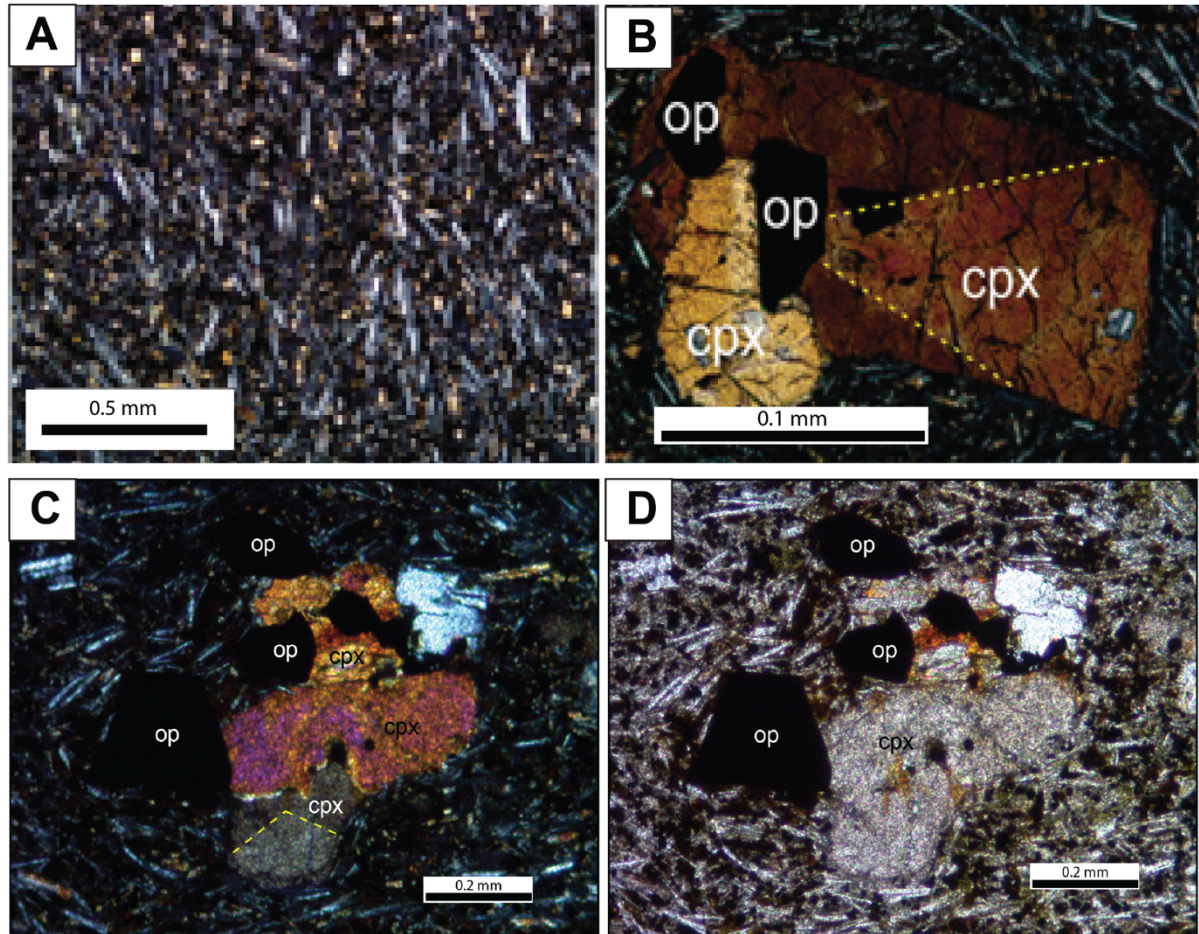
Eight samples dredged from a Davis Bank flank at 1940 m depth were petrographically studied and some of the most important petrographic characteristics are depicted in table 2 and figures 12, 13 and 14. The investigated samples are basanites (more than 10 wt.% normative olivine) characterized as a fine-grained mesocratic rock with porphyritic texture containing millimetric sparse phenocrysts of plagioclase, clinopyroxene and opaques. The somewhat stumpy groundmass, oxidized in some portions, is mainly composed of plagioclase/k-feldspar microliths and anhedral grains of clinopyroxene and opaque minerals (< 0.2 mm in size). The samples display a trachytoid groundmass with sub parallel alignment of lath-shaped feldspars (Figure 12, A), which is particularly noticeable where they flow wrapping around the outline of microphenocrysts marking the flow during the solidification of the lava. The most abundant phenocryst phase is plagioclase (Figure 13 A, B, C, D, E, F), which occur in euhedral to subhedral shapes, are 0.3 to 0.5 mm in size and display polysynthetic and carlsbad twinning. The clinopyroxene microphenocrysts (< 0.8 mm) are mainly subhedral and may display hourglass twinning (Figure 12, B, C, D) and

corroded borders. The opaque minerals also occur as microphenocrysts (Figure 14 A, B, C, D) characterized by euhedral (Figure 14 A, B) to anhedral (Figure 14 C, D) shapes and dimensions up to 0.4 mm. In most samples, microphenocrysts locally occur in clusters forming a glomeroporphyritic texture (Figure 13 A, B, E, F).

Table 2 - Summary of petrographic characteristics

Lithology	Phenocrysts	Matrix	Matrix/Pheno ratio	Observations
Basanite	plg, cpx, opaques;	cpx, plg/k-fdp, opaques;	95/05	microlitic texture, holocrystalline, glomeroporphyritic, hourglass texture in clinopyroxene;

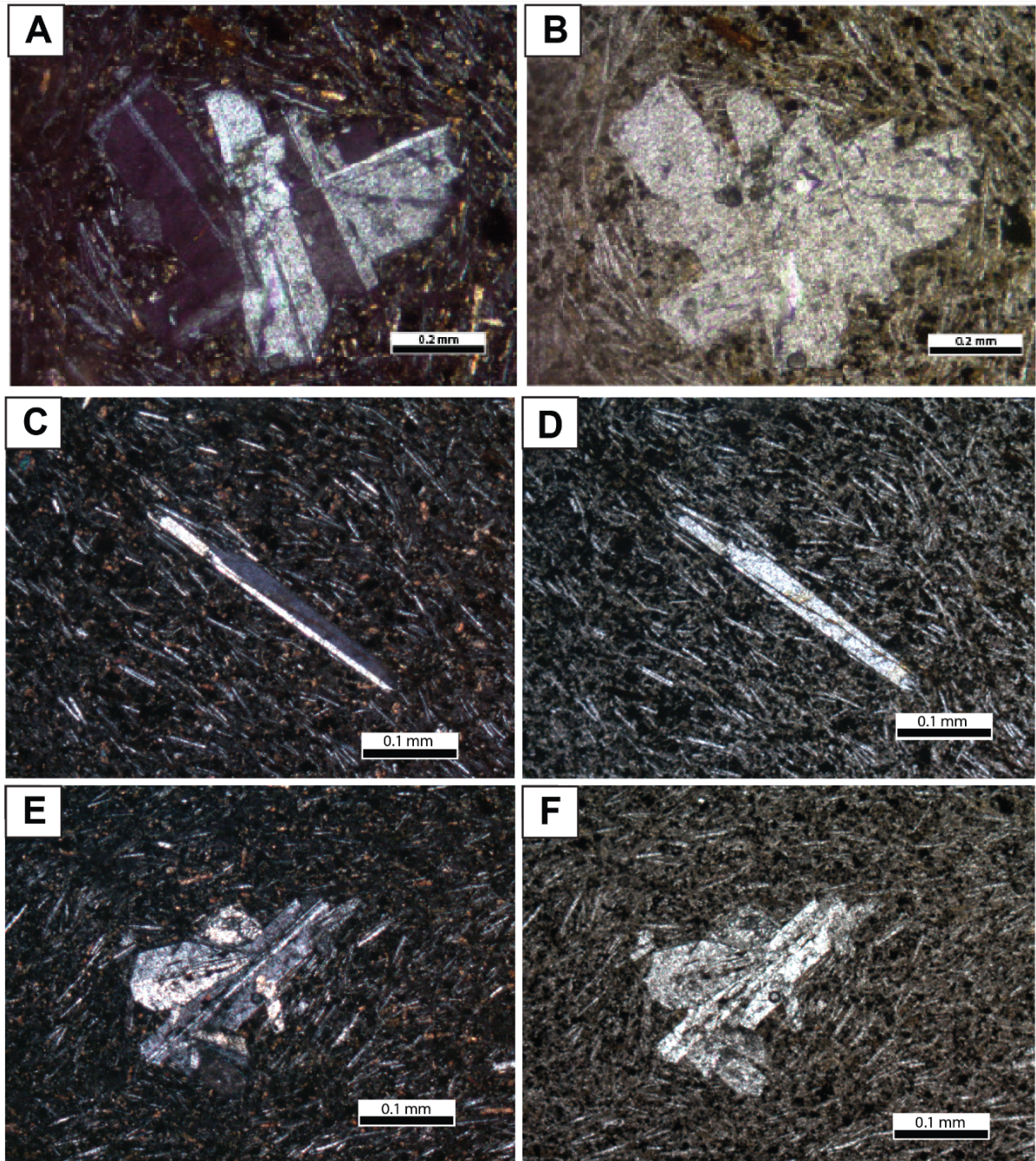
Figure 12 - Photomicrographs of Davis Bank basanite samples under polarized microscope, displaying the trachytic groundmass, clinopyroxene with hourglass twinning and opaque minerals



Subtitle: Picture depicts microglomeroporphyritic texture characterized by microphenocrysts of clinopyroxene and opaque minerals aggregated. (A) Crossed polarizers; pseudotrachytic/microlitic texture in basanite rock; (B, C) Crossed polarizers; Hourglass texture in clinopyroxene. (D) Parallel polarizers. Abbreviations are: cpx: clinopyroxene; op: opaque.

Source: The author, 2022.

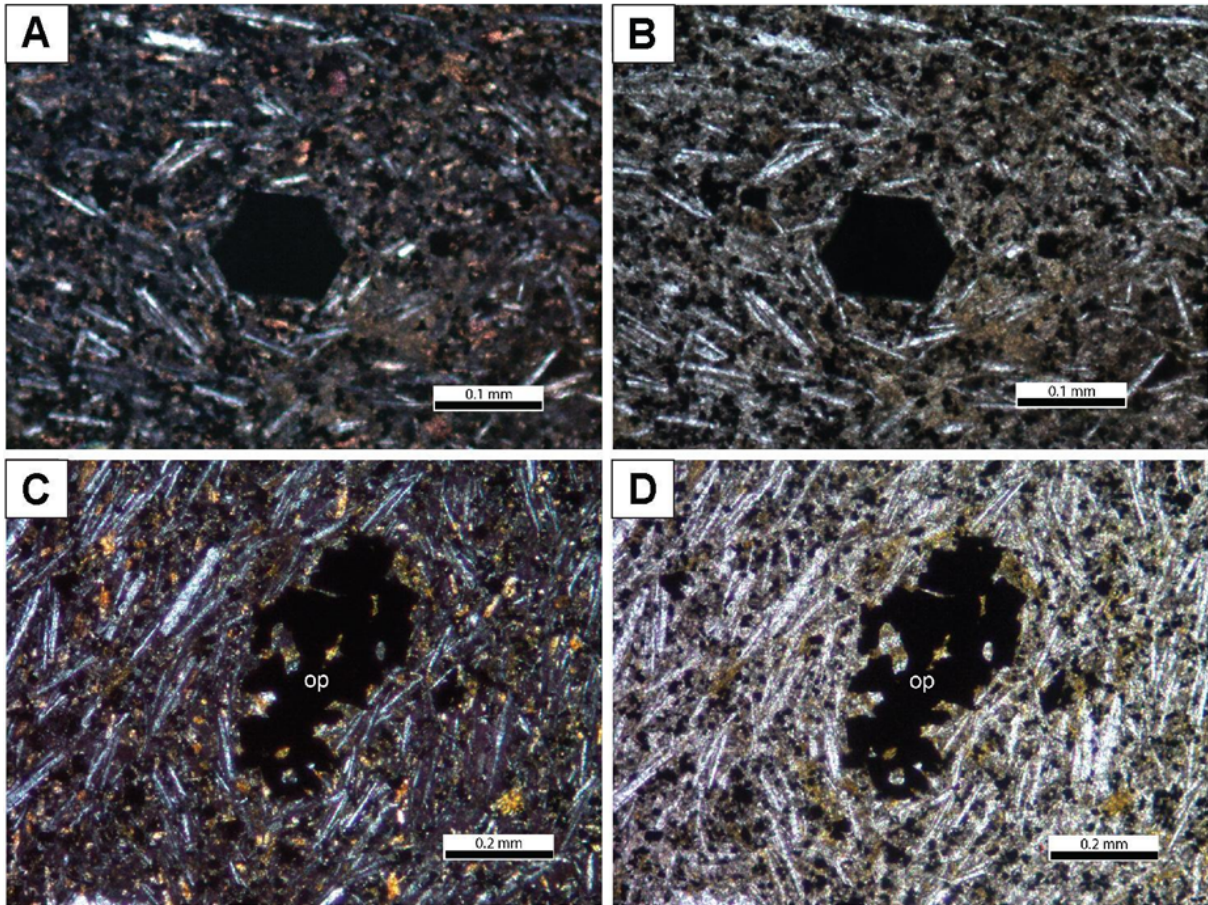
Figure 13 - Photomicrographs of plagioclase minerals in Davis Bank basanite samples under polarized microscope



Subtitle: A, C, E: crossed polarizers; and B, D, F: parallel polarizers. (A, B, E, F): Microglomeroporphyritic texture characterized by microphenocrysts of plagioclase aggregated. (C, D): Plagioclase crystal displaying carlsbad twinning and elongated in the direction of the oriented microliths in the groundmass.

Source: The author, 2022.

Figure 14 - Photomicrographs of opaque microphenocrysts in Davis Bank basanite samples under polarized microscope



Subtitle: A, C: crossed polarizers; and B, D: parallel polarizers. (A, B): Euhedral crystal of opaque mineral with hexagonal shape. (C, D): irregularly shaped opaque microphenocryst.

Source: The author, 2022.

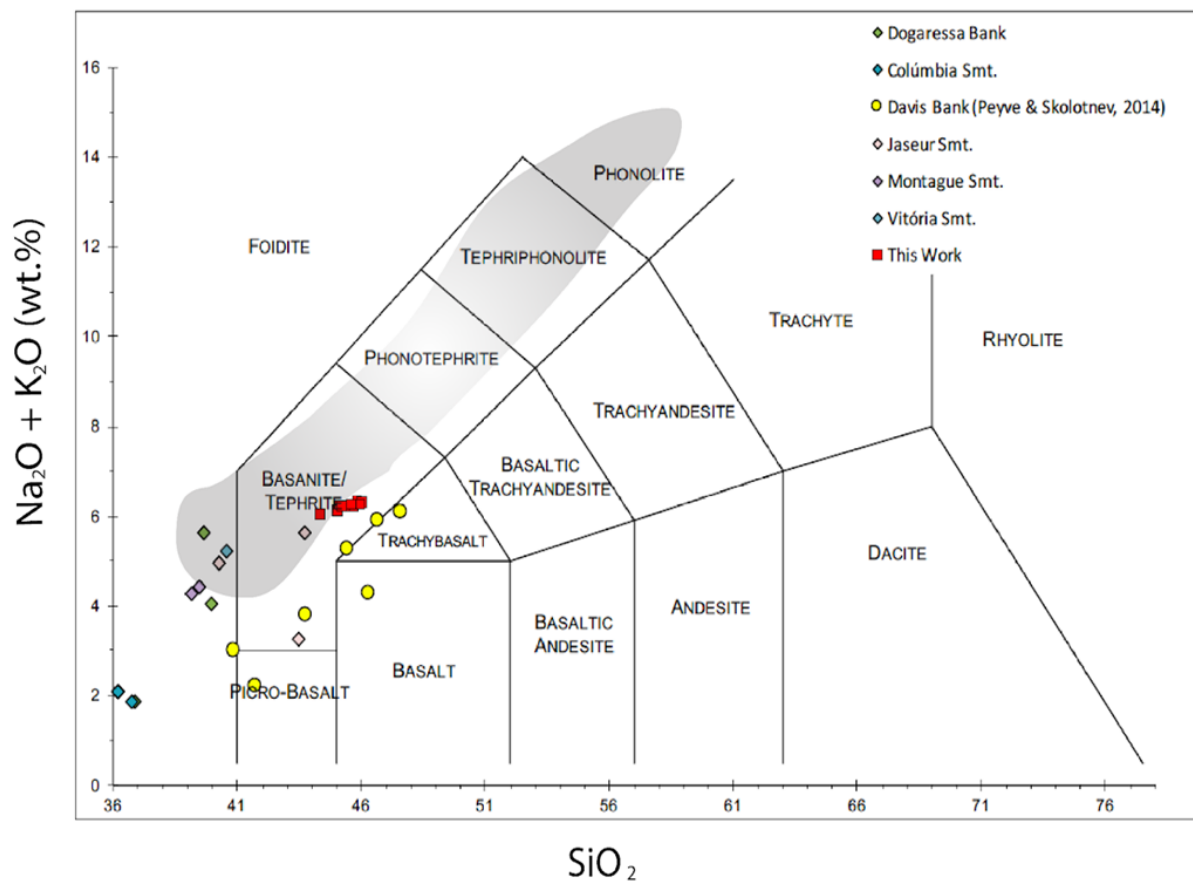
The alkaline basalt from the Vitória Seamount petrographically investigated by Maia *et al.* (2021) shows similarities with Davis Bank basanites. Plagioclases, clinopyroxenes and opaque minerals are the main mineral phases present in both magmatism. Both volcanic edifices are characterized by rocks of fine-grained pseudotrachytic groundmass mainly composed of lath-shaped plagioclase microliths. Clinopyroxene microphenocrysts also depict corroded borders and hourglass twinning, which according to Maia *et al.* (2021) attest the disequilibrium with melt.

5.2 Major and trace elements compositions for Davis Bank

Using the IUGS proposed TAS diagram (Le Maitre, 1989), Davis Bank volcanic rocks

are analyzed in this work plot on the basanite/tephrite field (Figure 15). Considering the proportion of normative olivine (*ca.* 11 wt.%), these rocks are classified as basanites (LE BAS; STRECKEISEN, 1991; LE MAÎTRE, 2005). This classification as basanite based on the 11 wt.% proportion of normative olivine may be interpreted carefully since it is in the limit of being considered tephrite or basanite and the LOI value, although being low, can influence this result. Previously studied samples from Santos (2016) and Jesus (2019) all plot within the same field. Rock compositions from Peyve and Skolotnev (2014), on the other hand, define a trend from subalkaline picro-basalt and basanite to subalkaline trachy-basalt, which is consistent with behavior of other major elements (Figures 16 and 17).

Figure 15 - Classification diagram based on Total Alkali vs. Silica (TAS) plot after Le Maitre (1989)



Subtitle: Samples from this work plot in the basanite/tephrite field. Data from the seamounts are from Fodor and Hanan (2000); Peyve and Skolotnev (2014); Santos (2016).

Source: The author. 2022.

Davis Bank rocks analyzed in this work have moderate LOI values (*ca.* 2 wt. %) and are composed of SiO₂-undersaturated alkaline rocks with sodic affinity having Na₂O + K₂O > 6.0; 45.2 wt. % (± 1.78) SiO₂ and MgO (4.2 ± 0.4 wt.%; Mg# *ca.* 43.5). Ni and Cr abundances are low (under the detection limit of 20 ppm), as well as Sc and Co contents (11 ppm, *ca.* 40

ppm, respectively). This composition indicates a more evolved magma (*e.g.* FREY *et al.*, 1978) when compared to some samples of Davis Bank from Peyve and Skolotnev (2014) (MgO = *ca.* 6.04 wt. %; Mg# 61; SiO₂ = 44.64 wt. %; Ni 132-371; Cr 241-584; Sc 21-30; Co 48.80-71.50) and to the other seamounts with SiO₂ ranging from 33.82 to 40.58 wt.%. (FODOR; HANAN, 2000; BONGIOLO *et al.* 2015; SANTOS 2013; 2016; SANTOS *et al.* 2018; MAIA *et al.* 2021). Whole-rock geochemical data are given in Table 3.

The Vitória Seamount (MAIA *et al.*, 2021) and other seamounts rocks from the Vitória- Trindade Ridge also plot in the alkaline field in the TAS diagram (Figure 15). Nevertheless, they are mostly ultrabasic rocks, as opposed to Davis Bank basanite. The Vitória Seamount alkaline basalt is characterized by a less evolved rock with low SiO₂ (40.6 wt.%) and high MgO (11 wt.%) contents (MAIA *et al.*, 2021), in contrast with Davis Bank samples analyzed in this work, which composition indicates a more evolved rock from a higher fractionated liquid, as discussed above.

Binary diagram SiO₂ (wt.%) *versus* MgO (wt.%) (Figure 16), when analyzing present data with previously published data, shows a linear trend of Davis Bank lavas suggesting a crystallization differentiation process. The linear trend is more evident in binary diagram MgO *vs.* Al₂O₃ (Figure 17), and this pattern repeats in other Fenner binary diagrams. Vitória Seamount alkaline basalt (MAIA *et al.*, 2021) apparently follows this linear trend observed in Davis Bank samples, with a lower differentiation process characteristic and plotting close to Montague Seamount samples and some samples from Jaseur Seamount and Dogaressa Bank (PEYVE; SKOLOTNEV, 2014; SANTOS, 2016).

Table 3 - VTR Seamounts whole rock composition from this work and bibliography

Sample	TRIM-04M	TRIM-04N	TRIM-04G	V2410/10	V2403/2	V2403/12	V2403/4	V2414/1	NA-12	TRIM-09
Data Source¹	a	a	new data	b	b	b	b	b	c	d
Volcanic Edifice	Davis	Davis	Davis	Davis	Dogar.	Dogar.	Dogar.	Jaseur	Colúmb.	Vitória
SiO₂	45.77	45.95	45.99	41.74	33.02	39.94	36.85	43.7	33.82	40.58
TiO₂	3.61	3.61	3.676	3.48	5.01	4.39	4.76	3.66	4.67	5.211
Al₂O₃	16.47	16.68	16.73	12.29	12.87	15.53	13.04	16.29	11.9	11
FeOt	10.13	10.07	9.92	11.3	4.6	3.25	6.94	2.44	15.7	13.93
MnO	0.18	0.19	0.193	0.17	0.26	0.19	0.2	0.18	0.45	0.172
MgO	4.11	4.42	4.27	9.62	8.56	5.53	11.22	3	15.11	11.02
CaO	9.31	9.35	9.35	11.27	13.75	10.01	11.62	10.09	15.05	9.89
Na₂O	3.34	3.35	3.3	1.34	1.39	1.87	1.4	3.74	0.7	4.3
K₂O	2.94	2.95	2.94	0.85	0.83	2.19	0.46	1.88	0.4	0.9
P₂O₅	1.04	1.06	1.12	0.66	3.73	0.9	1.34	2.09	1.79	0.63
LOI	1.98	2.16	2.35	2	-	-	-	-	15.1	1
Cr	< 20	< 20	< 20	584.3	668.8	114.1	348.4	12.9	-	370
Co	47	31	34	71.5	70.9	45.1	63.3	15.7	-	82
Ni	< 20	< 20	< 20	370.9	237	162.2	201.7	39.5	265	140
Sc	11	11	11	22.2	21.1	16	10.1	1	-	22
V	260	259	259	306.3	386.7	339.2	369.1	135.6	-	354
Ba	976	985	978	447	415	497	423		385	1011

¹ Data Source:

a

Santos, A.C., 2016. Petrology of Martin Vaz Island and Vitoria-Trindade Ridge Seamounts: Montague, Jaseur, Davis, Dogarossa and Columbia. Trace Elements, ⁴⁰Ar/³⁹Ar Dating and Sr and Nd Isotope Analysis Related to the Trindade Plume Evidence. Ph. D. Thesis. Universidade do Estado do Rio de Janeiro, Brazil.

b

Peyve, A.A., Skolotnev, S.G., 2014. Systematic variations in the composition of volcanic rocks in tectono-magmatic seamount chains in the Brazil Basin. *Geochem. Int.* 52, 111–130. <https://doi.org/10.1134/S0016702914020062>

c

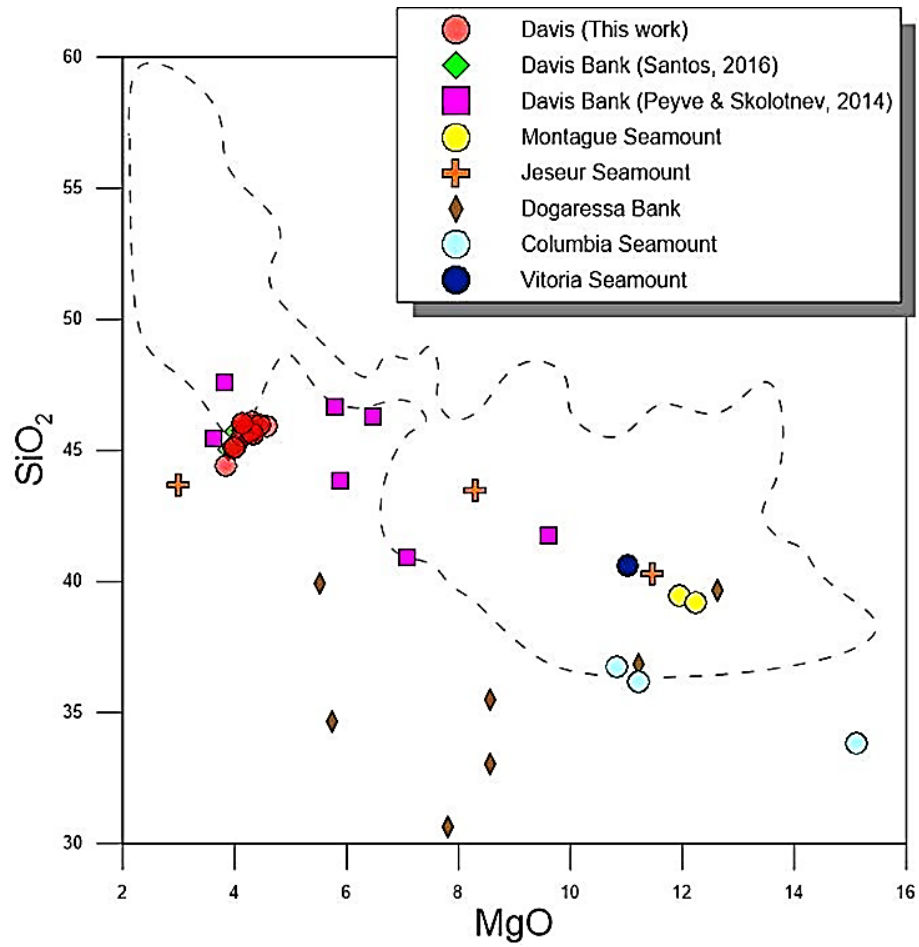
Fodor, R.V., Hanan, B.B., 2000. Geochemical evidence for the Trindade Hotspot trace: Columbia seamount ankaramite. *Lithos* 51, 293–304. [https://doi.org/10.1016/S0024-4937\(00\)00002-5](https://doi.org/10.1016/S0024-4937(00)00002-5).

d

Maia, T.M., Santos, A.C., Rocha-Júnior, E.R.V., Valeriano, C.M., Mendes, J.C., Jeck, I.K., Santos, W.H., Oliveira, A.L., Mohriak, W.U., 2021. First petrologic data for Vitória Seamount, Vitória-Trindade Ridge, South Atlantic: a contribution to the Trindade mantle plume evolution. *Journal of S. Am. Earth Sci.*, V. 109, 103304. <https://doi.org/10.1016/j.jsames.2021.103304>

Sample	TRIM-04M	TRIM-04N	TRIM-04G	V2410/10	V2403/2	V2403/12	V2403/4	V2414/1	NA-12	TRIM-09
Rb	60	58	59	15.4	14.6	45.3	5.1	14.2	1	21
Sr	1147	1145	1159	466	8688	452	2516	1655	985	745
Nb	108	107	109	51.1	64.4	80.8	67.9	142.1	57	68
Zr	423	415	412	220	303	416	330	537	161	237
Y	31	31	32	21	54	36	29	43	33	18
La	82.40	81.30	84.7	36.97	53.73	62.61	49.77	104.22	57.2	37
Ce	166	163	170	79.29	105.47	126.18	104.32	217.59	144.4	82.5
Pr	18.30	18.10	18.5	9.99	13.73	15.85	12.99	27.48	-	10
Nd	70.90	69.60	72.4	41.68	58.36	64.87	53.48	110.9	60.2	42.8
Sm	12.60	12.20	12.9	8.49	11.86	12.75	10.86	21.14	11.2	8.7
Eu	3.74	3.66	3.79	2.75	3.7	3.76	3.14	6.72	3.56	2.67
Gd	9.70	9.50	9.7	7.29	11.03	10.69	9.17	16.44	-	7.1
Tb	1.40	1.40	1.4	1	1.57	1.46	1.28	2.29	1.13	1
Dy	6.90	6.80	7	5.05	8.93	7.71	6.93	12.52	-	4.6
Ho	1.20	1.20	1.3	0.9	1.79	1.41	1.21	2.24	-	0.8
Er	3	3.10	3.2	2.17	4.79	3.63	2.94	5.45	-	1.8
Tm	0.42	0.41	0.42	0.27	0.63	0.47	0.37	0.74	-	0.21
Yb	2.70	2.50	2.6	1.45	3.75	2.69	2.22	4.27	2.05	1.2
Lu	0.40	0.37	0.42	0.2	0.58	0.39	0.31	0.57	0.27	0.18
Hf	8.30	8	8.6	5.39	8.16	9.31	7.88	13.18	-	5.8
Ta	6.70	6.40	6.8	3.46	4.27	5.25	4.56	11.86	-	4.5
U	2.10	2	2.1	1	3.51	2.12	1.28	1.35	-	0.9
Th	8.10	7.90	8.6	3.81	5.73	6.61	5.7	14.52	-	3.6
Pb	<5	<5	<5	-	-	-	-	-	-	-

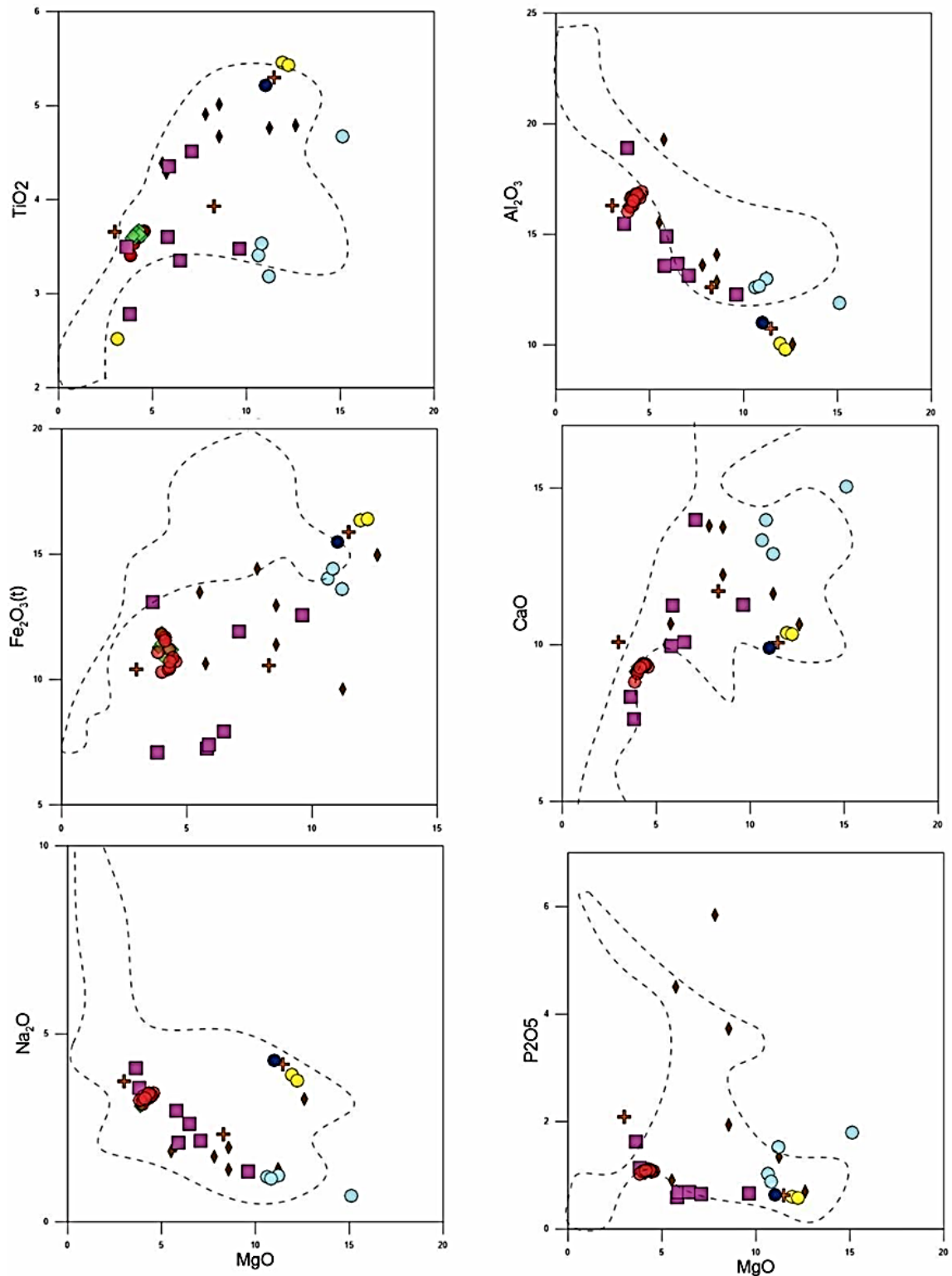
Source: The author, 2022.

Figure 16 - Fenner Variation Diagram for MgO vs. SiO₂ contents

Subtitle: For comparison the graph shows data from the Vitória-Trindade Seamounts from Peyve and Skolotnev (2014), Santos (2016), Jesus *et al.* (2020) and Fodor and Hanan (2000). References and symbols are listed in the figure. The field marked by the dotted line represents rocks from the Trindade and Martin Vaz Islands (Marques *et al.*, 1999; Siebel *et al.*, 2000; Greenwood, 2001; Bongiolo *et al.*, 2015; Santos, 2016, Unpublished data, Santos oral communication).

Source: The author, 2022.

Figure 17 - Fenner variation diagrams for Davis Seamount samples including major elements content

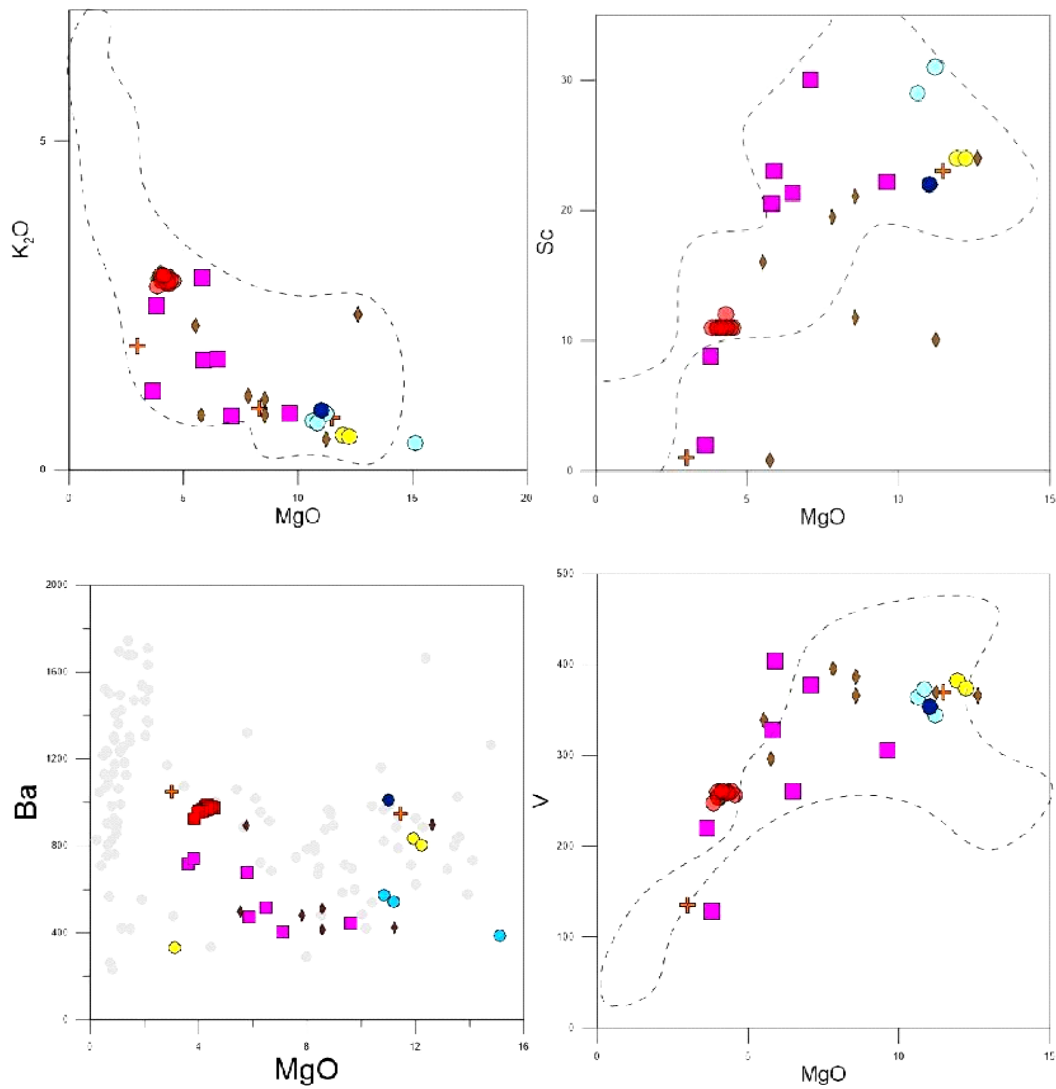


Subtitle: For comparison the graph also shows data from the other Vitoria-Trindade Seamounts from Peyve and Skolotnev (2014), Santos (2016), Jesus *et al.* (2020) and Fodor and Hanan (2000). References and symbols are the same as listed in figure 16. The field marked by the dotted line represents rocks from the Trindade and Martin Vaz Islands (Marques *et al.*, 1999; Siebel *et al.*, 2000; Greenwood, 2001; Bongiolo *et al.*, 2015; Santos, 2016, Unpublished data, Santos oral communication.

Source: The author, 2022.

Although it is difficult to observe a well-defined trend (regarding Davis samples which represent the same plumbing system) in most variation diagrams, a similar pattern as described for major element composition is also evident in compatible trace element composition of Davis Bank rocks in comparison to the other seamounts of the region, as seen in V (*ca.* 258 ppm) and Sc (*ca.* 11 ppm) plotted against MgO, while Ba contents show scatter pattern when plotted against MgO (Figure 18). Plots of trace elements against Th (used as a fractionation index; *e.g.* WEAVER, 1990; MARQUES *et al.*, 1999) illustrates the behavior of these elements (Figure 19). This is a useful trace element since it is a very incompatible element that has very low concentrations in sea water and is largely unaffected by seawater interaction or secondary alteration, as well as Nb, and La (WEAVER, 1991). As can be seen in figure 19 there is a strong positive correlation between Th and Zr, La, U and Ta for almost all seamounts' samples and some samples from the islands. The contents of Y also show positive correlation against Th contents for most seamounts and some samples from the islands, although with higher deviation from Montague Seamount and Dogaressa Bank. It is noteworthy that picrites from Dogaressa Bank (PEYVE; SKOLOTNEV, 2014) that deviate more in relation to the other volcanic edifices have anomalous chemical characteristics like very high P content and extremely high Sr isotopic ratios and were interpreted by these authors as being contaminated in the intermediate magma chamber by seawater. Similarly, one Montague Seamount sample (unpublished, SANTOS oral communication) that deviates significantly in some plots (Y vs. Th and U vs. Th) has an extremely high LOI (*ca.* 16) value with extremely high Sr isotopic ratios, probably from contamination of seawater as well. Thus, both samples should be disregarded.

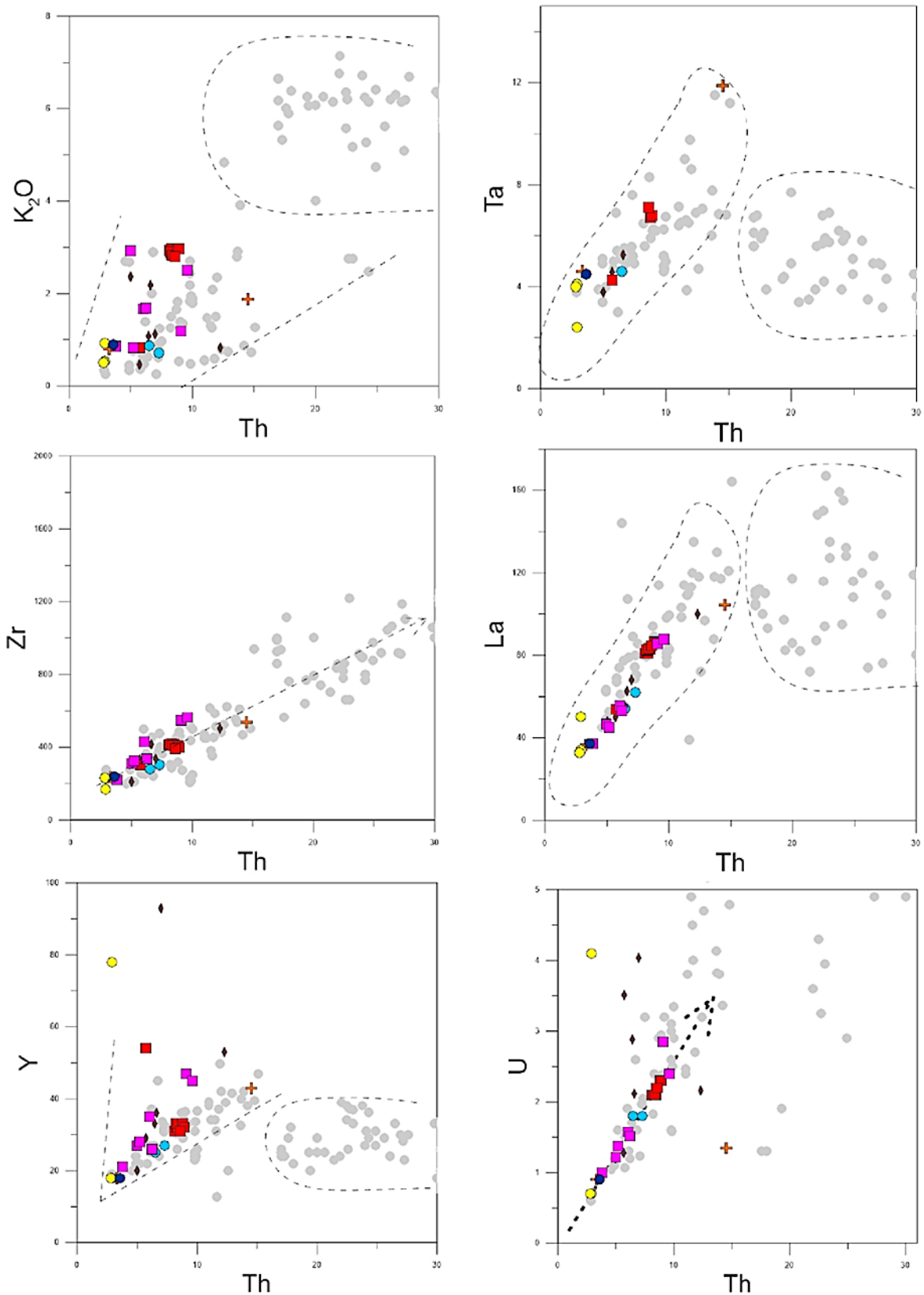
Figure 18 - Variation diagram between MgO (wt. %) and K₂O, V and Sc for Davis Seamount samples



Subtitle: For comparison the graph also shows data from the other Vitoria-Trindade Seamounts from Peyve and Skolotnev (2014), Santos (2016), Jesus *et al.* (2020) and Fodor and Hanan (2000). References and symbols are the same as listed in figure 16. The field marked by the dotted line represents rocks from the Trindade and Martin Vaz Islands (Marques *et al.*, 1999; Siebel *et al.*, 2000; Greenwood, 2001; Bongiolo *et al.*, 2015; Santos, 2016, Unpublished data, Santos oral communication).

Source: The author, 2022.

Figure 19 - Binary variation diagram between trace elements (ppm) and K₂O (wt.%) vs. Th (ppm) for the different alkaline rocks of Vitória-Trindade Ridge



Subtitle: Samples from VTR are from (Fodor and Hanan, 2000; Peyve and Skolotnev, 2014; Santos, 2016; Jesus *et al.*, 2019; Maia *et al.*, 2021). References and symbols are the same as listed in figure 16. The grey circles represent rocks from the Trindade and Martin Vaz Islands (Marques *et al.*, 1999; Siebel *et al.*,

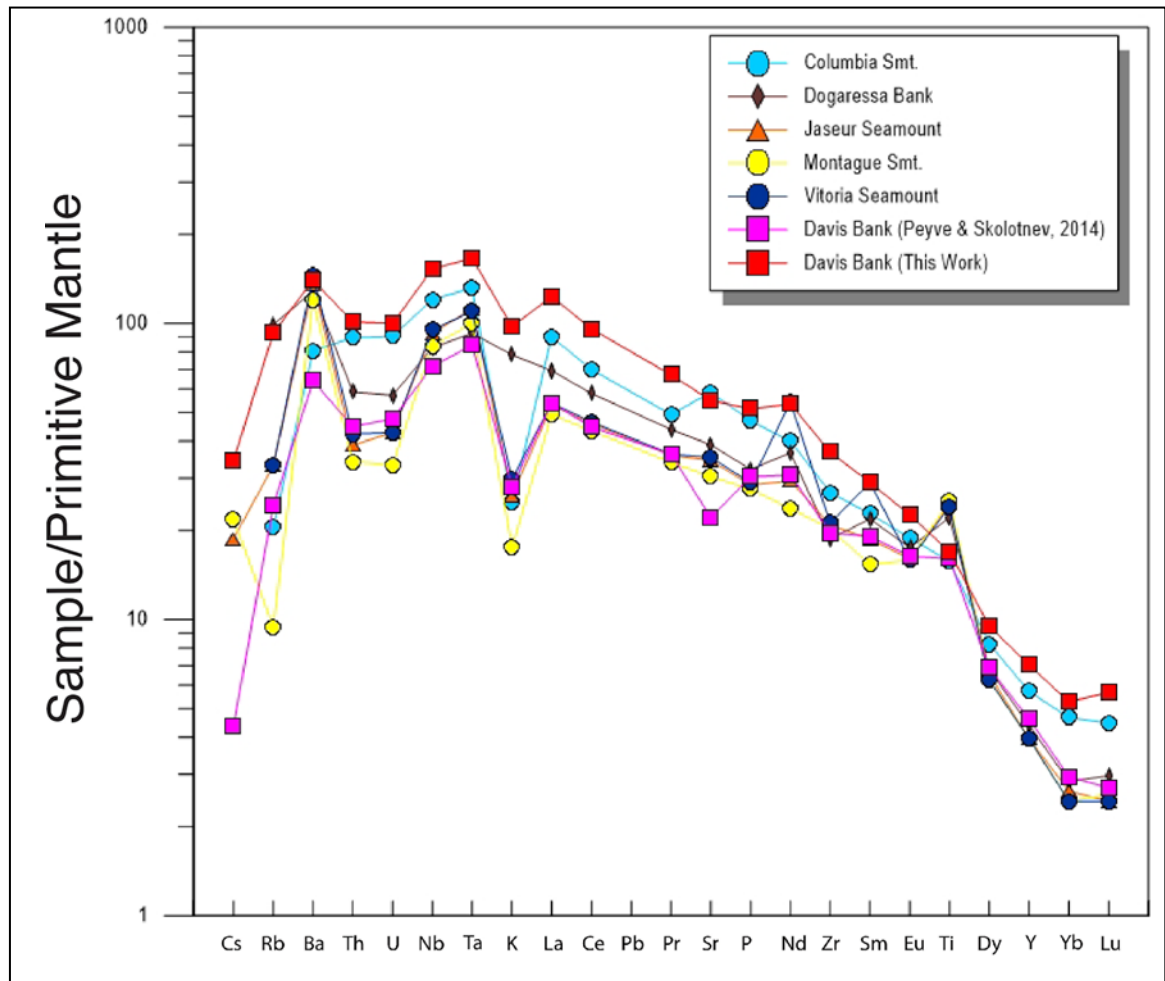
2000; Greenwood, 2001; Bongiolo *et al.*, 2015; Santos, 2016, Unpublished data, Santos oral communication).

Source: The author, 2022.

Figure 20 depicts the pattern of the trace elements in the Sun and McDonough (1989) primitive mantle-normalized spider diagram for Davis Bank basanite (this work) and picrobasalt (Peyve and Skolotnev, 2014), Vitória Seamount alkali basalt (MAIA *et al.*, 2021) and the other volcanic rocks from the submarine edifices for comparison. Davis Bank basanite has the most enriched pattern from all other seamounts and banks. The most differentiated samples from Davis Bank have the highest values of incompatible trace elements such as Zr (407–419 ppm) and La (80.4–83.9 ppm). Davis lava with higher SiO₂ and lower MgO content presents high to moderately incompatible trace elements (Ba *ca.* 972 ppm; La *ca.* 82 ppm; Rb *ca.* 57 ppm; Nb *ca.* 107 ppm; Zr *ca.* 412 ppm; Ce *ca.* 166 ppm; Sr *ca.* 1149 ppm; Th *ca.* 8.33 ppm) higher than picrobasalt from Davis Bank with lower SiO₂ and higher MgO (Ba *ca.* 455 ppm; La *ca.* 45 ppm; Rb *ca.* 24 ppm; Nb *ca.* 61 ppm; Zr *ca.* 293 ppm; Ce *ca.* 95 ppm; Sr *ca.* 580 ppm; Th *ca.* 5.08 ppm; Peyve and Skolotnev, 2014) which is also consistent with REE behavior pattern (Figure 21). The Vitória Seamount alkali basalt trace element composition (MAIA *et al.*, 2021) is more similar to less differentiated Davis Bank picrobasalt (Peyve and Skolotnev, 2014) presenting lower concentration of incompatible trace elements (such as Zr *ca.* 237 ppm; La *ca.* 37 ppm; Nb *ca.* 68 ppm), with exception for Ba content (*ca.* 1011 ppm) which is higher than Davis Bank's more evolved lava.

VTR rocks present positive Nb-Ta signal with depletion of K contents, much more evident in Vitória Seamount sample (MAIA *et al.*, 2021) and in the less differentiated picrobasalt sample from Peyve and Skolotnev (2014). This strong Nb-Ta signal and strong depletion in K and Rb contents is also more evident in other seamounts such as the melanephelinite from Montague Seamount. A positive Ba anomaly is also present in all samples investigated, especially in the Vitória Seamount alkali basalt (MAIA *et al.*, 2021), but less prominent in Davis Bank basanite analyzed in this work.

Figure 20 - Trace-element spider diagram normalized to primitive mantle (Sun and Mcdonough, 1989) for Davis Bank and other Vitória-Trindade Ridge seamounts



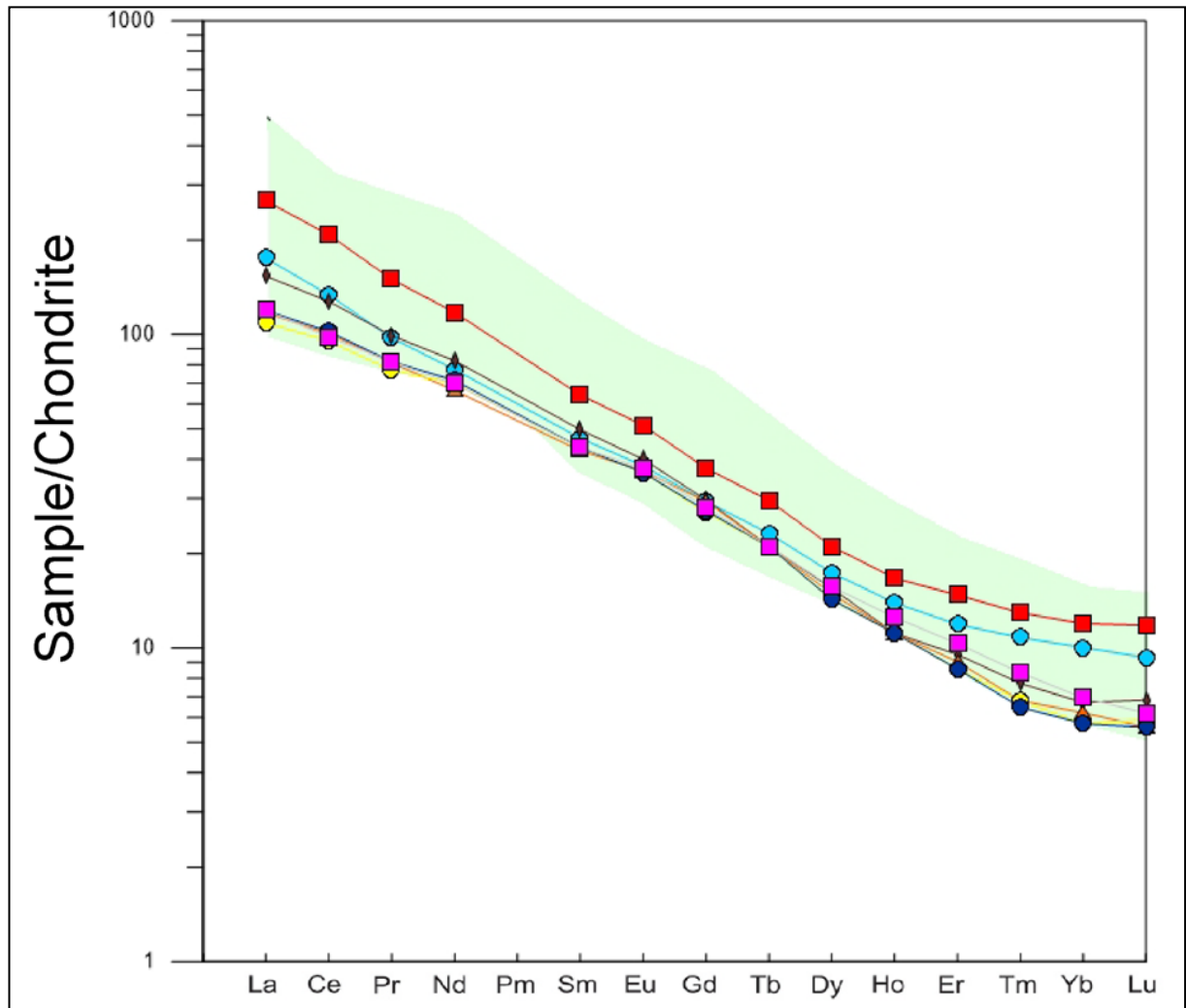
Source: The author, 2022.

Figure 21 shows Boynton (1984) Chondrite-normalized REE diagram for Davis Bank basanite from this work compared with one micro-basalt sample from Peyve and Skolotnev (2014), the alkali basalt from Maia *et al.* (2021) and the other rocks from the seamounts and the islands. Both Davis Bank basanite and micro-basalt samples and VTS alkaline basalt show a pattern with a stronger enrichment in LREE ($La/Sm_N = 4.1$ and $La/Yb_N = 22.5$; $La/Sm_N = 2.7$ and $La/Yb_N = 17.72$; $La/Sm_N = 2.68$ and $Sm/Yb = 7.25$, respectively; PEYVE; SKOLOTNEV, 2014; MAIA *et al.*, 2021) than HREE typical of alkaline rocks (FODOR; HANAN, 2000), as from other lavas from the Vitória-Trindade Ridge.

The difference in their patterns reflects difference in degree of differentiation, being the more strongly differentiated basanite ($MgO = 4.56$; TRIM-04F) the one with the higher enriched pattern and the least differentiated micro-basalt ($MgO = 9.62$; V2410/10; PEYVE; SKOLOTNEV, 2014) the one with lower enriched pattern. They may originate from each other by fractional crystallization. Davis Bank basanite La/Sm_N ratio similar to other alkaline

rocks such as Trindade Island ($\text{La/SmN} = 3$; $\text{La/YbN} = 25$ – unpublished data), Martin Vaz Archipelago ($\text{La/SmN} = 4$; $\text{La/YbN} = 32$; SANTOS *et al.*, 2018) and differs strongly from a ‘normal’ MORB (La/SmN ca. 0.50; REGELOUS *et al.*, 2009).

Figure 21 – Chondrite-normalized REE diagrams (values from Boynton, 1984) for the different alkaline rocks of Vitória-Trindade Ridge



Subtitle: Data sources and symbols as in Fig. 16. Green Field represents REE pattern of volcanic rocks from Trindade and Martin Vaz Islands (Marques *et al.*, 1999; Siebel *et al.*, 2000; Greenwood, 2001; Bongiolo *et al.*, 2015; Santos, 2016, Unpublished data, Santos oral communication).

Source: The author, 2022.

5.3 Sr-Nd-Pb-Hf isotopes

The bulk rock Sr-Nd-Pb-Hf isotopic compositions of the Davis Bank, as well as those of the Vitória seamount, are distinct from that of the depleted mantle and differ from the other seamounts and islands from the VTR, which are a little less enriched. The $^{87}\text{Sr}/^{86}\text{Sr}$ values of volcanic rocks of the Davis Bank range from 0.704014 to 0.704036, which are similar to the Vitória Seamount (0.704054 and 0.704031; MAIA *et al.*, 2021) and are at the higher end of the range defined by other VTR samples (0.703611– 0.704130; HALLIDAY *et al.*, 1992, MARQUES *et al.*, 1999, FODOR; HANAN, 2000; SIEBEL *et al.*, 2000; BONGIOLO *et al.*, 2015; SKOLOTNEV; PEIVE, 2017; SANTOS *et al.*, 2018a). In addition, they have a more radiogenic composition than the Abrolhos Volcanic Complex (AVC; 0.703607– 0.703946; FODOR *et al.*, 1989). The Davis Bank rocks have a $^{143}\text{Nd}/^{144}\text{Nd}$ signature ranging from 0.512622 and 0.512636, which expressed as ϵNd range from - 0.3 to 0 (chondritic signature), and are also similar to those of the Vitória Seamount (MAIA *et al.*, 2021) and slightly less radiogenic than those reported previously for the other VTR volcanic edifices ($^{143}\text{Nd}/^{144}\text{Nd} = 0.51272\text{--}0.512879$, $\epsilon\text{Nd} = \text{ca. } 3.028$; HALLIDAY *et al.*, 1992, MARQUES *et al.*, 1999, FODOR; HANAN, 2000; SIEBEL *et al.*, 2000; BONGIOLO *et al.*, 2015; SKOLOTNEV; PEIVE, 2017; SANTOS *et al.*, 2018a; and unpublished data).

In the $^{87}\text{Sr}/^{86}\text{Sr}$ versus $^{143}\text{Nd}/^{144}\text{Nd}$ space (Figure 22), Davis Bank samples deviate significantly from the depleted mantle array and from other VTR samples, trending towards an EMI-like end-member, as was also identified by Maia *et al.* (2021) for Vitória Seamount. The alkali basalt from Vitória Seamount (MAIA *et al.*, 2021) and one Martin Vaz melanephelinite sample (SANTOS *et al.*, 2018a) show Nd isotopic signature similar to those of Davis Bank (Table 4).

Table 4 – Sr - Nd - Pb isotope ratios of the Vitória-Trindade Ridge

Sample	Data Source ²	Volcanic Edifice	$^{87}\text{Sr}/^{86}\text{Sr}$	$\pm 2\sigma$	$^{143}\text{Nd}/^{144}\text{Nd}$	$\pm 2\sigma$	$^{206}\text{Pb}/^{204}\text{Pb}$	$\pm 2\sigma$	$^{207}\text{Pb}/^{204}\text{Pb}$	$\pm 2\sigma$	$^{208}\text{Pb}/^{204}\text{Pb}$	$\pm 2\sigma$
--------	--------------------------	------------------	---------------------------------	---------------	-----------------------------------	---------------	-----------------------------------	---------------	-----------------------------------	---------------	-----------------------------------	---------------

² Data Source:

a

Fodor, R.V., Hanan, B.B., 2000. Geochemical evidence for the Trindade Hotspot trace: Columbia seamount ankaramite. *Lithos* 51, 293–304. [https://doi.org/10.1016/S0024-4937\(00\)00002-5](https://doi.org/10.1016/S0024-4937(00)00002-5).

b

Peyve, A.A., Skolotnev, S.G., 2014. Systematic variations in the composition of volcanic rocks in tectono-magmatic seamount chains in the Brazil Basin. *Geochem. Int.* 52, 111–130. <https://doi.org/10.1134/S0016702914020062>

c

Maia, T.M., Santos, A.C., Rocha-Júnior, E.R.V., Valeriano, C.M., Mendes, J.C., Jeck, I.K., Santos, W.H., Oliveira, A.L., Mohriak, W.U., 2021. First petrologic data for Vitória Seamount, Vitória-Trindade Ridge, South Atlantic: a contribution to the Trindade mantle plume evolution. *Journal of S. Am. Earth Sci.*, V. 109, 103304. <https://doi.org/10.1016/j.jsames.2021.103304>

d

Siebel, W., Becchio, R., Volker, F., Hansen, M.A.F., Viramonte, J., Trumbull, R.B., Haase, G., Zimmer, M., 2000. Trindade and Martin Vaz islands, South Atlantic: isotopic (Sr, Nd, Pb) and trace element constraints on plume related magmatism. *J. S. Am. Earth Sci.* 13, 79–103. [https://doi.org/10.1016/S0895-9811\(00\)00015-8](https://doi.org/10.1016/S0895-9811(00)00015-8)

e

Halliday, A.N., Davies, G.R., Lee, D.C., Tommasini, S., Oaslick, C.R., Fitton, J.G., James, D.E., 1992. Lead isotope evidence for young trace element enrichment in the oceanic upper mantle. *Nature* 359, 623–627. <https://doi.org/10.1038/359623a0>

f

Marques, L.S., Ulbrich, M.N.C., Ruberti, E., Tassinari, C.G., 1999. Petrology, geochemistry and Sr-Nd isotopes of the trindade and Martin Vaz volcanic rocks (southern Atlantic Ocean). *J. Volcanol. Geoth. Res.* 93, 191–216. [https://doi.org/10.1016/S0377-0273\(99\)00111-0](https://doi.org/10.1016/S0377-0273(99)00111-0).

Sample	Data Source ₂	Volcanic Edifice	⁸⁷ Sr/ ⁸⁶ Sr	± 2σ	¹⁴³ Nd/ ¹⁴⁴ Nd	± 2σ	²⁰⁶ Pb/ ²⁰⁴ Pb	± 2σ	²⁰⁷ Pb/ ²⁰⁴ Pb	± 2σ	²⁰⁸ Pb/ ²⁰⁴ Pb	± 2σ
TRIM-04M		Davis Bank	0.704014	0	0.512622	0.000009						
TRIM-04N		Davis Bank	0.704036	5	0.512636	0.000004						
TRIM-04G		Davis Bank					19.1459	0.0008	15.585	0.0008	39.321	0.002
NA-12	a	Colúmbia Seamount	0.7039		0.512786		19.19		15.045		39.242	
V2403/2	b	Dogaressa Bank	0.70869		0.51275		19.4254		15.595		39.3818	
V2403/12	b	Dogaressa Bank	0.70413		0.51272		19.0116		15.5902		39.0813	
V2403/4	b	Dogaressa Bank	0.70775		0.51277		19.3465		15.6171		39.486	
V2414/1	b	Jaseur Seamount	0.70405		0.51277							
TRIM-09B1	c	Vitória Seamount	0.704031	0.000007	0.512635	0.000003						
TRIM-09B2	c	Vitória Seamount	0.704054	0.000005	0.512629	0.000004						
10745	d	Trindade Island	0.703766	0.000008	0.512837	0.000006	19.012	0.003	15.574	0.004	38.924	0.012

g

Bongiolo, E.M., Pires, G.L.C., Geraldes, M.C., Santos, A.C., Neumann, R., 2015. Geochemical modeling and Nd-Sr data links nephelinite-phonolite successions and xenoliths of Trindade Island (South Atlantic Ocean, Brazil). *J. Volcanol. Geoth. Res.* 306, 58–73. <https://doi.org/10.1016/j.jvolgeores.2015.10.002>

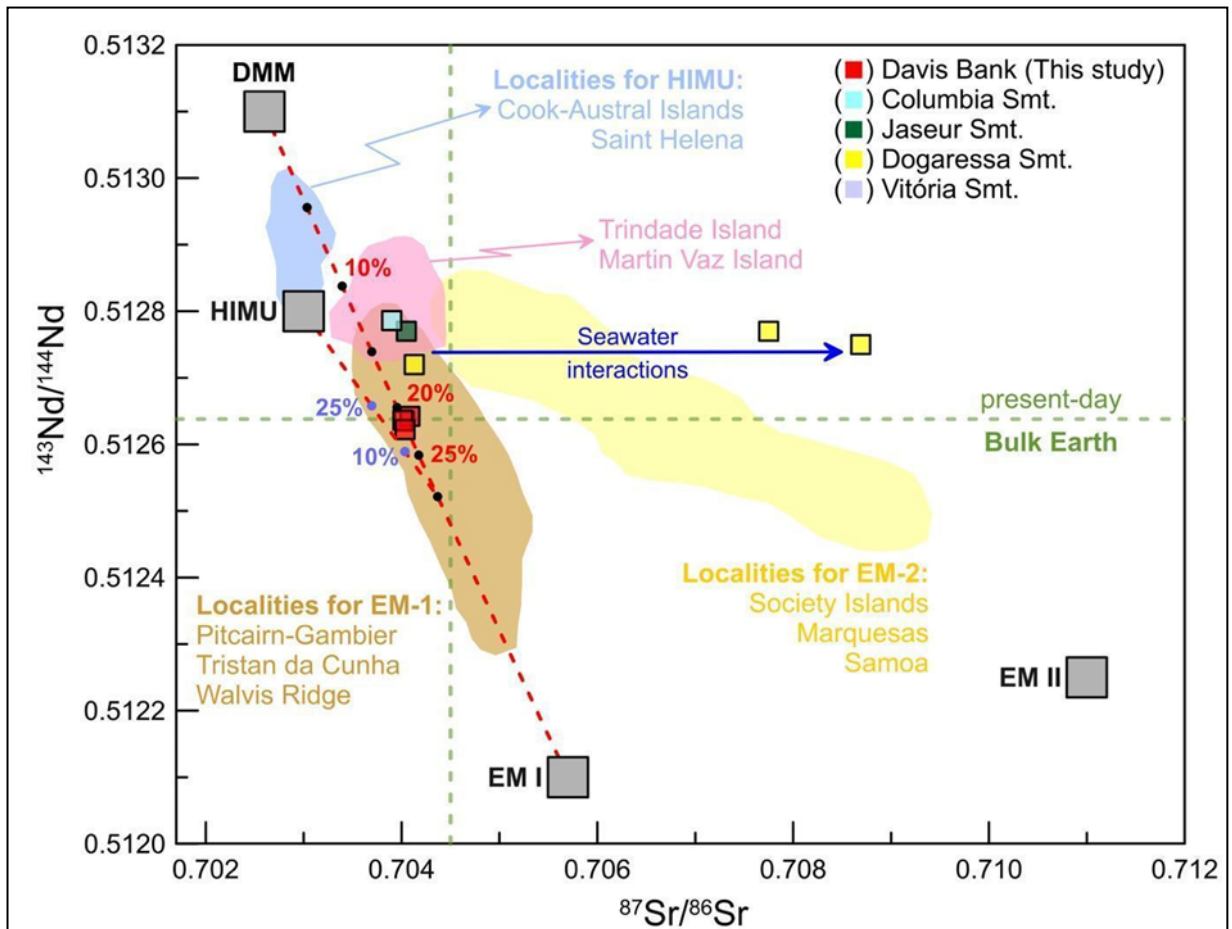
h

Santos, A.C., Geraldes, M.C., Siebel, W., Mendes, J., Bongiolo, E., Santos, W.H., Garrido, T.C.V., Rodrigues, S.W.O., 2018a. Pleistocene alkaline rocks of Martin Vaz volcano, South Atlantic: low-degree partial melts of a CO₂-metasomatized mantle plume. *Int. Geol. Rev.* 61, 296–313. <https://doi.org/10.1080/00206814.2018.1425921>

Sample	Data Source ₂	Volcanic Edifice	⁸⁷ Sr/ ⁸⁶ Sr	± 2σ	¹⁴³ Nd/ ¹⁴⁴ Nd	± 2σ	²⁰⁶ Pb/ ²⁰⁴ Pb	± 2σ	²⁰⁷ Pb/ ²⁰⁴ Pb	± 2σ	²⁰⁸ Pb/ ²⁰⁴ Pb	± 2σ
10764	d	Trindade Island	0.703896	0.00000 9	0.512784	0.000007	19.241	0.002	15.591	0.003	39.239	0.00 9
10763	d	Trindade Island	0.703898	0.00000 8	0.512774	0.000007	19.179	0.001	15.578	0.002	39.140	0.00 4
10761	d	Trindade Island	0.703828	0.00000 9	0.512752	0.000008	19.209	0.008	15.588	0.008	39.199	0.02 5
Hit-4	d	Trindade Island	0.703860	0.00001 0	0.512787	0.000007	19.274	0.007	15.579	0.007	39.221	0.02 5
10770	d	Trindade Island	0.703961	0.00000 8	0.512762	0.000011	19.220	0.005	15.576	0.005	39.172	0.01 7
10771	d	Trindade Island	0.703861	0.00001 2	0.512777	0.000013	19.208	0.002	15.561	0.002	39.116	0.00 9
10769	d	Trindade Island	0.703915	0.00000 8	0.512799	0.000006	19.170	0.001	15.578	0.002	39.165	0.00 5
10759	d	Trindade Island	0.703837	0.00000 8	0.512815	0.000005	19.228	0.003	15.584	0.004	39.203	0.01 4
TD3	e	Trindade Island	0.703611	0.00001 1	0.512762	0.000008	19.047		15.564		38.816	
TD4	e	Trindade Island	0.703804	0.00001 3	0.512772	0.000008	19.143		15.535		39.023	
TD5	e	Trindade Island	0.703837	0.00009	0.512799	0.000009	19.152		15.523		39.02	
TR-80	f	Trindade Island	0.70374	0.00011	0.51279	0.000043						
TR-93	f	Trindade Island	0.70372	0.00011	0.512869	0.000038						
TR-98	f	Trindade Island	0.70364	0.00011	0.512826	0.000042						
EMB-02A	g	Trindade Island	0.704072	0.00000 6	0.512768	0.000004						
EMB-04A	g	Trindade Island	0.704251	0.00000 5	0.512762	0.000005						
EMB-06A	g	Trindade Island	0.703795	0.00000 9	0.51277	0.000005						

Sample	Data Source ₂	Volcanic Edifice	⁸⁷ Sr/ ⁸⁶ Sr	± 2σ	¹⁴³ Nd/ ¹⁴⁴ Nd	± 2σ	²⁰⁶ Pb/ ²⁰⁴ Pb	± 2σ	²⁰⁷ Pb/ ²⁰⁴ Pb	± 2σ	²⁰⁸ Pb/ ²⁰⁴ Pb	± 2σ
EMB-09A	g	Trindade Island	0.703693	5	0.512792	0.000006						
EMB-11A	g	Trindade Island	0.704182	5	0.512842	0.000002						
EMB-14A	g	Trindade Island	0.703918	9	0.512754	0.000005						
EMB-15A	g	Trindade Island	0.703761	7	0.512759	0.000006						
EMB-16A	g	Trindade Island	0.704209	7	0.512764	0.000006						
EMB-19A	g	Trindade Island	0.703826	8	0.51277	0.000007						
MV2	f	Martin Vaz Archipelago	0.70364	0.00011	0.512879	0.000039						
10774	d	Martin Vaz Archipelago	0.703907	0.00008	0.512788	0.000005	19.276	0.003	15.596	0.003	39.252	0.008
10773	d	Martin Vaz Archipelago	0.704207	0.00011	0.512785	0.000007	19.325	0.004	15.599	0.005	39.340	0.007
MVA-01	h	Martin Vaz Archipelago	0.703690	8	0.512773	0.000007						
MVA-05A	h	Martin Vaz Archipelago	0.703871	0	0.512788	0.000007						
MVA-10	h	Martin Vaz Archipelago	0.703946	7	0.512784	0.000007						
MVA-12	h	Martin Vaz Archipelago	0.703774	9	0.512627	0.000008						

Figure 22 - Plot of ternary mixing calculations between DMM, EMI and HIMU-type pyroxenite to describe $^{87}\text{Sr}/^{86}\text{Sr}$ and $^{143}\text{Nd}/^{144}\text{Nd}$ isotopic variability of Davis bank and other VTR rocks

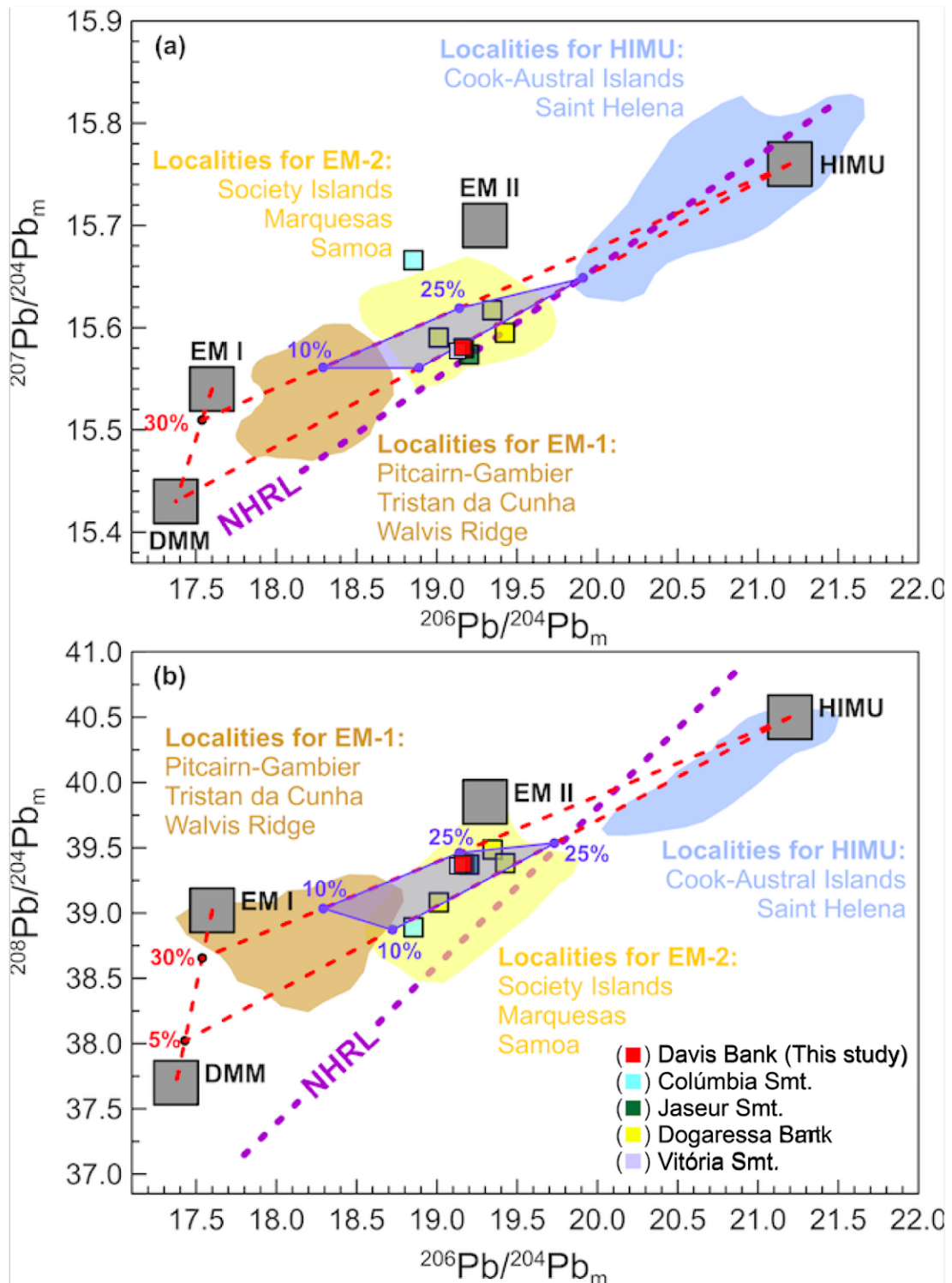


Subtitle: Modeling assumes three-component mixing between asthenospheric mantle (represented by DMM; $^{87}\text{Sr}/^{86}\text{Sr} = 0.7026$, $[\text{Sr}] = 160 \mu\text{g/g}$, $^{143}\text{Nd}/^{144}\text{Nd} = 0.5131$, $[\text{Nd}] = 9.6 \mu\text{g/g}$), EMI ($^{87}\text{Sr}/^{86}\text{Sr} = 0.7057$, $[\text{Sr}] = 495 \mu\text{g/g}$, $^{143}\text{Nd}/^{144}\text{Nd} = 0.5121$, $[\text{Nd}] = 30.6 \mu\text{g/g}$) and HIMU-type pyroxenite ($^{87}\text{Sr}/^{86}\text{Sr} = 0.7030$, $[\text{Sr}] = 757 \mu\text{g/g}$, $^{143}\text{Nd}/^{144}\text{Nd} = 0.5128$, $[\text{Nd}] = 45.7 \mu\text{g/g}$). The parameters for the DMM, EMI, EMII and HIMU are from Zindler and Hart (1986), Salters and Stracke (2004), Workman and Hart (2005), Jackson and Dasgupta (2008), Gurenko *et al.* (2009), Hofmann (2014) and Marques *et al.* (2018). The Sr and Nd contents of the EMI and HIMU end-members are based on data from the GEOROC database (<http://georoc.mpch-mainz.gwdg.de/georoc/>), whereas for the melt DMM, the Sr and Nd contents were calculated considering a partial melting degree of *ca.* 3% (based on the study by Maia *et al.*, 2021; bulk $D_{\text{Sr}} = 0.0185$ and $D_{\text{Nd}} = 0.0317$).

Source: The author, 2022.

Lead isotopic analysis yielded moderately radiogenic ratios of $^{206}\text{Pb}/^{204}\text{Pb} = 19.146$, $^{207}\text{Pb}/^{204}\text{Pb} = 15.585$ and $^{208}\text{Pb}/^{204}\text{Pb} = 39.321$. The following $^{207}\text{Pb}/^{204}\text{Pb}$ versus $^{206}\text{Pb}/^{204}\text{Pb}$ and $^{208}\text{Pb}/^{204}\text{Pb}$ versus $^{206}\text{Pb}/^{204}\text{Pb}$ correlation diagrams (Figure 23) show the isotopic compositions of the analyzed samples plotted together with the previously published data from VTR and the fields for South Atlantic plume-related rocks, for comparison. On Pb isotope correlation diagrams, Davis Bank Pb isotopic signature matches most data from VTR (HALLIDAY *et al.*, 1992; SIEBEL *et al.*, 2000; FODOR AND HANAN, 2000; PEYVE; SKOLOTNEV, 2014), and all these samples plot above the Northern Hemisphere Reference Line (NHRL; HART, 1984), with $\Delta 7/4 = 1.1$ and $\Delta 8/4 = 57.5$ for the Davis Bank. The $^{206}\text{Pb}/^{204}\text{Pb}$ ratio correlates positively with $^{208}\text{Pb}/^{204}\text{Pb}$ ratios ($r^2 = 0.84$) and less significantly with $^{207}\text{Pb}/^{204}\text{Pb}$ even when an outside Colúmbia seamount is discarded ($r^2 = 0.34$), for samples from Davis Bank and other VTR rocks.

Figure 23 - Plot of ternary mixing calculations between DMM, EMI and HIMU-type pyroxenite to describe measured (m) $^{206}\text{Pb}/^{204}\text{Pb}$, $^{207}\text{Pb}/^{204}\text{Pb}$ and $^{208}\text{Pb}/^{204}\text{Pb}$ isotopic variability of Davis bank and other VTR rocks



Subtitle: Modeling assumes three-component mixing between asthenospheric mantle (represented by DMM; $^{206}\text{Pb}/^{204}\text{Pb} = 17.375$, $^{207}\text{Pb}/^{204}\text{Pb} = 15.430$, $^{208}\text{Pb}/^{204}\text{Pb} = 37.700$, $[\text{Pb}] = 0.46 \mu\text{g/g}$), EMI ($^{206}\text{Pb}/^{204}\text{Pb} = 17.600$, $^{207}\text{Pb}/^{204}\text{Pb} = 15.540$, $^{208}\text{Pb}/^{204}\text{Pb} = 39.020$, $[\text{Pb}] = 2.82 \mu\text{g/g}$) and HIMU-type pyroxenite ($^{206}\text{Pb}/^{204}\text{Pb} = 21.200$, $^{207}\text{Pb}/^{204}\text{Pb} = 15.760$, $^{208}\text{Pb}/^{204}\text{Pb} = 40.500$, $[\text{Pb}] = 2.73 \mu\text{g/g}$). The parameters for the DMM, EMI, EMII and HIMU are from Zindler and Hart (1986), Salters and Stracke (2004), Workman and Hart (2005), Jackson and Dasgupta (2008), Gurenko *et al.* (2009), Hofmann (2014) and Marques *et al.* (2018). The Pb content of the EMI and HIMU end-members are based on data from the GEOROC database (<http://georoc.mpch-mainz.gwdg.de/georoc/>), whereas for the melt

DMM, the Pb content was calculated considering a partial melting degree of *ca.* 3% (based on the study by Maia *et al.*, 2021; $D_{Pb} = 0.0092$).

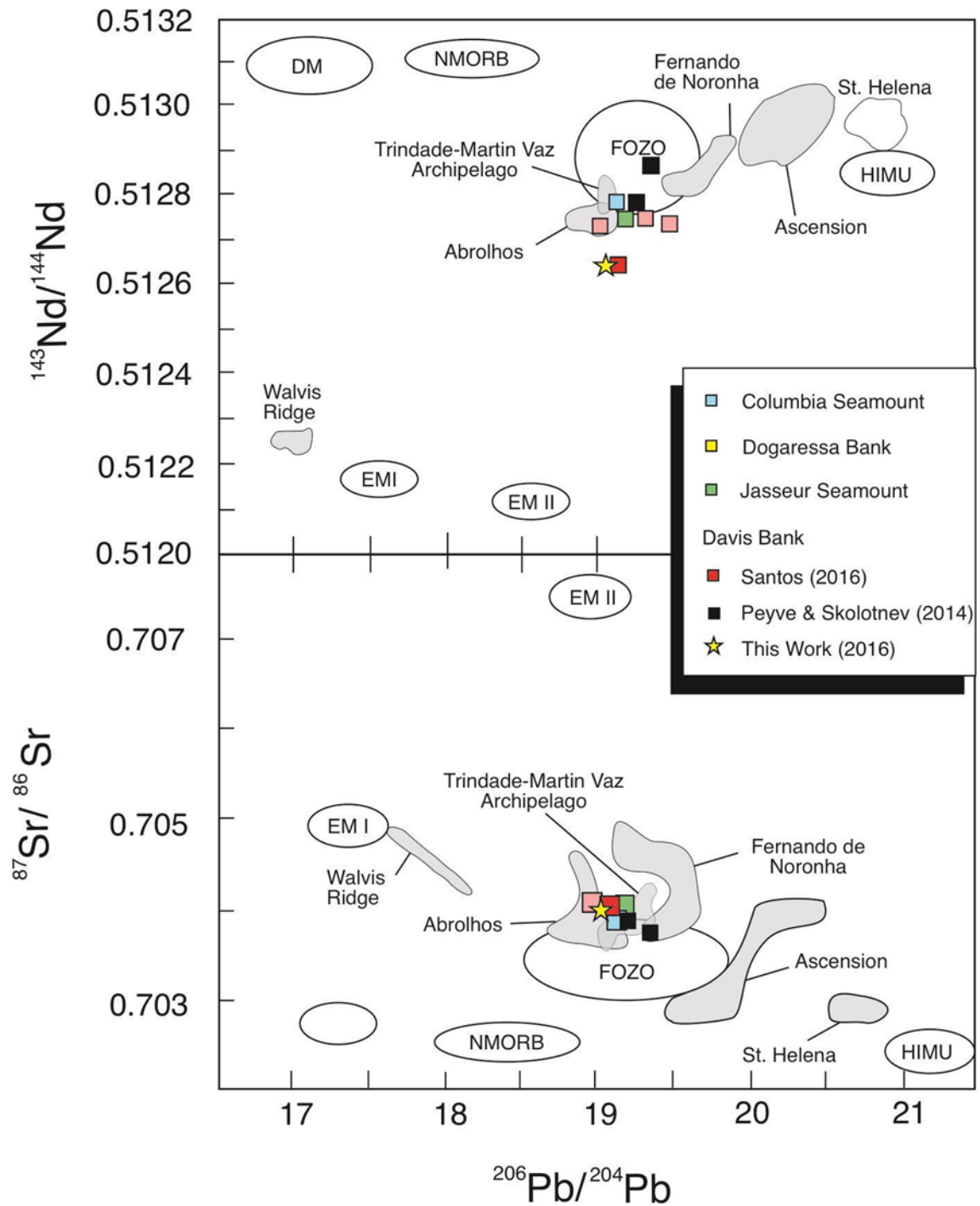
Source: The author, 2022.

The $^{87}\text{Sr}/^{86}\text{Sr}$ *versus* $^{206}\text{Pb}/^{204}\text{Pb}$ correlation diagram (Figure 24) highlights the proximity in values yielded for all VTR for these isotopic systems. Notwithstanding, when observing $^{143}\text{Nd}/^{144}\text{Nd}$ *versus* $^{206}\text{Pb}/^{204}\text{Pb}$ correlation diagram (Figure 24) Davis bank isotopic composition shows significant variation, suggesting that what caused the enrichment in unradiogenic Nd did not significantly affect Sr-Pb isotopic systems.

The three-dimensional Sr–Nd–Pb-isotope diagram permits the identification of EM I as the third component of the VTR mantle source, whereas EM II does not appear to contribute to the source composition (Figure 25). This diagram is useful in distinguishing between EM I and EM II on multicomponent mixtures (MATA *et al.*, 1998).

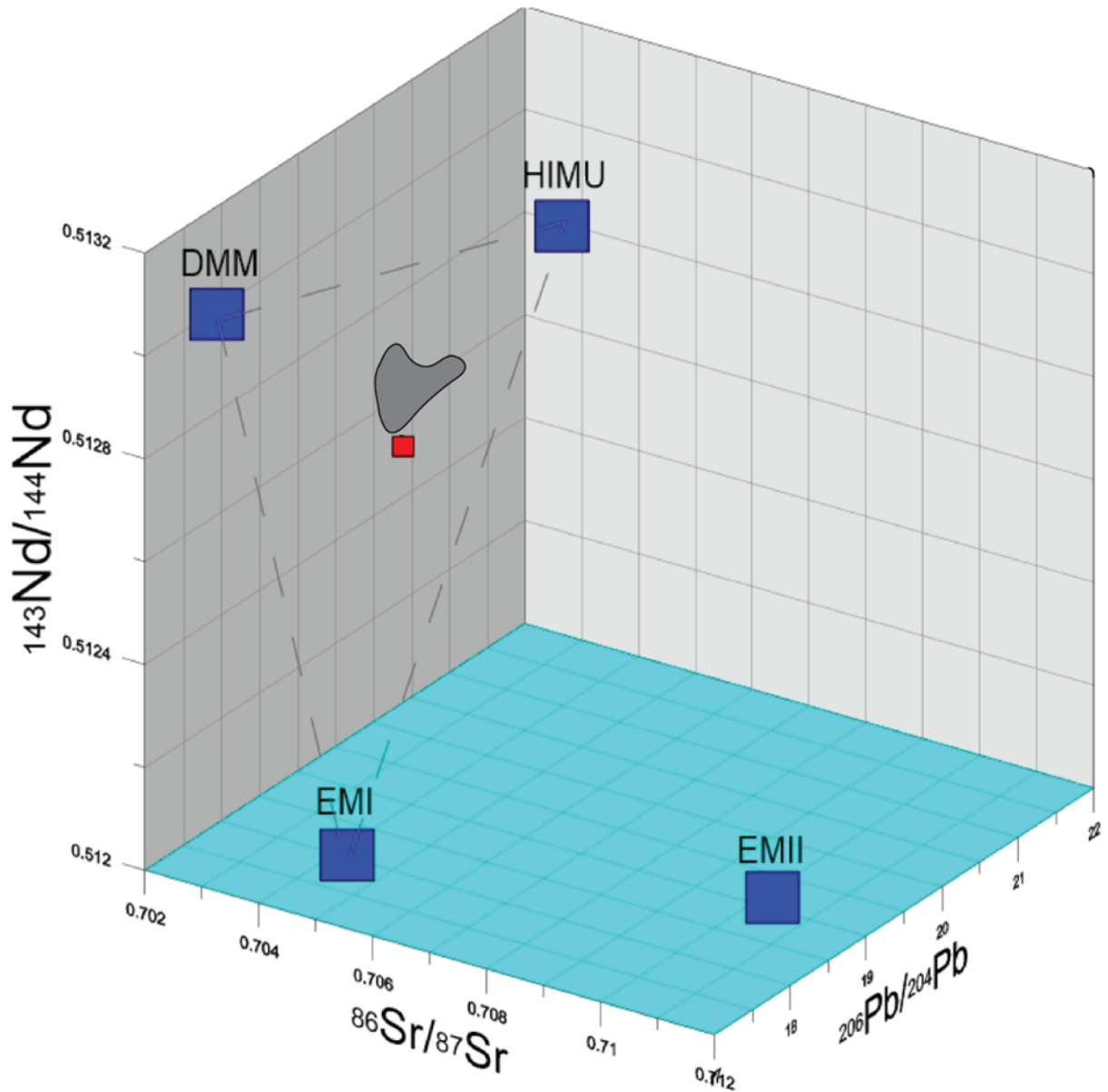
Two Hf isotopic ratios were obtained from Davis Bank, one from a duplicate sample. There is no data available on $^{176}\text{Hf}/^{177}\text{Hf}$ for the VTR and data from other hotspots from the South Atlantic are scarce, making it harder to draw comparisons with the other volcanic features. Similarly to what is registered by the Nd isotopic system, $^{176}\text{Hf}/^{177}\text{Hf}$ of samples from Davis Bank (0.282834 and 0,282766) from this work are significantly unradiogenic when compared to the VTR (SANTOS, unpublished data), plotting beneath the Nd–Hf mantle array. As can be seen in the Hf-Nd diagram (Figure 26), the samples also deviate from the depleted component and tend towards an EMI-like end-member, analogous to what is seen in the Sr-Nd diagram (Figure 22). Davis Bank samples are more enriched in unradiogenic Hf while $^{206}\text{Pb}/^{204}\text{Pb}$ remains constant compared to other samples from the VTR as can be seen in $^{176}\text{Hf}/^{177}\text{Hf}$ *versus* $^{206}\text{Pb}/^{204}\text{Pb}$ diagram (Figure 27), deviating from the depleted component towards an EM-like end-member.

Since the Hf data along the VTR has not yet been published our comparison and discussion will be slightly restricted.

Figure 24 – VTR plots in $^{206}\text{Pb}/^{204}\text{Pb}$ versus $^{87}\text{Sr}/^{86}\text{Sr}$ and $^{206}\text{Pb}/^{204}\text{Pb}$ versus $^{143}\text{Nd}/^{144}\text{Nd}$ correlation diagram

Source: The author, 2022.

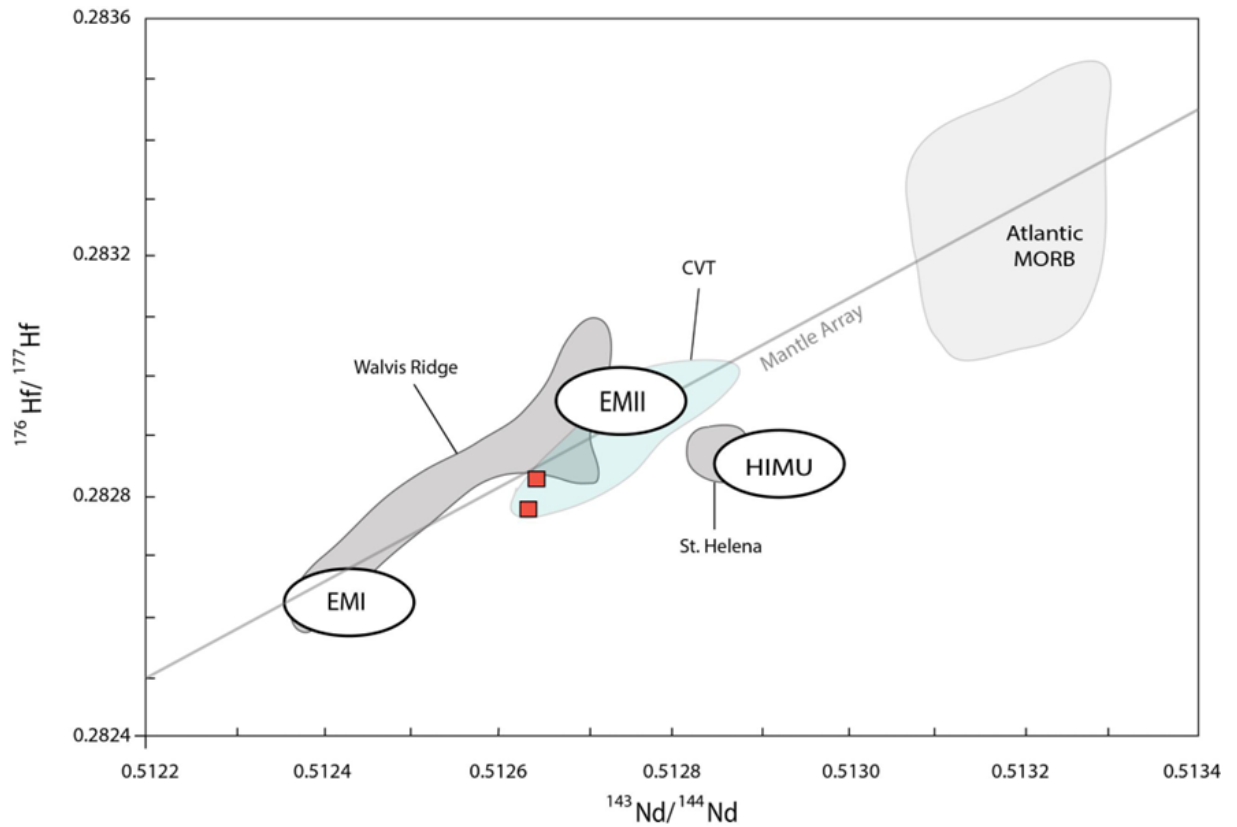
Figure 25 – Three-dimensional isotopic plot for Vitória-Trindade Ridge (VTR) samples and mantle end members



Subtitle: VTR samples are plotted as the gray field and Davis Bank sample is plotted as red square. The parameters for the DMM, EMI, EMII and HIMU are from Zindler and Hart (1986), Salters and Stracke (2004), Workman and Hart (2005), Jackson and Dasgupta (2008), Gurenko *et al.* (2009), Hofmann (2014).

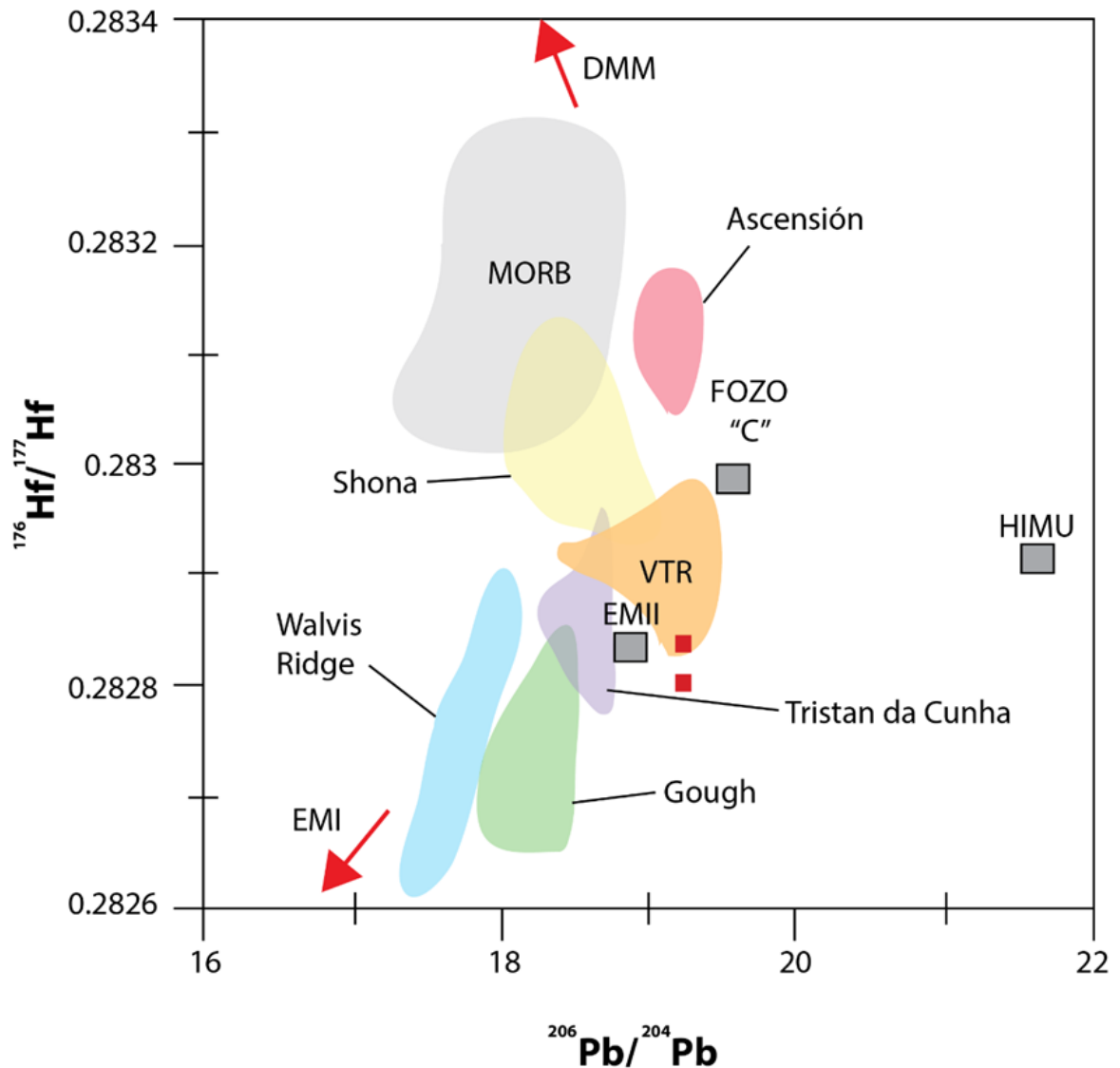
Source: The author, 2022.

Figure 26 – $^{143}\text{Nd}/^{144}\text{Nd}$ versus $^{176}\text{Hf}/^{177}\text{Hf}$ correlation diagram for Davis Bank samples



Subtitle: Trindade unpublished samples plotted as green field. Source: The author, modified from Geldmacher *et al.* (2011).

Source: The author, 2022.

Figure 27 - $^{176}\text{Hf}/^{177}\text{Hf}$ versus $^{206}\text{Pb}/^{204}\text{Pb}$ for VTR magmatic rocks

Subtitle - Davis Bank sample is depicted as the red square (this study) and VTR data is depicted as orange field (Santos, unpublished data). Mantle components: MORB (Saunders *et al.*, 1988; Nowel *et al.*, 1998; Andres *et al.*, 2002; Workman & Hart, 2005; Chauvel *et al.*, 2008; Hofmann, 2014); EM I (Salters & White, 1998; Eisele *et al.*, 2002), EM II (Salters & White, 1998), and HIMU (Salters & White, 1998 and references therein; Stracke *et al.*, 2005); FOZO (Stracke *et al.*, 2005); and "C" (Hanan and Graham, 1996; Hanan *et al.*, 2000). Additional data: Walvis Ridge (Hart *et al.* 1986), Ascension (Hart *et al.*, 1986), Gough, Shona and Tristan da Cunha (Schwindrofska *et al.*, 2016 and references therein).

Source: The author, 2022.

6 DISCUSSIONS

6.1 Magma genesis

The behavior of major, minor and trace elements suggest that fractional crystallization may have played an important role in the evolution of many magmatic systems from the Vitória- Trindade Ridge. Most samples from the seamounts, especially Davis bank basanites have low concentrations of MgO, Ni and Cr, which are more differentiated, and fractionation of olivine and clinopyroxene is likely. For these samples, decreasing CaO and increasing Al₂O₃ leads to decreasing CaO/Al₂O₃ ratios with decreasing MgO and increasing SiO₂, which is also consistent with clinopyroxene fractionation (JUNG *et al.*, 2006). Increasing Al₂O₃ contents and the lack of negative Eu anomalies indicate that plagioclase was not a major fractionating mineral phase at this stage, implying that fractionation took place at pressures > 5 kbar, equivalent to depths >15 km within the lower crust (JUNG *et al.*, 2006). The fact that the more differentiated rocks have lower abundances of Ni, Cr and V with decreasing MgO indicates that olivine, clinopyroxene and Fe–Ti oxides were important fractionating mineral phases in the petrogenesis of the more the more evolved magmas of the VTR.

One micro-basalt sample from Davis Bank (PEYVE; SKOLOTNEV, 2014) with Mg# 60, MgO 9.62 wt.% and Ni 371ppm is likely to have undergone minimum fractionation and may be representative of a more primitive magma from which basanites samples from this work may have evolved. Davis' more differentiated basanite shows the highest values of incompatible trace elements as Zr (407–419 ppm) and La (80.4 – 83.9 ppm) likely related to evolution from clinopyroxene and plagioclase fractionation.

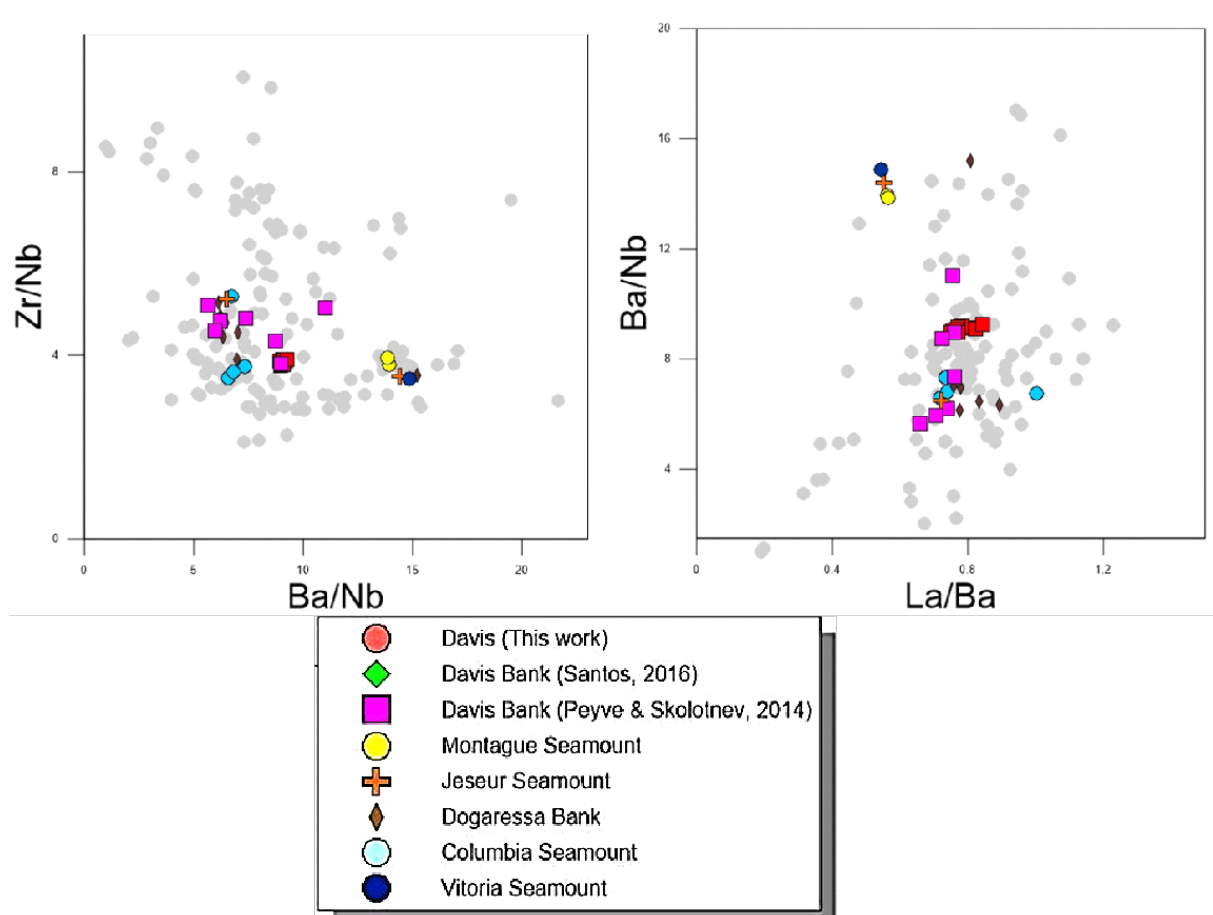
All samples from the VTR are characterized by a marked depletion in K and Rb relative to other incompatible trace elements (Figure 20), which is commonly interpreted as the presence of a residual minor K-bearing phase in the source region (GERLACH *et al.*, 1987). This suggests, according to Sun and McDonough (1989), that potassium in the melts could be buffered by residual amphibole, phlogopite and clinopyroxene (under very high pressure) during source enrichment processes and/or magma generation (*e.g.* SUN; HANSON 1975; CLAGUE; FREY, 1982). The behavior of K may also reflect metasomatic processes that occurred in mantle sources (MARQUES *et al.*, 1999). Weaver *et al.* (1990) also pointed to the strong K depletion in Fernando de Noronha and Trindade nephelinites and basanites. These authors highlight that St. Helena HIMU-type OIB also displays such relative K depletion

(WEAVER *et al.* 1987) and suggest that it may be a characteristic of the HIMU-like magma source. Nonetheless, Weaver *et al.* (1990) points that the magnitude of the K depletion is greater in Fernando de Noronha and Trindade, and implies that, although K depletion at source might be a function of a HIMU component (as indicated by isotopic evidence, *e.g.* Lead isotopic ratios) such stronger depletion as in VTR may have been enhanced during partial melting, and the presence of a residual K-bearing minor phase (*e.g.*, phlogopite, amphibole - see Bongiolo *et al.*, 2015 for modeling details) is still required at small degrees of melting.

The steep pattern of REE may indicate the presence of garnet as residual phase, but also clinopyroxene. High Ce/Yb (*ca.* 20 up to 66), Ce/Y (1.33 – 5.42), Sm/Yb (2.27 up to 6.93), Nd/Sm (4.7 – 5.6), Cr/Y (up to 27), Tb/Yb (0.3 – 0.7) and low Sm/Nd (0.15 – 0.21) suggest melting in the presence of garnet (*i.e.* depths > 80 km - see Maia *et al.*, 2021 for details concerning chemical modeling to Vitória Seamount). Variable (Tb/Yb)_N (=chondrite-normalized Tb/Yb) and (La/Yb)_N (= chondrite-normalized La/Yb) ratios (*ca.* 2 to 4 and *ca.* 15 to 55, respectively, Figure 28), but with similar Yb concentrations, indicates Yb is buffered, which is consistent to different degrees of partial melting in the presence of garnet as a residual phase (GEORGE; ROGERS 2002; MARTINS *et al.*, 2010).

Davis samples have low ratios of Ti/Zr, Zr/Nb, Y/Nb, Ba/Nb, Ba/Th, Nb/Th. Ratios of Zr/Nb are low in samples from the seamounts and banks of the VTR and display restricted variation, ranging from 3.5 to 5.3. Primitive alkaline volcanic rocks with OIB affinities commonly have low Zr/Nb ratios ranging from *ca.* 2 to 4 (WEAVER, 1991), whereas the continental crust has higher and more variable Zr/Nb ratios ranging from *ca.* 8 to 14 (TAYLOR; MCLENNAN, 1985; RUDNICK; FOUNTAIN, 1995). The Zr/Nb ratios along with low Y/Nb (<1) can further attest the geochemically enriched nature of the samples (LE ROEX, 2010). Ba/Nb and Ba/Th ratios along the VTR are variable (*ca.* 5-16; *ca.* 69-288, respectively) and when plotted against La/Ba and Zr/Nb (Figure 28) one group may be distinguished deviating from other VTR seamounts, characterized by higher Ba/Nb and Ba/Th ratios of (*ca.* 14, *ca.* 285, respectively) and lower La/Ba and Zr/Nb represented by the alkaline basalt from Vitória Seamount (MAIA *et al.*, 2021), two samples from Jaseur Seamount (SANTOS, 2016) and two samples from Montague seamount (SANTOS, 2016), along with a few samples from the Trindade and Martin Vaz Islands. All samples cited have LOI below 2.

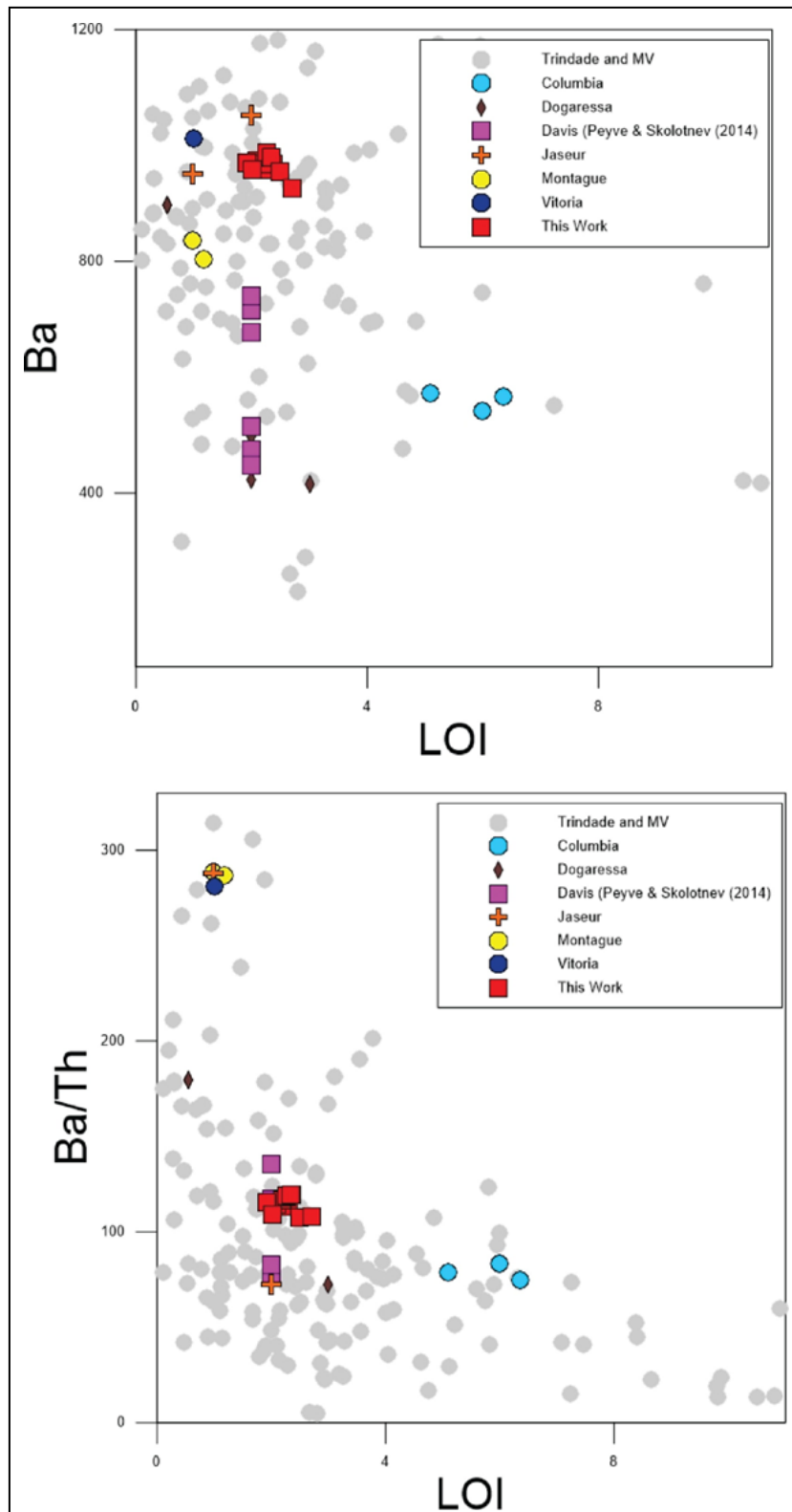
Figure 28 - Variations in selected incompatible trace element ratios in lavas from the Vitória- Trindade Ridge



Subtitle: The alkaline rocks of Vitória-Trindade Ridge (Fodor and Hanan, 2000; Peyve and Skolotnev, 2014; Santos, 2016; Jesus *et al.*, 2019; Maia *et al.*, 2021). The grey circles represent rocks from the Trindade and Martin Vaz Islands (Marques *et al.*, 1999; Siebel *et al.*, 2000; Greenwood, 2001; Bongioiolo *et al.*, 2015; Santos, 2016, Unpublished data, Santos oral communication). Red dotted line highlights the group of rocks that deviate from the rest of the VTR seamounts.

Source: The author, 2022.

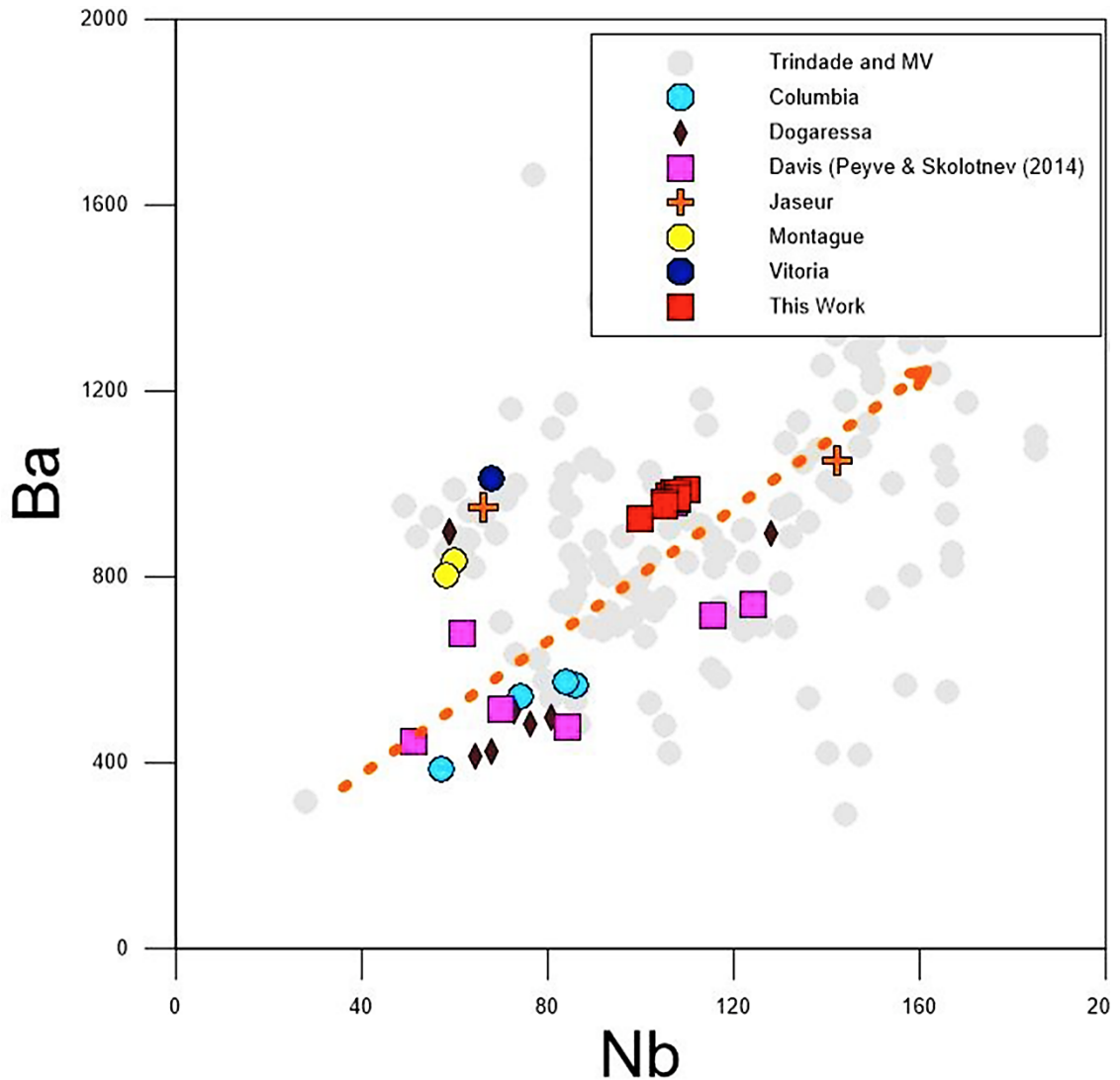
All seamounts show positive Ba anomaly. There is no obvious correlation between Ba and LOI or between Ba/Th and LOI (Figure 29). Nonetheless, Ba shows a reasonably good correlation with Zr (not shown) and Nb (Figure 30), although samples from seamounts do not represent the same magmatic suite. Observing figure 31 it becomes clear that the full spectrum of Ba/Nb ratios found in samples from this region occur in samples with low LOI values, and samples with the highest Ba/Nb ratios are amongst the least altered. On the other hand, samples with higher LOI values do not have raised Ba/Nb ratios. Ba abundances and Ba/Nb and Ba/Th ratios are considered reasonably robust with respect to alteration and the measured ratios are believed to closely reflect those in the original magma. We believe that the high Ba/Nb and Ba/Th (Figures 29 and 32) ratio reflects a compositional characteristic of the mantle source region and might be related to continental sediments into the mantle.

Figure 29 - Variation between Ba and Ba/Nb *versus* LOI in lavas from the VTR

Subtitle: The alkaline rocks of Vitória-Trindade Ridge (Fodor and Hanan, 2000; Peyve and Skolotnev, 2014; Santos, 2016; Jesus *et al.*, 2019; Maia *et al.*, 2021). Rocks from the Trindade and Martin Vaz Islands (Marques *et al.*, 1999; Siebel *et al.*, 2000; Greenwood, 2001; Bongioiolo *et al.*, 2015; Santos, 2016, Unpublished data, Santos oral communication).

Source: The author, 2022.

Figure 30 - Variation between Ba and Nb in lavas from the VTR

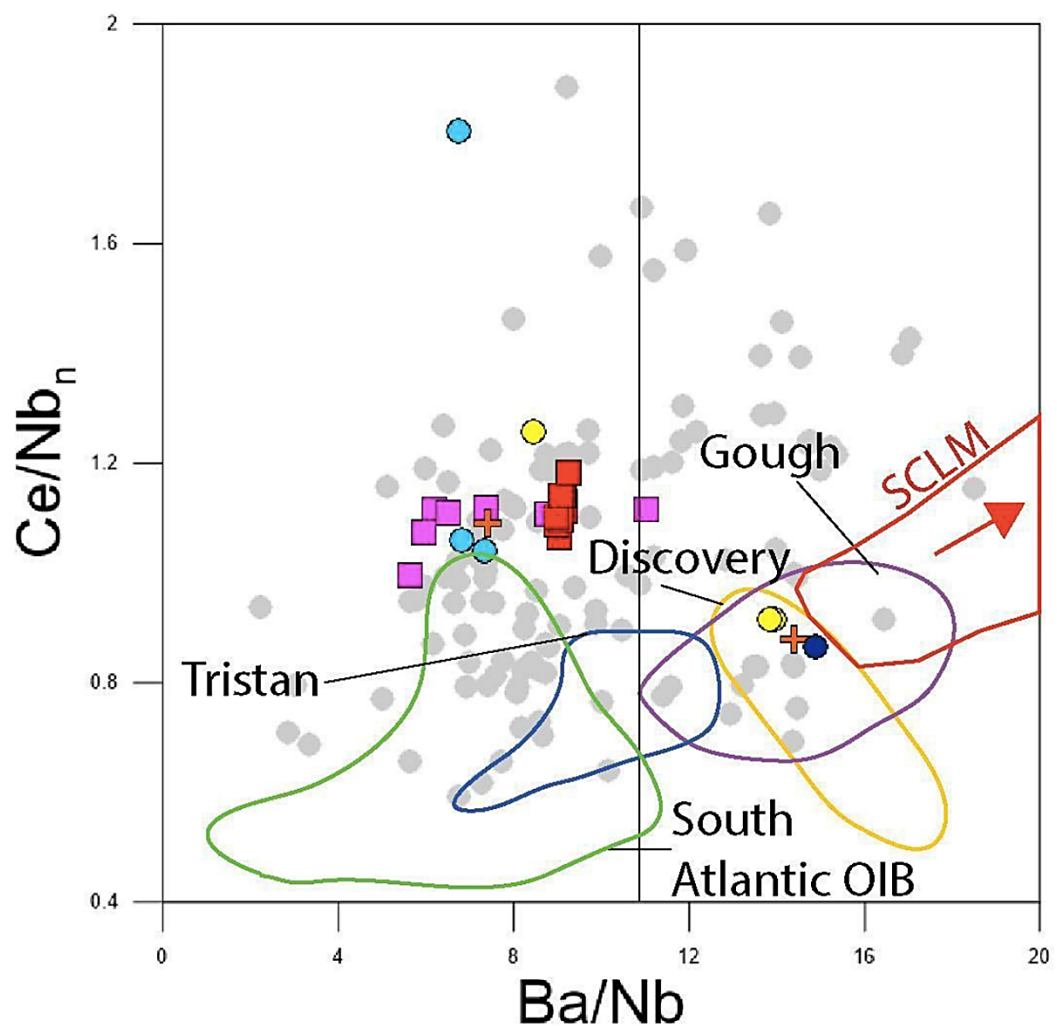


Subtitle: The alkaline rocks of Vitória-Trindade Ridge (Fodor and Hanan, 2000; Peyve and Skolotnev, 2014; Santos, 2016; Jesus *et al.*, 2019; Maia *et al.*, 2021). Rocks from the Trindade and Martin Vaz Islands (Marques *et al.*, 1999; Siebel *et al.*, 2000; Greenwood, 2001; Bongiolo *et al.*, 2015; Santos, 2016, Unpublished data, Santos oral communication). Orange dotted arrow highlights the reasonably positive correlation between samples from the seamounts and most samples from the Trindade and M.V. islands.

Source: The author, 2022.

According to Le Roex *et al.* (2010), high Ba/Nb ratios (<10), as seen in Vitória Seamount and a group of rocks plotted closely (*ca.* 14.9; MAIA *et al.*, 2021), are extremely unusual for within-plate oceanic magmatism and must reflect either relative enrichment in Ba or relative depletion in Nb in the source region, or fractionation of the Ba/Nb ratio during partial melting processes. High Ba/Nb ratio is accompanied by $Ce/Nb_n < 1$ (Vitória Seamount $Ce/Nb_n = 0.87$; MAIA *et al.*, 2021) (Figure 31) reflecting relative enrichment in Ba rather than depletion in Nb.

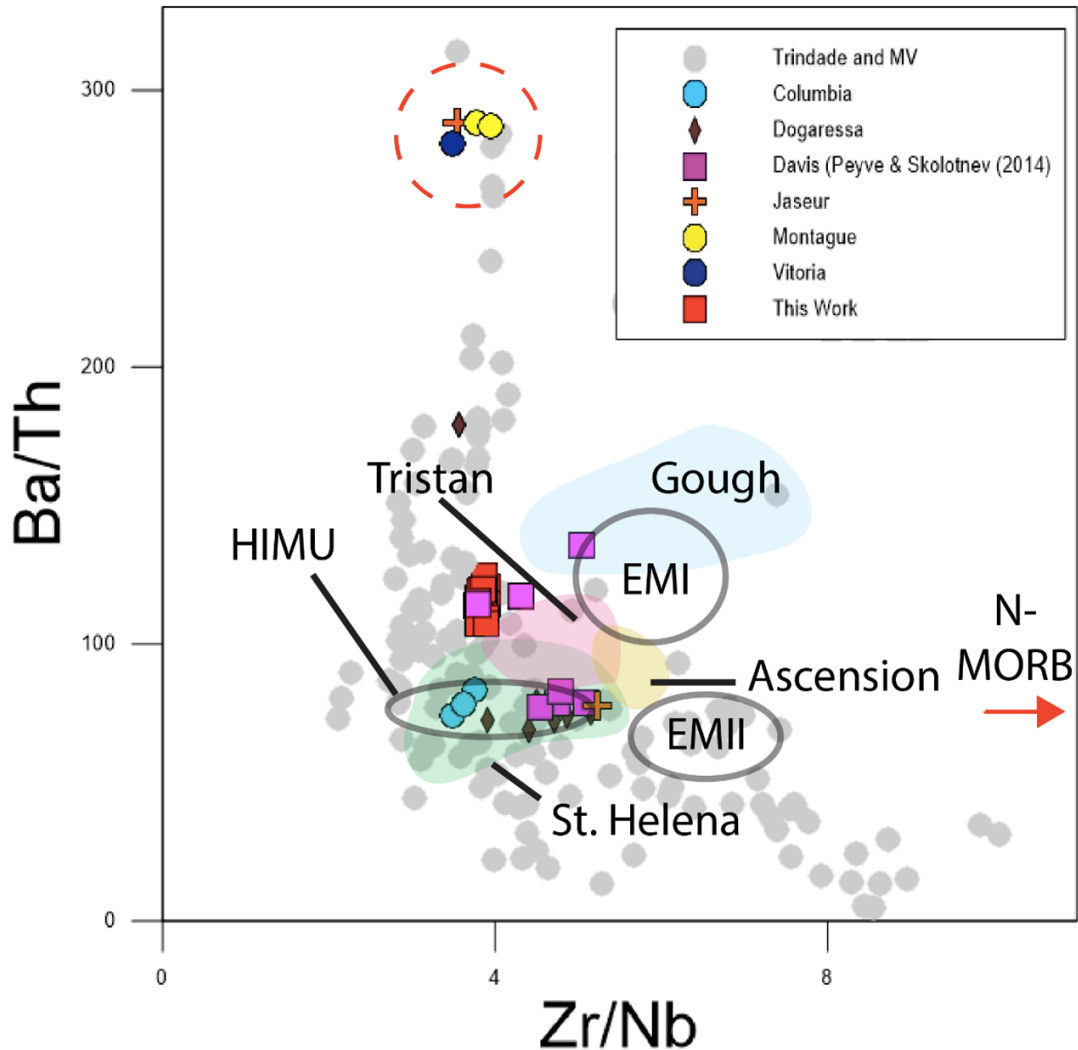
Figure 31 - Ce/Nb_n vs Ba/Nb in lavas from VTR



Subtitle: Shown for comparison are data from Le Roex *et al.* (2010) and references therein: Tristan da Cunha (Le Roex *et al.*, 1990), Gough Island (Le Roex, 1985), South Atlantic OIB (Ascension, St. Helena, Bouvet, Marion and Prince Edward Islands and Vema seamount—see reference sources in Fig. 8 caption) and SCLM from Karoo flood basalts (Rehacek, 1995). The vertical line represents the maximum Ba/Nb ratio typically found in OIB.

Source: The author, 2022. Modified from Le Roex *et al.* (2010).

Figure 32 - Variations in Ba/Th versus Zr/Nb in lavas from the Vitória-Trindade Ridge (VTR)



Subtitle: Additional data from South Atlantic plume-related rocks and mantle end members are from Le Roex *et al.* (2010) and references therein. It is noteworthy that a group formed by samples from Vitória Seamount (Maia *et al.*, 2021), Jaseur Seamount (Santos, 2016 and Peyve and Skolotnev (2014) and Montague Seamount (Santos, unpublished data) deviate significantly from the VTR samples with very high values of Ba/Th.

Source: The author, 2022.

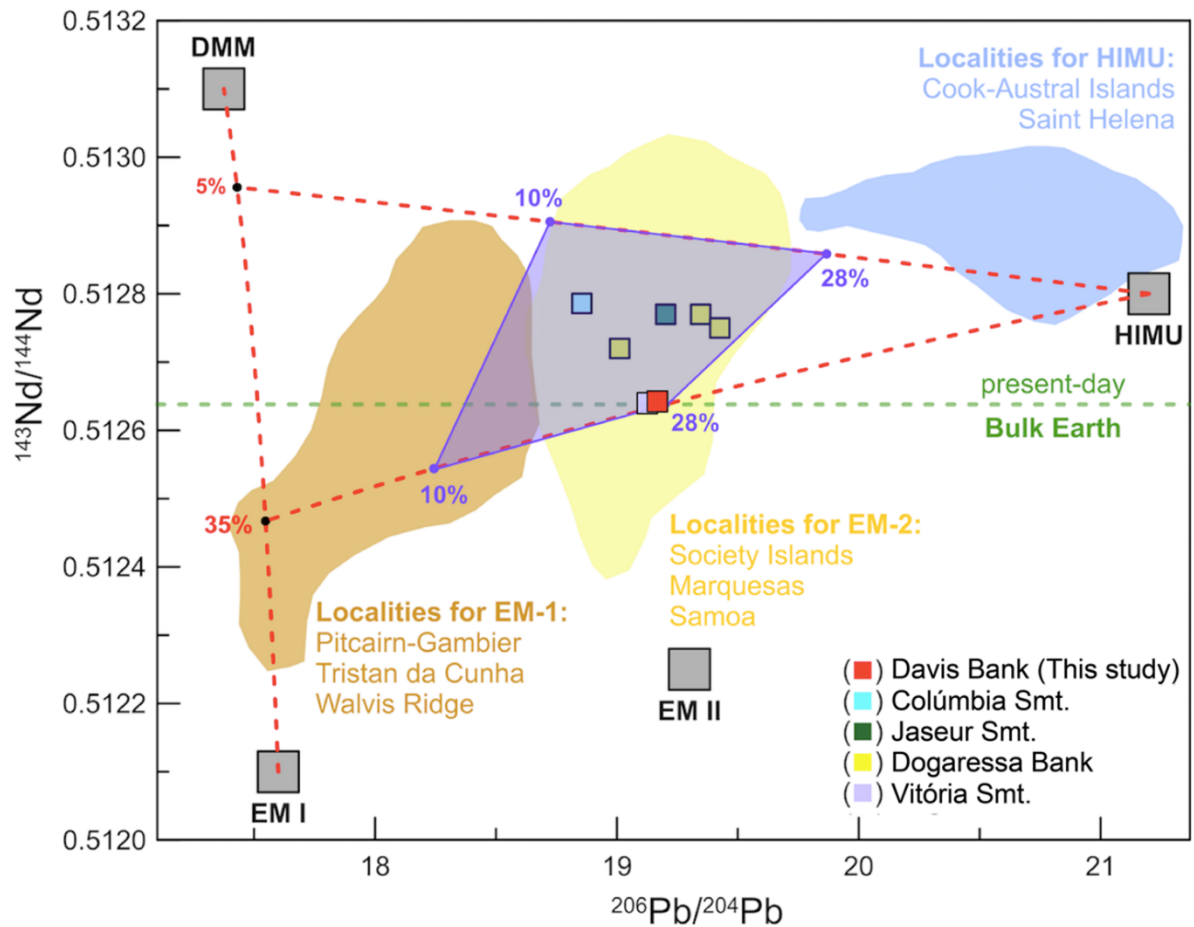
The high values of Ba in the Vitória Seamount have been acknowledged before by Maia (2019), who suggested that the origin of such enrichment may reflect partial melting of volatile-enriched metasomatic events. According to Le Roex *et al.* (2010), melting of a recycled SCLM component eroded from the base of the Gondwana lithosphere and rafted within the shallow convecting oceanic mantle have been invoked to account for unusual trace element characteristics of OIB, including high Ba/Nb ratios (*e.g.* WEAVER *et al.*, 1986; LE ROEX *et al.*, 1989; LE ROUX *et al.*, 2002; GOLDSTEIN *et al.*, 2008). According to Kelemen *et al.* (2014), small partial melts degree of eclogite may also have characteristics normally attributed to an aqueous fluid component from arc-like magmas, such as high Ba/La,

Pb/Ce and Sr/Nd, which we can also apply to the high ratios of Ba/Nd and Ba/Th. Therefore, partial melts of eclogite cannot be discarded to explain such characteristics, given its difficulty distinguishing from aqueous components only by means of these trace elements.

6.2 Identification and quantification of source components involved in the Davis Bank magmatism

Overall, the $^{87}\text{Sr}/^{86}\text{Sr}$ and $^{143}\text{Nd}/^{144}\text{Nd}$ ratios of the VTR (Figure 22) indicate a mixture between DMM and EMI, with Davis Bank and Vitória Seamount lavas tending towards a more significant contribution of the EMI end-member. The moderately elevated radiogenic $^{206}\text{Pb}/^{204}\text{Pb}$ content from Davis Bank sample reported herein as well as from the other seamounts and the islands cannot be explained by a mixing only involving DMM and EMI components. It may be indicative of a contribution of a HIMU mantle component, as suggested by Pires and Bongiolo (2016) for the Trindade Island. Therefore, a heterogeneous three- component mantle source (DMM, EMI, HIMU) in variable proportions could be envisaged to explain isotopic variations seen in the VTR volcanic bodies. This is also shown on diagrams $^{206}\text{Pb}/^{204}\text{Pb}$ versus $^{143}\text{Nd}/^{144}\text{Nd}$ (Figure 33) which reveal that a two-component mixing model does not explain the variations in the VTR and that the mantle source from which these rocks were derived possibly included a mixture between a HIMU-type component and depleted mantle material with a significant admixture of an EM-like component. $^{176}\text{Hf}/^{177}\text{Hf}$ ratios from Davis Bank correlate positively to $^{143}\text{Nd}/^{144}\text{Nd}$ ratios and correlation diagrams of $^{176}\text{Hf}/^{177}\text{Hf}$ versus $^{206}\text{Pb}/^{204}\text{Pb}$ also reinforce these rocks isotopic ratio can be explained by a mixture between a HIMU-type component and an EM-like component, with a less significant DMM component when compared to other VTR samples. All diagrams reinforce the similarities between isotopic signatures from Davis Bank and Vitória Seamount.

Figure 33 - Plot of ternary mixing calculations between DMM, EMI and HIMU-type pyroxenite to describe $^{143}\text{Nd}/^{144}\text{Nd}$ and $^{206}\text{Pb}/^{204}\text{Pb}$ isotopic variability of Davis bank and other VTR rocks



Subtitle: Modeling assumes three-component mixing between asthenospheric mantle (represented by DMM; $^{143}\text{Nd}/^{144}\text{Nd} = 0.5131$, $[\text{Nd}] = 9.6 \mu\text{g/g}$, $^{206}\text{Pb}/^{204}\text{Pb} = 17.375$, $[\text{Pb}] = 0.46 \mu\text{g/g}$), EMI ($^{143}\text{Nd}/^{144}\text{Nd} = 0.5121$, $[\text{Nd}] = 30.6 \mu\text{g/g}$, $^{206}\text{Pb}/^{204}\text{Pb} = 17.600$, $[\text{Pb}] = 2.82 \mu\text{g/g}$) and HIMU-type pyroxenite ($^{143}\text{Nd}/^{144}\text{Nd} = 0.5128$; $[\text{Nd}] = 45.7 \mu\text{g/g}$, $^{206}\text{Pb}/^{204}\text{Pb} = 21.200$, $[\text{Pb}] = 2.73 \mu\text{g/g}$). The parameters for the DMM, EMI, EMII and HIMU are from Zindler and Hart (1986), Salters and Stracke (2004), Workman and Hart (2005), Jackson and Dasgupta (2008), Gurenko *et al.* (2009), Hofmann (2014) and Marques *et al.* (2018). The Sr and Nd contents of the EMI and HIMU end-members are based on data from the GEOROC database (<http://georoc.mpch-mainz.gwdg.de/georoc/>), whereas for the melt DMM, the Sr and Nd contents were calculated considering a partial melting degree of *ca.* 3% (based on the study by Maia *et al.*, 2021; bulk $D_{\text{Nd}} = 0.0317$ and $D_{\text{Pb}} = 0.0092$).

Source: The author, 2022.

Model mixing calculations between DMM component and EMI for Nd and Sr isotopic compositions suggest that EMI contributions ranging from 5% to 30% can account for the

observed Davis rocks compositions. As is clear from isotope correlation diagrams of $^{206}\text{Pb}/^{204}\text{Pb}$ versus $^{143}\text{Nd}/^{144}\text{Nd}$, $^{207}\text{Pb}/^{204}\text{Pb}$ and $^{208}\text{Pb}/^{204}\text{Pb}$ isotope ratios, as well as $^{87}\text{Sr}/^{86}\text{Sr}$ versus $^{143}\text{Nd}/^{144}\text{Nd}$, only the DMM and EMI components cannot explain the isotopic variations in VTR lavas, requiring a third component that can explain the more radiogenic $^{206}\text{Pb}/^{204}\text{Pb}$, $^{207}\text{Pb}/^{204}\text{Pb}$ and $^{208}\text{Pb}/^{204}\text{Pb}$ isotopic ratios. The best-fit in terms of Nd, Pb and Sr isotopic compositions is attained through the partial melting of a DMM-type depleted contributor mixed with EMI (< 24% in the mixing) and HIMU-type components (up to 20% in the mixing). The results of the mixing calculations are shown in Figs. 22, 23 and 34. Note that in these figures the mass balance models were performed in a binary way. First, a mixing process between the DMM and EMI components was modeled and then the result of the calculated composition was modeled with the third component (HIMU). To compute the ternary contributions of each component, the results were renormalized to 100%, providing contributions of up to 24% of EMI and up to 20% of HIMU in the peridotitic mantle source.

6.3 A genetic model for Davis Bank source components

In the precedent section we concluded that the isotope characteristics of the magmas erupted along the VTR can be explained considering the mantle sources incorporating in variable proportions three end-members with characteristics similar to those of the DMM, HIMU and EMI mantle components. We envision an asthenospheric component that is similar to the DMM, but that was hybridized by fluids and/or magmas related to the recycling of MORB-eclogite related to the Neoproterozoic subduction processes that occurred in Western Gondwana leading to the formation of several orogenic belts from the Brasiliano Event (*e.g.* HEILBRON *et al.* 2020), as well as due to the presence of detached continental lithosphere that remained in the asthenosphere after the breakup of Africa and South America during the Mesozoic.

The EMI component is ascribed to processes by which the Brazilian Neoproterozoic continental lithosphere was detached and contaminated a zone of the South Atlantic asthenosphere, as proposed by Hawkesworth *et al.* (1986), Bizzi *et al.* (1995) and Maia *et al.* (2021). Circumstantial evidence comes from the study by Hawkesworth *et al.* (1986) who proposed that the Walvis Ridge basalts were originated from mixtures of delaminated enriched subcontinental lithosphere and more typical “normal” oceanic compositions lying within the oceanic mantle array. In this context, we point out that the origin of the enriched

component

(EMI) would be associated with the recycling of detached fragments of South American continental lithosphere, which may have been left behind during the breakup of Western Gondwanaland and later thermally remobilized by the Trindade hotspot. Indeed, the EMI component is commonly interpreted to have a shallow origin from metasomatized delaminated subcontinental lithospheric mantle. The role of ancient slabs subducted during the Brasiliano Orogeny in the origin of VTR isotopic enrichment has been recognized by several authors (MARQUES *et al.*, 1999; SIEBEL *et al.*, 2000; BONGIOLO *et al.*, 2015; SANTOS 2013, 2016; SANTOS *et al.*, 2018a; MAIA *et al.*, 2021) based on T_{DM} Nd age models ranging from 420-640 Ma, which coincides with the Brasiliano Event.

Furthermore, the origin of the HIMU signature in OIB magmas is commonly associated with mantle plumes originating at the core–mantle boundary or D" layer (*e.g.* HOFMANN; WHITE, 1982). However, Halliday *et al.* (1995) proposed that a HIMU-type component could also have a shallow origin derived through the metasomatism of the oceanic lithospheric mantle. It is noteworthy that Halliday *et al.* (1992, 1995), based on Pb isotopes, attributed the HIMU component of the Trindade mantle source to young strong enrichments in U and Th relative to Pb. Another model for the origin of the HIMU component was invoked by Gurenko *et al.* (2009) and Day *et al.* (2010) to explain the petrogenesis of the Canary Islands lavas, whose origin of the HIMU component would be associated with the recycling of MORB-eclogite, which when melted reacted with the mantle peridotite and produced a "reaction pyroxenite".

Geldmacher *et al.* (2011) discussing hafnium isotopic variations in East Atlantic intraplate volcanism, pointed out that the lower Hf and Nd but higher Pb isotope ratios of the Canary domain samples (compared to the Madeira Archipelago), similar to what is seen in Davis Bank analyzed samples, could not just reflect an increased contribution of the enriched recycled component in the magma source, suggesting that such enriched components exist as pyroxenitic or eclogitic veins (garnet-pyroxenites) within the depleted peridotitic mantle matrix (*e.g.* ZINDLER *et al.* 1984; ALLÈGRE; TURCOTTE 1986; HIRSCHMANN; STOLPER 1996).

We suggest the presence of a HIMU-type pyroxenite mantle source component in the Davis Bank from recycling oceanic crust, indicating the occurrence of MORB-eclogite (mafic) recycled lithologies involved during mantle melting. Experimental studies carried out by Sobolev *et al.* (2005, 2007) and Mallik and Dasgupta (2012) suggested that the partial melting of these MORB-eclogite components produces Si-rich liquid that react with the

surrounding peridotite mantle, converting it to olivine-free reaction-pyroxenite (and such as basanites,

tephrites). As reviewed by Rocha-Júnior *et al.* (2013, 2020), experimental petrology data has been used to argue that pyroxenite or eclogite are important constituents in the mantle sources of OIB. According to the experiments carried out by Sobolev *et al.* (2005, 2007) and Mallik and Dasgupta (2012), pyroxenite might be generated by hybridizing mantle peridotite with MORB-eclogite recycled components, where a series of progressive mixing and reactions processes might re-homogenize the eclogitic components back into the peridotitic mantle, producing a source consisting of different proportions of peridotite and pyroxenite which will yield a “hybrid melt”.

Based on geochemical and isotope data from VTR rocks, including Davis Bank, it seems likely that these rocks have been generated from a source consisting of different proportions of peridotite and olivine-poor components (*e.g.*, pyroxenite, garnet pyroxenite, or eclogite), which occur by partial melting of the MORB-eclogite and injection of its silicic melts into the surrounding mantle peridotite, yielding a “hybrid pyroxenite”. Note that the high-TiO₂ contents of the Davis rocks, along with the depletions in Rb, K, U and Sr in relation to fluid-immobile incompatible elements like Nb and Ta (Figure 20; This work; PEYVE; SKOLOTNEV, 2014; JESUS *et al.*, 2019; SANTOS, oral communication) are robust evidence for signatures inherited from recycled oceanic crust in the mantle source, as well as a consequence of dehydration of oceanic crust during subduction (DAY *et al.*, 2010; HOFMANN, 2014). Evidence for alkaline basaltic melts derived from pyroxenite fraction in the peridotite mantle (reaction between MORB-eclogite and subsolidus peridotite) can be statistically distinguished from peridotite-derived melts through a polynomial relationship of major element log-ratios called FCKANTMS marker, which is used to identify the source lithology for natural basalts (YANG *et al.*, 2019). For instance, crustal material recycling and mantle metasomatism can result in mineralogical and compositional heterogeneities, producing a variety of mafic and ultramafic rocks, *e.g.*, metasomatized peridotite, pyroxenite, hornblendite. If we consider only Davis Bank rocks with MgO > 10 wt.% (sample V2410/10 from PEYVE; SKOLOTNEV, 2014), the FCKANTMS value is 0.27, which is higher than those melts derived from normal peridotite. Hence, based on this statistical model in the log-ratio space, the source lithology of the Davis Bank should have been influenced by olivine-free pyroxenite.

In this context, we propose that the HIMU-type flavor identified in Davis Bank is explained by pyroxenite fractions in the VTR mantle source related to recycled oceanic crust that was converted into eclogite-MORB after the subduction process. Moreover, as highlighted by Bodinier *et al.* (2008), when partial melting of a hybridized mantle (marble-

caked

mantle)

occurs, preferential melting of eclogite or pyroxenite lithologies explain chemical and isotopic variations observed in oceanic rocks, which may explain the slight compositional variability observed in different magmatic activities of the VTR.

Subducted slabs of Neoproterozoic oceanic lithosphere detached during the evolution of the Neoproterozoic-Cambrian Brasiliano/Pan-African Orogenic System, may have been incorporated into the upper mantle and contaminated the local mantle underneath the South Atlantic Ocean. The Brasiliano Event resulted in the amalgamation of West Gondwana and involved multiple orogenic systems with partially coeval stages of subduction and collision (e.g. Heilbron *et al.*, 2020), including the Araçuaí-Ribeira Orogenic System (AROS, HEILBRON *et al.*, 2017; TEDESCHI *et al.*, 2016). Neoproterozoic Magmatic Arcs of Western Gondwana date from 980 to 550 Ma (PEIXOTO *et al.*, 2017; HEILBRON *et al.*, 2020), which means subduction may have started sometime prior to that, and we speculate oceanic slabs may have up to 1.3 Ga. It is noteworthy that the sources of the northern Paraná basalts (MARQUES *et al.*, 2018; ROCHA-JÚNIOR *et al.*, 2013, 2020), several occurrences of small-volume ultramafic alkaline magmatism that surround the Paraná Basin, and some oceanic basalts in the South Atlantic, all appear to be related to the EMI component (BIZZI *et al.*, 1995; HAWKESWORTH *et al.*, 1986). As discussed by these authors, the oceanic basalts with EMI flavor in the South Atlantic are ascribed to processes by which the Brazilian Neoproterozoic continental lithosphere was delaminated and contaminated a zone of the South Atlantic asthenosphere. In addition to the Paraná basalts and alkaline rocks that border the Paraná Basin having EMI affinity, they also have similar Nd model ages, ranging from 0.8 to 1.3 Ga, indicating that the mantle source that gave rise to these rocks was metasomatized by slab-derived fluids of a mid- to late-Proterozoic event such as the Brasiliano. The isotopic and temporal overlapping of different magmatic events cannot be accidental and lead us to believe that these events were, directly or indirectly, affected by Neoproterozoic subduction processes (events of the Brasiliano/Pan-African orogenic cycles). Robust elemental and isotopic geochemistry data on Neoproterozoic plutonic and volcanic rocks of the Mantiqueira Province, which includes the Ribeira and Araçuaí belts, testifies to the consumption of an oceanic realm to generate the orogen (CAXITO *et al.*, 2021). Valeriano *et al.* (2016) suggest break-off and sinking of subducted oceanic lithospheric slab into the asthenosphere during the terminal stages of collisional orogeny generating tholeiitic magma from melting of the asthenosphere.

6.4 On the heterogeneity of the VTR magmatism

Radiogenic isotope ratios are reliable indicators of source heterogeneity, since they do not change during partial melting and crystal fractionation processes, in contrast to incompatible trace-element ratios. It is noteworthy that Davis Bank basanite analyzed in this work have clearly less radiogenic Nd and Hf isotopic signature ($^{143}\text{Nd}/^{144}\text{Nd}$ 0.512612; $^{176}\text{Hf}/^{177}\text{Hf}$ 0.282834) in comparison to other VTR rocks ($^{143}\text{Nd}/^{144}\text{Nd}$ = 0.51272–0.512879; $^{176}\text{Hf}/^{177}\text{Hf}$ 0.282834–0.282984 – SANTOS, unpublished data).

Davis Bank also displays several distinct characteristics from the other seamounts and the islands. Isotopic analyses carried out in Davis Bank, alongside with whole-rock chemistry and mineral chemistry (JESUS *et al.*, 2019; REGO *et al.*, 2021) confirm those suggestions. For instance, Davis Bank lavas show an enrichment in incompatible elements (normalized La/Sm *ca.* 4.1 and La/Yb *ca.* 21.7) higher than the alkaline rocks from other seamounts (La/SmN = *ca.* 2.57; La/YbN = *ca.* 20 – compiled from MAIA *et al.*, 2021), and more basic compositions with lower content of MgO (4.0 wt.%), higher SiO₂ content (*ca.* 45 wt.%), which differs from the ultrabasic seamounts (*ca.* 37 SiO₂ wt.%; *ca.* 10 MgO wt.%) like the ankaramites from Colúmbia Seamount (FODOR; HANAN, 2000) and Dogaressa Bank (Skototnev *et al.*, 2010), melanephelinites from Montague and Jaseur Seamounts (SANTOS, 2016) and alkaline basalt from Vitória Seamount (MAIA *et al.*, 2021). Santos (personal communication) suggests that Davis Bank is a primitive magma that underwent exceedingly small amounts of phase crystallization. Such differences on the enrichment of incompatible elements cannot be assigned solely to the distinct degrees of magmatic evolution, given that isotope ratios, especially Nd and Hf, of Davis Bank are different from most other occurrences from the VTR, with the exception of the Vitória seamount (see below).

Indeed, although authors have previously reported a restricted range in isotopic signature along the VTR (*e.g.* SKOLOTNEV; PEIVE, 2017), the dredged samples from the Davis Bank (this study) and Vitória Seamount (MAIA *et al.*, 2021) clearly pointing to the heterogeneity of the mantle sources feeding the magmatism along the VTR. Our conclusion is at odds with the idea about the possible homogeneity of the VTR magma source as previously proposed by Peyve and Skolotnev (2014) and Bongiolo *et al.* (2015).

As can be seen in figure 22, two samples from Dogaressa seamount are strongly radiogenic in Sr isotopes. We suggest that this increase in the Sr isotopic compositions of the Dogaressa seamount rocks can potentially be attributed to the interaction with seawater or too

a limited extent of assimilation of anhydrite-rich, evaporitic sediments, which may be found in the sedimentary sequences that underlies the oceanic basin. Therefore, these samples will not be considered to assess mantle sources.

6.5 Davis Bank distinct characteristics and similarities with the Vitória Seamount

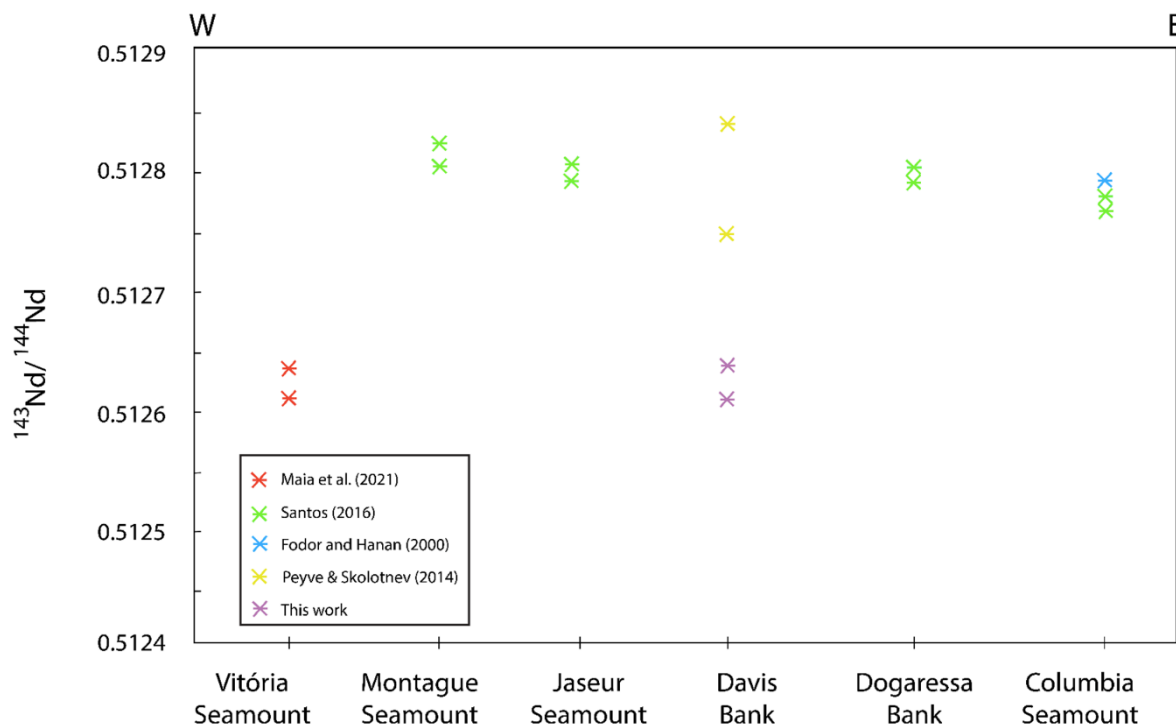
As aforementioned, Vitória Seamount alkaline basalt and Davis Bank basanite analyzed in this work have similar Nd and Hf isotopic signature ($^{143}\text{Nd}/^{144}\text{Nd}$ 0.512612; $^{176}\text{Hf}/^{177}\text{Hf}$ 0.282834) which deviates from the other VTR rocks ($^{143}\text{Nd}/^{144}\text{Nd}$ 0.51272–0.512879 $^{176}\text{Hf}/^{177}\text{Hf}$ 0.282834–0.282984 – SANTOS unpublished data; Figure 27). Such similarities are conspicuous given that the Vitória Seamount is localized 315 km apart from Davis Bank, that these eruptions may have occurred within a time lapse of only 15 Ma as speculated by Maia *et al.* (2021), and that other paleo volcanoes (Congress Bank, Montague Seamount, Jaseur Seamount, Colúmbia Bank) localized between them have more radiogenic Nd and Hf isotopic signature (PEYVE; SKOLOTNEV, 2014; SANTOS – unpublished data).

As outlined before, Davis Bank is not only the most voluminous volcanic building of the VTR but also displays several distinct characteristics from the other seamounts and the islands, besides chemical characteristics. Davis Bank shows higher magma viscosity (*ca.* 7.20 log (Poise); JESUS *et al.*, 2019), which according to Jesus *et al.* (2019) reflects its size and volume compared to other small seamounts from the Vitória-Trindade Ridge. Recent geothermobarometry studies have been carried out in Davis Bank (REGO *et al.*, 2021) revealing that the thermodynamic conditions of Davis Bank crystallization rocks differ from the other VTR records, being associated with a shallower magmatic chamber.

Furthermore, Davis Bank has a well-marked N–S division between a western negative anomaly and an eastern positive anomaly (REGO *et al.*, 2021), which we speculate can be a reflection of different lithologies, as the differences observed in the Nd isotopic composition and whole rock chemistry between basanites analyzed in this work and lavas studied from Peyve and Skolotnev (2014) which were dredged on the opposite flank of the volcanic edifice. Such differences within a single volcano (Figure 34) may indicate the presence of small-scale heterogeneities in the mantle sources feeding the volcanism and the absence of significant magma mingling/homogenization before eruption.

Such distinctiveness of chemical composition as compared to other seamounts in the Vitória-Trindade Ridge (Vitória Seamount, Jaseur Seamount, Dogaressa Bank, Montague Seamount, Colúmbia Seamount and Bank; unpublished data) is conspicuous and may evoke a more complex evolutionary history for the Vitória-Trindade Ridge.

Figure 34 - Nd isotopic signature along the seamounts from Vitória-Trindade Ridge



Source: The author, 2022.

6.6 On the origin of the Vitória-Trindade Ridge

For most researchers, the origin of the VTR is attributed to the effect of the South American Plate passing above the Trindade hotspot (*e.g.*, GIBSON *et al.*, 1995; VANDECAR *et al.*, 1995). However, only sparse geochronological data have been published so far for the Vitória-Trindade Ridge, especially concerning seamounts and banks. Some authors use the supposed progressivity of the dated volcanic episodes to support the Trindade Plume hypothesis (*e.g.*, SKOLOTNEV *et al.*, 2011; SANTOS *et al.*, 2021). However, besides the islands (ranging from 3.9 Ma to 0.17 Ma; CORDANI, 1970; PIRES *et al.*, 2016; SANTOS *et al.*, 2021) and Davis Bank (*ca.* 21 Ma; SANTOS, 2016; SKOLOTNEV AND PEIVE, 2017; QUARESMA, submitted), the only dated volcanic edifice by radioisotopic geochronology is the Jaseur Seamount (29.8 ± 6.6 Ma by U–Pb zircon dating; SKOLOTNEV *et al.*, 2011), but

the age obtained has a large uncertainty that can even overlap with the Davis Bank age and therefore make this result barely usable.

The lack of robust geochronological data on the seamounts and banks prevents thoroughly testing the idea of the VTR formation due to the passage of the lithosphere over a fixed plume in the mantle. Furthermore, the role of the Vitória-Trindade Fracture Zone in the ascent of the magma and evolution of the VTR can't be overlooked (ALVES *et al.*, 2006; BARÃO *et al.*, 2020), and its influence should be considered when discussing the origin of the magmatic episodes. Only larger precise and accurate geochronology data will be able to address if the age progression is entirely related to the movement of the plate, or if channeling of the magma through easy crustal pathways induces some level of randomness in the age progression.

It is clear the importance of structural control in the formation and evolution of this unique sub-latitudinal linear geological structure (FERRARI; RICCOMINI, 1999; BARÃO *et al.*, 2020). Indeed, for some authors, its development is related to the tectonic framework of the South Atlantic Ocean (HEINE *et al.*, 2013; COLLI *et al.*, 2014). During the Gondwana breakup and the opening of the South Atlantic Ocean, a system of fractures representing weakened zones of the lithosphere formed. For instance, the Vitória-Trindade Fracture Zone (VTFZ), along which lies the Vitória-Trindade volcanic ridge (*e.g.* FERRARI; RICCOMINI, 1999; ALVES *et al.*, 2006). Hence, one hypothesis about the formation of this volcanic ridge considers the role of the fracture zone as a conduit for the ascent of magmas generated in a sub-lithospheric thermal anomaly (*e.g.*, ALVES *et al.*, 2006). In this perspective, the existence of the Trindade Plume and the magnitude of this anomaly are still controversial.

Although the origin of such alkaline magmatic episodes is still argued, the Vitória-Trindade Ridge reflects important Cenozoic oceanic tectonic-magmatic activity in this planet region. Several authors highlight the contemporaneity of alkaline intrusion and episodes of tectonic reactivation on the onshore Brazilian territory (*e.g.*, COGNÉ *et al.*, 2012). The onshore emplacement of alkaline bodies during the Late Cretaceous and the Paleocene (COGNÉ *et al.*, 2012), with emphasis on the Poços de Caldas – Cabo Frio Lineament has been linked to coeval tectonic uplift events in the Brazilian coast due to reactivation of the main intraplate structures such as the shear zones parallel to the coast and to transfer zones (*e.g.*, SOUZA *et al.*, 2021).

The voluminous volcanic activity at the Davis Bank build-up may have started in the Oligocene (*ca.* 31 Ma), as suggested by Skolotnev *et al.* (2011), lasting for 10 Ma until Early Miocene. A tectonic reactivation on the Brazilian territory at that time is proposed. Japsen *et al.* (2012), Cogné *et al.* (2012) and Souza *et al.* (2021) interpreted a reactivation of transfer zones in the Neogene, marking an uplift phase starting approximately at the Oligo-Miocene boundary on NE and SE Brazil. Similarly, Cogné *et al.* (2012) highlight the increase in sediment supply during the Miocene in Campos and Santos basins as support for the Neogene fast cooling event recorded in samples from SE and NE Brazil (COGNÉ *et al.*, 2012; JAPSEN *et al.*, 2012). Along with increase in sediment input rate, during the Oligo-Miocene turbidite flows are also recorded in the Espírito Santo Basin from the Rio Doce Canyon System (EUGENE *et al.*, 2004) and in the Campos basin (ARIENTI *et al.*, 2012).

Both tectonic events are synchronous to important tectonic episodes on a broader scale, leading some authors (*e.g.*, MEISLING *et al.*, 2001) to propose a correlation between them. For instance, the supposed Neogene uplift event in the Brazilian passive margin has also been linked to the Andes Orogeny as it coincides with the peak of the Andean uplift during the Quechuan Phase (25–0 Ma; COGNÉ *et al.* 2012; JAPSEN *et al.*, 2012). Japsen *et al.* (2012) suggest that the uplift experienced throughout Brazil during the Oligo-Miocene has a common cause with the Andean uplift and the increase in spreading velocity of the South Atlantic. Similarly, Colli *et al.* (2014) linked the two main phases of the Andes uplift, including the uplift peak during the Oligo-Miocene, to phases of fast-spreading rates of the South Atlantic, owing to an active role of the asthenospheric mantle causing dynamic topography and rapid plate motion velocity changes.

Indeed, this region corresponds to an anomalous positive dynamic topography (COWIE; KUSZNIR, 2018), indicating a hot mantle thermal structure or upwelling convection, as suggested by Stanton *et al.* (2021) for the Abrolhos Volcanic Complex (AVC). There are several discussions about geodynamic models that attempt to explain these rapid variations (short time interval) in the lateral movements of the plates and in the vertical movements of uplift that would not have an isostatic cause. Works like Colli *et al.* (2014, 2018), Iaffaldano and Bunge (2005), and O'Connor *et al.* (2018) invoke an active role of the asthenosphere with a pressure-driven flow (poiseuille flow) that would result in dynamic topography. For example, O'Connor *et al.* (2018) pointed out that under the South Atlantic there would be the occurrence of fast flow channels which, together with the occurrence of hotspots referring to small overlying “plumelets”, would be driven by pulses of larger and deeper Plumes. O'Connor *et al.* (2018) also mentions that these uplift

events observed on both sides of the Atlantic are synchronous to the pulse events of the African Superplume (CIVIERO *et al.*, 2019). Moore *et al.* (2008) called attention to the temporal links between tectonic processes and plate movements on the one hand, and episodes of alkaline volcanism in South Africa on the other, which raises the discussion about the nature of the mantle processes involved in the generation of magma.

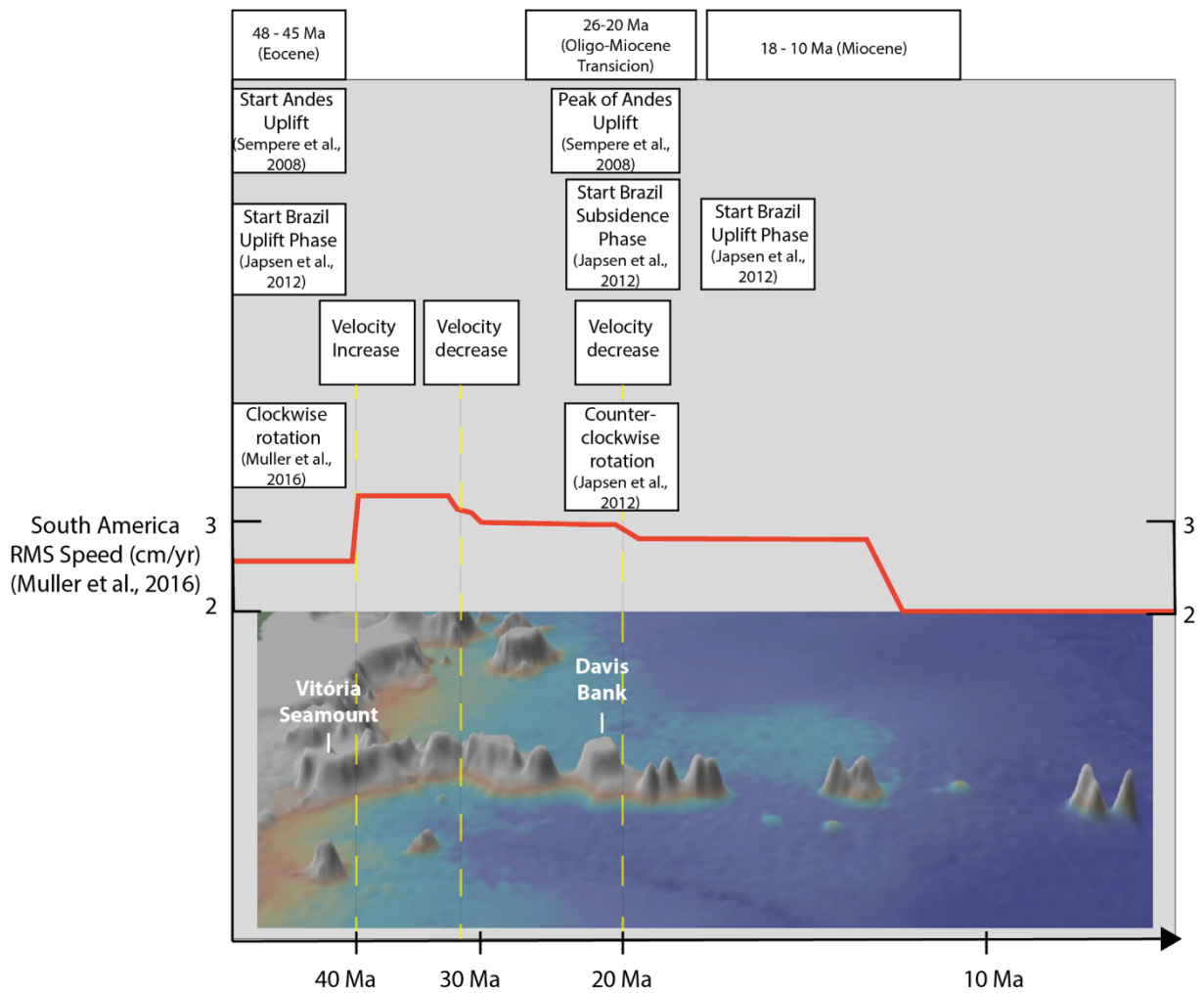
Celli *et al.* (2020) presented a tomographic model of upper mantle and transition zone beneath the South Atlantic and identified low-velocity anomalies beneath major hotspots, including the pronounced low velocities at 80 Myr — corresponding to the age of the lithosphere under the Trindade hotspot. Celli *et al.* (2020) described the pattern of these anomalies as being overly complex and deeply interconnected. O'Connor *et al.* (2018) suggest an interplay between the active role of the fast-flowing asthenosphere fed by these larger and deeper plumes (*e.g.* African Superswell) and the tectonic setting.

In regards to the VTR, changes in orientation in the alignment of the paleo volcanoes have been linked in the past (FERRARI; RICCOMINI, 1999) to changes both in speed and in the direction of movement of the South American Plate, and would indicate a change in direction of the main tensor acting on the regional scale that would be reflecting the change direction of the general strain of the South American plate (FERRARI; RICCOMINI, 1999; BARÃO *et al.*, 2020). An inflexion in the VTR of about 18° occurs around the W34° coordinate (MOTOKI *et al.* 2012) close to the Davis Bank, that could be due to small direction variations from the structures of the transfer zone but could as well be reflecting a change in direction of the South American Plate, of the possible existence of the Trindade Plume or a combination of both. The distance between the Jaseur Seamount radiometrically dated from *ca.* 29 Ma, Davis Bank (*ca.* 21 Ma) and the Martin Vaz Island (*ca.* 3.6 Ma) do not correlate to the mean velocity of the South American absolute plate motion at this time (MÜLLER *et al.*, 2016) if we were to consider the VTR as a track resulting from the drift of the plate over a fixed hotspot model. This would, then, invalidate the fixed plume model or it may imply that the Trindade hotspot did not remain stationary and would have accelerated eastwards during the Miocene.

All the aforementioned correlations are merely speculative. There is no consensus on the Neogene tectonic reactivations in the Brazilian territory and the associations with the emplacement of alkaline intrusions and in a global scale, the events such as the peak of the uplift in the Andes during the Oligo-Miocene and increase in South Atlantic spreading velocities. Nonetheless, we consider the temporal links between the Oligo-Miocene complex

tectonic scenario and the conspicuous distinct characteristics of the Davis Bank rocks that are most possibly related to the source of magmatism and therefore could provide important insights on the evolution of the VTR. A summary of the main events and contemporaneity with the VTR volcanic edifices is presented in figure 35.

Figure 35 - Andean uplift and South American Plate tectonic events



Source: The author, 2022.

6.7 A model for the Vitória-Trindade Ridge magmatism

Celli *et al.* (2020) observed through their tomographic model, strong low-velocity seismic wave anomaly under a large portion of the Vitória-Trindade Ridge at depths of *ca.* 100- 250 km, which may indicate either anomalous hot asthenosphere or anomalous compositional contrasts. This seismic evidence shows little correlation to the concept of a classic narrow deep-seated plume. Yet, a recent seismic tomographic study (CIVIERO *et al.*, 2021) has shown, for the Canary/Morocco region a significant heterogeneity in the shape and lateral extension of mantle upwellings rooted in the Central-East Atlantic Anomaly stacked beneath the 660 km seismic discontinuity.

Nevertheless, as aforementioned tomographic images by Celli *et al.* (2020) depict a very complex and interconnected pattern of low-velocity anomalies in the mantle beneath the South Atlantic Ocean, apparently not existent beneath the 260 km depth. Also, the origin of the AVC is commonly linked to the VTR, due to its proximity, and attributed to the Trindade Plume (THOMPSON *et al.*, 1989; GIBSON *et al.*, 1995; SIEBEL *et al.*, 2000). Nevertheless, Stanton *et al.* (2021), based on extensive geophysical mapping using seismic reflection data, suggested magmatic activity affecting sediments as recent as the Middle Miocene and, thus, contemporary to the Davis Bank magmatic episode thus, also invalidating a link between the VTR and the AVC to a fixed Trindade Plume.

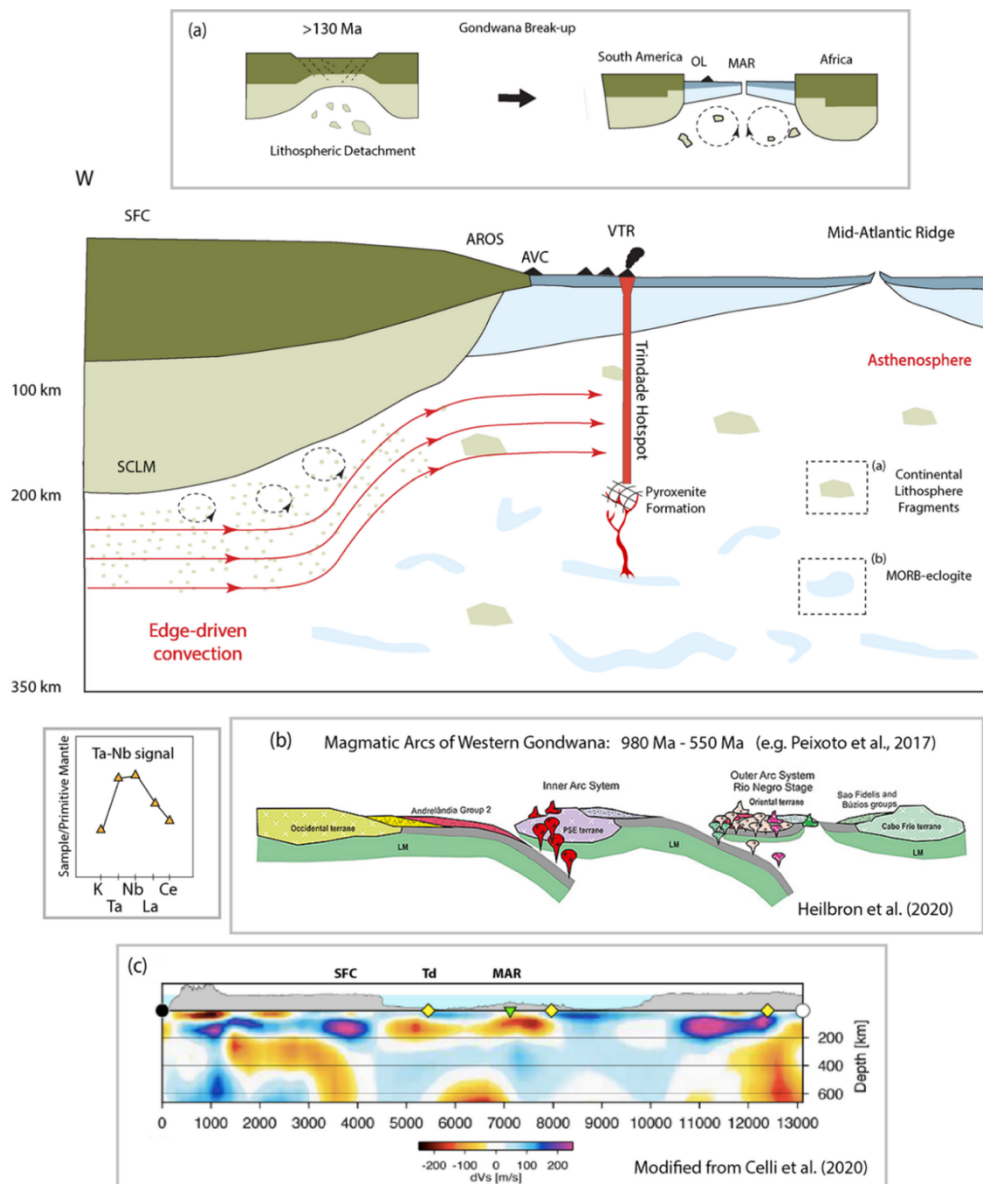
We further suggest that an analog for the VTR could be the Fernando de Noronha Island, where Knesel *et al.* (2011) and Perlingeiro *et al.* (2013) proposed such alkaline magmatism to be a manifestation of the upwelling flow from an edge-driven convection model (EDC, KING; ANDERSON, 1998), rather than tracking passage over a deep-seated mantle plume. The EDC is an alternative model to the formation of some intraplate volcanism assumed to be formed above regions where differences in lithospheric thickness cause thermal contrasts driving small- scale convective flows (KING; ANDERSON, 1998). According to Knesel *et al.* (2011), the Vitória-Trindade Ridge is also geometrically favorable for the EDC mechanism.

To illustrate the envisioned origin of the enriched components of the VTR mantle source, Figure 36 shows a hypothetical model with a hybridized mantle beneath the VTR and the tectonic events that may have led to the incorporation of fragments of recycled oceanic crust and subcontinental lithosphere into the local mantle, integrating models from different authors (KING; ANDERSON, 1998; ALLÈGRE; TURCOTTE, 1986; HAWKESWORTH *et*

al., 1986; BIZZI *et al.*, 1995; MAIA *et al.*, 2021; SOBOLEV, 2005; MALLIK; DASGUPTA, 2012;

HEILBRON *et al.*, 2020). The presence of such recycled materials at the convective mantle may account for the large, shallow, and interconnected pattern of seismic anomalies that have been observed underneath many intraplate volcanism regions across the South Atlantic (O'CONNOR *et al.*, 2018; CELLI *et al.*, 2020). Although we acknowledge the occurrence of the EDC mechanism in the envisioned model for the genesis of the VTR due to the favorable geometry of the region, as pointed out by Knesel *et al.* (2011), we argue that such a mechanism cannot explain the formation of volcanic ridge aligned perpendicular to the coastline, since EDC is expected to sustain volcanism in an elongated zone that is parallel to the lithospheric boundary (MANJÓN-CABEZA CÓRDOBA; BALLMER, 2021). The EDC in this scenario may only regionally contribute to the heterogeneity of the mantle through the process of lithospheric erosion. The presence of anomalous fertile sources (*e.g.*, pyroxenite) within an asthenosphere close to the melting point can account for the generation of a melting anomaly, rather than the need to invoke anomalously high temperatures (LUSTRINO, 2005). Such melting anomaly patches confined to the asthenospheric mantle would move slower than the overlying lithospheric plate, giving an illusion of a fixed hotspot (ANDERSON, 2005). The term hotspot here is used as the definition by Courtillot *et al.* (2003) of a Tertiary hotspot of shallow origin not related to deep mantle plumes.

Figure 36 – Schematic sketch depicting the envisioned model for the three-component mantle source of the VTR magmatism, and the tectonic setting associated



Subtitle: Figure depicts edge-driven convection in the asthenosphere (King and Anderson, 1998) and a hybridized (marble-cake) mantle (Allègre and Turcotte, 1986) with subcontinental lithosphere fragments detached during the Gondwana breakup (Hawkesworth *et al.*, 1986; Bizzi *et al.*, 1995; Maia *et al.*, 2021) (EMI) and recycled slabs of oceanic lithosphere subducted during the Brasiliano Event and converted into MORB-eclogite, which reacts with the subsolidus peridotite forming pyroxenite (e.g. Sobolev *et al.*, 2005; Mallik and Dasgupta, 2012) (HIMU), embedded in the peridotitic mantle (DMM). The Ta-Nb signal of Davis Bank lava (sample V2410/5; Peyve and Skolotnev, 2014) showing a positive anomaly is depicted as evidence of recycled dehydrated subducted oceanic crust signature in the mantle source. (a) Tectonic model of continental lithosphere detachment during the Gondwana breakup sometime prior to 130 Ma and the South Atlantic Ocean opening during the Mesozoic; (b) Tectonic model from Heilbron *et al.* (2020) of subduction processes during the Brasiliano Event which resulted in the amalgamation of West Gondwana and involved multiple orogenic systems which ages of magmatic arcs range from 980-550 Ma (compilation from Peixoto *et al.*, 2017); (c) W-E cross-sections tomographic image across the study area from Celli *et al.* (2020).

Source: The author, 2022.

7 FINAL CONCLUSIONS

(1) Based on data presented herein, it can be concluded that Davis Bank samples characterize a very fine-grained basanite with a trachytic groundmass mainly composed of lath-shaped plagioclase microliths and a glomeroporphyritic texture, composed basically of plagioclase, clinopyroxene and opaque minerals. These minerals are observed in the matrix as well as occurring as microphenocrysts, which indicate two distinct moments of crystallization.

(2) Magmas erupted at Davis Bank and analyzed in this work are SiO₂-undersaturated alkaline rocks with sodic affinity having Na₂O + K₂O > 6.0 classified as basanites, exhibit significantly evolved compositions with SiO₂ 4.2 ± 0.4 wt.%, Mg# *ca.* 43.53 and low Ni and Cr abundances (under the detection limit of 20 ppm) as well as Sc and Co contents (11 ppm, *ca.* 40 ppm, respectively). The compositional range is larger than reported for Davis Bank lavas by Peyve and Skolotnev (2014). Although the behavior of major, minor and trace elements suggest that fractional crystallization may have played an important role in the evolution of these rocks, it cannot solely explain chemical differences observed, given that Nd and Hf isotopic variation between Davis samples analyzed in this work and those from Peyve and Skolotnev (2014) indicate a source of heterogeneity.

(3) The combined Sr-Nd-Pb-Hf isotope data presented here suggest a wider range of isotopic ratios for the VTR in general, especially in view of the more unradiogenic Nd and Hf isotopic ratios in Davis Bank samples, as also reported for Vitória Seamount samples, which challenges some interpretations about the homogeneity of the mantle source of the VTR. The enriched Sr-Nd-Pb-Hf signatures of both volcanic edifices preclude the generation of Davis Bank magma via exclusive melting of depleted mantle source and confirm the previous conjecture of several authors about the significant contribution of the EMI and HIMU mantle components in the source of the Vitória-Trindade Ridge magmatism. Data also suggest that those components evolved in an environment with low Sm/Nd and slightly high Rb/Sr, U/Pb and Th/Pb ratios. Thus, the isotopic variations along the ridge could be explained by a heterogeneous three-component mantle source (DMM, EMI, HIMU) with variable mixing proportions.

(4) Modeling of the isotopic data suggests that the best fit in terms of Nd, Pb, and Sr isotopic composition is achieved by partial melting of a depleted mantle represented by a dominant asthenospheric component (DMM) hybridized by the addition of EMI (< 24% in the mixing) and HIMU (up to 20% in the mixture) melts.

(5) The three isotopically different mantle components identified here may be explained by a lithologically heterogeneous mantle. The origin of the EMI component in the source of the magmatism studied can be attributed to detached metasomatized fragments of subcontinental lithospheric mantle slabs left at shallow levels, as previously suggested by Marques *et al.* (1999). As an alternative to the hypothesis of the HIMU mantle component in the VTR source characterized as a deep mantle material ascending from a plume, we believe in a model with ubiquitous heterogeneities in a depleted mantle matrix, in which the Brasiliano Orogeny played a major role regarding the incorporation of enriched materials into the mantle. Recycled slabs of Neoproterozoic oceanic lithosphere subducted during the Brasiliano Event, converted into MORB-eclogite, may have contaminated the local mantle underneath the Vitória-Trindade Ridge. We invoke a HIMU-type pyroxenite formed by partial melting of the MORB-eclogite and injection of its silicic melts into the surrounding mantle peridotite.

(6) Davis Bank samples analyzed in this work represent a more fertile alkaline magmatic episode in the VTR evolution, given chemical and specially Nd-Hf isotopic data presented herein, which point to a heterogeneity at the source of the magmatism of the VTR. Davis Bank intense magmatic episode (volume calculated in *ca.* 14,000 km³) is contemporary to important tectonic events in the Brazilian coastal territory such as coastal uplift, increasing inflow sediments, drainage diversion, offshore volcanism and reactivation of structures on the passive margin. It is clear the role of the VTFZ in the emplacement of these alkaline bodies, which are under the influence of a compressive regime due to stresses from South Atlantic ridge-push and far-field stresses of the Andean Orogeny. We speculate if spatio-temporal isotopic variation along the VTR is linked to Andean uplift events and rapid changes in South Atlantic spreading due to dynamic topography caused by an active role of the asthenospheric mantle. In addition, the role of structural control in the evolution of this linear ridge should not be overlooked and additional geochronological data are necessary to properly test its role in channeling magma to the surface.

REFERENCES

- ALBERONI, A.A.L. *et al.*, 2020. The new Digital Terrain Model (DTM) of the Brazilian Continental Margin: detailed morphology and revised undersea feature names. *Geo-Mar Lett* 40, 949–964. <https://doi.org/10.1007/s00367-019-00606-x>
- ALLÈGRE, C.J., TURCOTTE, D.L., 1986. Implications of a two-component marble-cake mantle. *Nature*, v. 323, p. 123-127.
- ALMEIDA, F.F.M., 1986. Distribuição regional e relações tectônicas do magmatismo pós-Paleozóico no Brasil. *Revista Brasileira de Geociências*, v. 16, p. 325-349.
- ALMEIDA, F.F.M., 1991. O alinhamento magmático de Cabo Frio. In: *II Simpósio De Geologia do Sudeste*. SBG, São Paulo, pp. 423–428.
- AMANTE, C.; EAKINS, B.W., 2009. ETOPO1 Global Relief Model converted to PanMap layer format. NOAA-National Geophysical Data Center, PANGAEA, <https://doi.org/10.1594/PANGAEA.769615>
- ALVES, E.C. *et al.*, 2006. Zona de Fratura de Vitória-Trindade no Atlântico Sudeste e suas implicações tectônicas. *Rev. Bras. Geofís.* 24, 117–127.
- ANDERSON, D.L., 1994. The sublithospheric mantle as the source of continental flood basalts, *Earth Planet. Sci. Lett.*, 123, 269-280.
- ANDERSON, D.L., 2000. The thermal state of the upper mantle: No role for mantle plumes. *Geophysical Research Letters*, 27, 3623 – 3626.
- ANDERSON, D.L., 2001. Top-Down Tectonics?. *Science*, 293, 2016-2018.
- ANDERSON, D.L., 2002. Plate tectonics as a far - from - equilibrium self - organised system, in Plate Boundary Zones (eds S. Stein and J. Freymuller), *American Geophysical Union*, Washington, DC, pp. 411 – 425.
- ANDERSON, D.L., 2005. Large igneous provinces, delamination, and fertile mantle. *Elements*, 1: 271-275.
- ANDERSON, D.L., 2007. The eclogite engine: Chemical geodynamics as a Galileo thermometer. In: FOULGER, G.R. & JURDY, D.M. (Eds.), *Plates, Plumes, and Planetary Processes. Geological Society of America Special Paper*, 430: 47-64.
- ANDERSON, D.L. Speculations on the nature and cause of mantle heterogeneity. *Tectonophysics*, 416: 7-22, 2006.

ARIENTI, L.M. *et al.*, 2012. Turbidite Systems in the Campos Basin Oligo-Miocene and Miocene, Brazil. Conference: 32nd Annual GCSSEPM Foundation Bob Perkins Research Conference - New Understanding of the Petroleum Systems of the World. At: Houston, Texas. <https://doi.org/10.5724/gcs.12.32.0410>

ARMIENTI, P., GASPERINI, D., 2007. Do we really need mantle components to define mantle composition? *J. Pet.* 48, 693–709.

BALLMER, M.D. *et al.*, 2007. Non - hotspot volcano chains originating from small - scale sublithospheric convection. *Geophysical Research Letters*, 34: L23310, doi:10.1029/2007GL031636,2007.

BARÃO, L.M., TRZASKOS, B., ANGULO, R.J., De Souza, M.C., DAUFENBACH, H.F., SANTOS, F.A., VASCONCELLOS, E.M.G., 2020. Deformational structures developed in volcanic sequences as a product of tectonic adjustments in the South Atlantic Ocean. *J. S. Am. Earth Sci.*, 104, 102812. <https://doi.org/10.1016/j.jsames.2020.102812>.

BIZZI, L.A., DE WIT, M.J., SMITH, C.B., MCDONALD, I., ARMSTRONG, R.A., 1995. Heterogeneous enriched mantle materials and Dupal-type magmatism along the SW margin of the São Francisco craton, Brazil. *J. Geodyn.* 20 (4), 469–491. [https://doi.org/10.1016/0264-3707\(95\)00028-8](https://doi.org/10.1016/0264-3707(95)00028-8).

BODINIER, J.-L. *et al.*, 2008. Origin of pyroxenite–peridotite veined mantle by refertilization reactions: evidence from the Ronda peridotite (Southern Spain). *Journal of Petrology*, 49.5: 999-1025.

BONGIOLO, E.M., PIRES, G.L.C., GERALDES, M.C., SANTOS, A.C., NEUMANN, R., 2015. Geochemical modeling and Nd-Sr data links nephelinite-phonolite successions and xenoliths of Trindade Island (South Atlantic Ocean, Brazil). *J. Volcanol. Geoth. Res.* 306, 58–73. <https://doi.org/10.1016/j.jvolgeores.2015.10.002>

BOYNTON, W.V., 1985. Cosmochemistry of the rare earth elements: Meteorite studies (Chapter 3). In: *Rare Earth Element Geochemistry* (P. Henderson. ed.). First Edition. (Developments in Geochemistry 2). Elsevier (Ed), Amsterdam, p. 115-1522.

BUNGE, H.-P., 2005. Low plume excess temperature and high core heat flux inferred from nonadiabatic geotherms in internally heated mantle circulation models. *Physics of the Earth and Planetary Interiors*, 153(1–3), 3–10, 10.1016/j.pepi.2005.03.017.

CAMPBELL, I.H., GRIFFITHS, R.W., 1990. Implications of mantle plume structure for the evolution of flood basalts. *Earth and Planetary Science Letters*, 99: 79 – 93.

CAXITO, F.A., BASTO, C.F., SANTOS, L.C.M.L., DANTAS, E.L., MEDEIROS, V.C., DIAS, T.G., BARROTE, V., HAGEMANN, S., ALKMIM, A.R., LANA, C.C., 2021. *Neoproterozoic magmatic arc volcanism in the Borborema Province, NE Brazil: possible flare-ups and lulls and implications for western Gondwana assembly.* *Gondwana Res.* 92, 1–25. <https://doi.org/10.1016/j.gr.2020.11.015>.

CELLI, N.L., LEBEDEV, S., SCHAEFFER, A.J., RAVENNA, N., GAINA, C., 2020. The upper mantle beneath the South Atlantic Ocean. South America and Africa from waveform tomography with massive data sets. *Geophys. J. Int.* 221, 178–204. <https://doi.org/10.1093/gji/ggz574>.

CIVIERO, C. *et al.*, 2019. The seismic signature of Upper-Mantle Plumes: application to the Northern East African Rift. *Geochemistry, Geophysics, Geosystems*, 20.12: 6106-6122.

CIVIERO, C. *et al.*, 2021. The role of the seismically slow Central-East Atlantic anomaly in the genesis of the Canary and Madeira volcanic provinces. *Geophysical Research Letters*, 2021, 48.13: e2021GL092874.

CHAFFEY, D.J., CLIFF, R.A., WILSON, B.M., 1989. Characterization of the St. Helena source. In: Saunders, A.D., Norry, M.J. (Eds.), *Magmatism in the Ocean Basins*, vol. 42. *Geological Society, London, Special Publications*, pp. 257–276. <https://doi.org/10.1144/GSL.SP.1989.042.01.16>.

CHAUVEL, C., HOFMANN, A.W., VIDAL, P., 1992. HIMU-EM: the French Polynesian connection. *Earth and Planetary Science Letters*, 110: 99–119.

CHASE, C. G., 1981. Oceanic island Pb: two-stage histories and mantle evolution. *Earth Planet Sci Lett*, 52: 277±284.

CLAGUE, D.A., FREY, F.A., 1982. Petrology and trace element geochemistry of the Honolulu Volcanics, Oahu: Implications for the oceanic mantle below Hawaii. *J. Petrol.* 23, 447-504, 1982.

CLASS, C., LE ROEX, A.P., 2006. Continental material in the shallow oceanic mantle — how does it get there? *Geology*, 34, 129–132.

COBBOLD, P.R., MEISLING, K.E., MOUNT, V.S., 2001. Reactivation of an obliquely rifted margin, Campos and Santos Basins, southeastern Brazil. *AAPG (Am. Assoc. Pet. Geol.) Bull.* 85, 1925–1944. <https://doi.org/10.1306/8626D0B3-173B-11D7-8645000102C1865D>.

COGNÉ, N., GALLAGHER, K., COBBOLD, P.R., RICCOMINI, C., GAUTHERON, C., 2012. Post-breakup tectonics in southeast Brazil from thermochronological data and combined inverseforward thermal history modeling. *J. Geophys. Res.* 117, B11413. <https://doi.org/10.1029/2012JB009340>.

COLLI, L., STOTZ, I., BUNGE, H.P., SMETHURST, M., CLARK, S., IAFFALDANO, G., TASSARA, A., GUILLOCHEAU, F., BIANCHI, M.C., 2014. Rapid South Atlantic spreading changes and coeval vertical motion in surrounding continents: evidence for temporal changes of pressure-driven upper mantle flow. *Tectonics* 33, 1304–1321. <https://doi.org/10.1002/2014TC003612>.

GHELICKHAN, S., BUNGE, H.-P., OESER, J., 2018. Retrodictions of Mid Paleogene mantle flow and dynamic topography in the Atlantic region from compressible high resolution adjoint mantle convection models: sensitivity to deep mantle viscosity and

tomographic input model. *Gondwana Res.* 53, 252–272.
<https://doi.org/10.1016/j.gr.2017.04.027>.

CONRAD, C.P., LITHGOW-BERTELLONI, C., 2006. Influence of continental roots and asthenosphere on plate-mantle coupling. *Geophysical Research Letters*, 33:L05312. <https://doi.org/10.1029/2005GL025621>

CORDANI, U.G., 1970. Idade do vulcanismo do Oceano Atlântico Sul. *Boletim do Instituto de Geociências e Astronomia (IGA-USP)*, vol. 1, pp. 9–75.

CORDANI, U.G., BLAZEKOVIĆ, A., 1970. Idades radiométricas das rochas vulcânicas dos Abrolhos. In: *Congresso Brasileiro de Geologia*, Brasília, Brazil.

CORDANI, U.G., RAMOS, V.A., FRAGA, L.M., CEGARRA, M., DELGADO, I., SOUZA, K.G.D., SCHOBENHAUS, C., 2016. Tectonic map of South America. CGMW-CPRM-SEGEMAR. <http://rigeo.cprm.gov.br/jspui/handle/doc/16750>.

COURTILLOT, V. *et al.*, 2003. Three distinct types of hotspots in the Earth's mantle. *Earth and Planetary Science Letters*, 205: 295 – 308.

CONTRERAS, J., ZÜHLKE, R., BOWMAN, S., BECHSTADT, T., 2010. Seismic stratigraphy and subsidence analysis of the southern Brazilian margin (Campos, Santos and Pelotas basins). *Mar. Petrol. Geol.* 27 <https://doi.org/10.1016/j.marpetgeo.2010.06.007>, 1952–1980.

COWIE, L., KUSZNIR, N., 2018. Renormalisation of global mantle dynamic topography predictions using residual topography measurements for “normal” oceanic crust. *Earth Planet. Sci. Lett.* 499 (3), 145–156. <https://doi.org/10.1016/j.epsl.2018.07.018>.

CHRISTENSEN, U. R., HOFMANN A. W., 1994. Segregation of subducted oceanic crust in the convecting mantle. *J Geophys Res* 99: 19867±19884.

CROUGH, S.T., MORGAN, W.J., HARGREAVES, R.B, 1980. Kimberlites: their relation to mantle hot spots. *Earth and Planetary Science Letters*, v.50. p. 260–274.

CROUGH, S.T., 1983. Hotspot swells. *Annual Reviews in Earth and Planetary Sciences*, 11: 165 – 193.

DASGUPTA R., JACKSON M. G., LEE C.-T. A., 2010. Major element chemistry of ocean island basalts — Conditions of mantle melting and heterogeneity of mantle source. *Earth Planet. Sci. Lett.* 289, 377–392.

DAY, J. M. D. *et al.*, 2009. Pyroxenite-rich mantle formed by recycled oceanic lithosphere: oxygen–osmium isotope evidence from Canary Island lavas. *Geology*, 37, 555–558.

DAY, J.M.D., *et al.*, 2010. Evidence for distinct proportions of subducted oceanic crust and lithosphere in HIMU-type mantle beneath El Hierro and La Palma, Canary Islands. *Geochem. Cosmochim. Acta* 74, 6565–6589. <https://doi.org/10.1016/j.gca.2010.08.021>.

DUNCAN, R.A., 1981. Hotspots in the southern oceans - An absolute frame of reference for motion of the Gondwana continents. *Tectonophysics*, v. 74 (1-2). p. 29-42.

DUNCAN, R.A.; RICHARDS, M.A. Hotspots, mantle plumes, flood basalts, and true polar wander. *Rev. Geophys.* 29, 31-50, 1991.

ELLAM, R.M., 1992. Lithospheric thickness as a control on basalt geochemistry. *Geology* 20, 153±156.

EUGENE, B., FIDUK, J., LOVE, F., GIBBS, P., LARSEN, S.B., FARROW, G., 2004. The Rio Doce Canyon System in the Northern Espirito Santo Basin, Offshore Brazil: A Model for Interpreting Ancient Deep-Water Sand Transportation Fairways. Search and Discovery Article #30028. Adapted from extended abstract for presentation at AAPG Annual Convention, Dallas, TX, April 18-21.

EWART, A., *et al*, 2004. Petrology and geochemistry of early cretaceous bimodal continental flood volcanism of the NW Etendeka, Namibia. Part 1. Introduction, mafic lavas and re-evaluation of mantle source components. *J. Petrol.* 45 (1), 59–105.

FARLEY, K.A., NATLAND, J.H., CRAIG, H., 1992. Binary mixing of enriched and undegassed (primitive?) mantle components (He, Sr, Nd, Pb) in Samoan lavas. *Earth and Planetary Science Letters*, 111, 183±199.

FERRARI, A., RICCOMINI, C., 1999. Campo de esforços Plio Pleistocênico na Ilha de Trindade (Oceano Atlântico Sul, Brasil) e sua relação com a tectônica regional. *Rev. Bras. Geociencias* 29, pp. 195–202.

FODOR, R.V., HANAN, B.B., 2000. *Geochemical evidence for the Trindade Hotspot trace: Columbia seamount ankaramite*. *Lithos* 51, 293–304. [https://doi.org/10.1016/S0024-4937\(00\)00002-5](https://doi.org/10.1016/S0024-4937(00)00002-5).

FODOR, R.V., MCKEE, E.H., ASMUS, H.E., 1983. K-Ar ages and the opening of the South Atlantic Ocean: basaltic rock from the Brazilian margin. *Marine Geology*, v. 54, M1-M8.

FODOR, R.V., MUKASA, S.B., GOMES, C.B., CORDANI, U.G., 1989. Ti-rich eocene basaltic rocks, abrolhos platform, Offshore Brazil, 18°S: petrology with respect to South Atlantic magmatism. *J. Petrol.* 30, 763–786. <https://doi.org/10.1093/petrology/30.3.763>.

FOULGER, G.R., 2007. The “ Plate ” model for the genesis of melting anomalies. In: *Plates, Plumes, and Planetary Processes (eds G.R. Foulger and D.M. Jurdy)*, Geological Society of America , Boulder, CO , pp. 1 – 28 .

FOULGER, G.R.; ANDERSON, D.L., 2005. A cool model for the Iceland hotspot. *Journal of Volcanology and Geothermal Research*, 144: 1-22.

FOULGER , G.R., NATLAND , J.H., 2003. Is “ hotspot ” volcanism a consequence of plate tectonics? *Science*, 300: 921 – 922.

FOULGER, G.R., 2010. Plates vs. Plumes: A Geological Controversy. *Economic Geology*, 106 (3): 525–526.

FOULGER, G.R. (2010), *Plates vs. Plumes: A Geological Controversy*, pp. 328+xii, Wiley-Blackwell, ISBN 978-1-4051-6148-0.

FOULGER, G.R. The “plate” model for the genesis of melting anomalies. In: FOULGER, G.R. & JURDY, D.M. (Eds.), *Plates, Plumes, and Planetary Processes. Geological Society of America Special Paper*, 430: 1-28, 2007.

FRANÇA, R.L., DEL REY, A.C., TAGLIARI, C.V., BRANDÃO, J.R., FONTANELLI, P.D.R., 2007. Bacia do Espírito Santo. *Bol. Geociencias Petrobras* 15 (2), 501–509.

GALER, S.J.G., ABOUCHAMI, W., 1998. Practical application of lead triple spiking for correction of instrumental mass discrimination. *Mineralogical Magazine* 62 (A), 491–492.

GELDMACHER, J., *et al.*, 2011. Hafnium isotopic variations in East Atlantic intraplate volcanism. *Contributions to Mineralogy and Petrology*, 162.1: 21-36.

GEORGE RM, ROGERS NW, 2002. Plume dynamics beneath the African plate inferred from the geochemistry of the Tertiary basalts of Southern Ethiopia. *Contrib Mineral Petrol* 144:286–304.

GERALDES, M.C.; MOTOKI, A.; COSTA, A.; MOTA, C.E.; MOHRIAK, W.U., 2013. Geochronology (Ar/Ar and K-Ar) of the South Atlantic post-break-up magmatism. *Geological Society London Special Publications*, v. 369, n. 1, p. 41-74.

GERLACH, D.C., STORMER, J.C., MUELLER, P.A., 1987. Isotopic geochemistry of Fernando de Noronha. *Earth and Planetary Sciences Letters*, 85:129-144. doi: [https://doi.org/10.1016/0012-821X\(87\)90027-6](https://doi.org/10.1016/0012-821X(87)90027-6)

GIBSON, S.A., THOMPSON, R.N., LEONARDOS, O.H., DICKIN, A.P., MITCHELL, J.G., 1995. The Late Cretaceous impact of the Trindade mantle plume: evidence from large-volume, mafic, potassic magmatism in *SE Brazil*. *J. Petrol.* 36, 189–229. <https://doi.org/10.1093/petrology/36.1.189>.

GIBSON, S.A., THOMPSON, R.N., WESKA, R.K., DICKIN, A.P., LEONARDOS, O.H., 1997. Late Cretaceous rift-related upwelling and melting of the Trindade starting mantle plume head beneath western Brazil. *Contrib. Mineral. Petrol.* 126, 303–314. <https://doi.org/10.1007/s004100050252>.

GOLDSTEIN, S.L. *et al.*, 2008. Origin of a 'Southern Hemisphere' geochemical signature in the Arctic upper mantle. *Nature*, 453 (7191), 89–93.

GREEN, T.H., GREEN, D.H., RINGWOOD, A.E., 1967, The origin of high-alumina basalts and their relationships to quartz tholeiites and alkali basalts. *Earth and Planetary Science Letters*, v. 2, p. 41–51.

GRIFFITHS, R.W., CAMPBELL, I.H., 1990. Stirring and structure in mantle plumes.

Earth and Planetary Science Letters, 99: 66 – 78.

GURENKO, A.A. *et al.*, 2009. Enriched, HIMU-type peridotite and depleted recycled pyroxenite in the Canary plume: A mixed-up mantle. *Earth and Planetary Science Letters* 277, 514-524.

HALLIDAY, A.N., DAVIES, G.R., LEE, D.C., TOMMASINI, S., OASLICK, C.R., FITTON, J.G., JAMES, D.E., 1992. Lead isotope evidence for young trace element enrichment in the oceanic upper mantle. *Nature* 359, 623–627. <https://doi.org/10.1038/359623a0>.

HALLIDAY, A.N., LEE, D.C., TOMMASINI, S., DAVIES, G.R., PASLICK, C.R., FITTON, G.J., JAMES, D.E., 1995. Incompatible trace elements in OIB and MORB and source enrichment in the sub-oceanic mantle. *Earth Planet. Sci. Lett.* 133, 379–395.

HART, S.R. 1984. A large-scale isotopic anomaly in the Southern Hemisphere mantle. *Nature (London)*, 309: 753–757.

HART, S.R., 1988. Heterogeneous mantle domains: signatures, genesis and mixing chronologies. *Earth Planet Sci. Lett.* 90, 272–296. [https://doi.org/10.1016/0012-821X\(88\)90131-8](https://doi.org/10.1016/0012-821X(88)90131-8).

HART, S.R. *et al.*, 1992. Mantle plumes and entrainment: Isotopic evidence. *Science*, 256, 517±520.

HAURI, E.H., WHITEHEAD, J.A., HART, S.R., 1994. Fluid dynamic and geochemical aspects of entrainment in mantle plumes. *Journal of Geophysical Research*, 99, 24275±24300.

HACKSPACHER, P.C., GODOY, D.F., RIBEIRO, L.F.B., HADLER NETO, J.C., FRANCO, A.O.B., 2007. Modelagem térmica e geomorfologia da borda sul do Cráton do São Francisco: termocronologia por traços de fissão em apatita. *Rev. Bras. Geociencias* 37 (4 - Suppl. o), 76–86.

HAWKESWORTH, C.J., MANTOVANI, M.S.M., TAYLOR, P.N., PALACZ, Z., 1986. Evidence from the Paraná of south Brazil for a continental contribution to Dupal basalts. *Nature* 322, 356–359. <https://doi.org/10.1038/322356a0>.

HEILBRON, M., TUPINAMBÁ, M., VALERIANO, C.M., ARMSTRONG, R., EIRADO, L.G.S., MELO, R.S., SIMONETTI, A., SOARES, A.C.P., MACHADO, N., 2013. The Serra da Bolívia Complex: *The record of a new Neoproterozoic arc-related unit at Ribeira belt. Precambrian Research*, 238:158-175. <https://doi.org/10.1016/j.precamres.2013.09.014>

HEILBRON, M. CORDANI, U.G., ALKMIM, F.F., REIS, H.L.S., 2017. Tectonic genealogy of a miniature continent. In: M. Heilbron, U. Cordani, F. Alkmim (Eds.), *The São Francisco Craton and its Margins: Tectonic Genealogy of a Miniature Continent*, vol. 17, Springer, Regional Geological Reviews, pp. 321-331 https://doi.org/10.1007/978-3-319-01715-0_17.

HEILBRON, M., VALERIANO, C.M., PEIXOTO, C., TUPINAMBÁ, M., NEUBAUER, F., DUSSIN, I., CORRALES, F., BRUNO, H., LOBATO, M., ALMEIDA, J.C.H., SILVA, L.G.E., 2020. Neoproterozoic magmatic arc systems of the central Ribeira belt, SE-Brazil, in the context of the West-Gondwana pre-collisional history: A review. *Journal of South American Earth Sciences*, 102710. <https://doi.org/10.1016/j.jsames.2020.102710>

HEINE, C., ZOETHOURT, J., MULLER, R.D., 2013. Kinematics of the South Atlantic rift. *Solid Earth*, 4:215–253. <https://doi.org/10.5194/se-4-215-2013>

HERBOZO, G., KUKOWSKI, N., CLIFT, P.D., PECHER, I., BOLAÑOS, R., 2020. Cenozoic increase in subduction erosion during plate convergence variability along the convergent margin off Trujillo, Peru. *Tectonophysics*, V. 790, 228557, <https://doi.org/10.1016/j.tecto.2020.228557>.

HERZ, 1977. *Timing of spreading in the South Atlantic: Information from Brazilian alkalic rocks Geological Society of America Bulletin*, January, v. 88(1), p. 101-112.

HIROSE, K., 1997. Partial melt compositions of carbonated peridotite at 3 GPa and role of CO₂ in alkali-basalt magma generation. *Geophysical Research Letters*, 24(22), 2837–2840. <https://doi.org/10.1029/97gl02956>

HIRUMA, S.T., RICCOMINI, C., MODENESI-GAUTIERRI, M.C., HACKSPACHER, P.C., HADLER NETO, J.C., FRANCO-MAGALHÃES, A.O.B., 2010. Denudation history of the Bocaina Plateau, Serra do Mar, southeastern Brazil: relationships to Gondwana breakup and passive margin development. *Gondwana Res.* 18, 674–687. <https://doi.org/10.1016/j.gr.2010.03.001>.

HIRSCHMANN, M.M; STOLPER, E.M., 1996. A possible role for garnet pyroxenite in the origin of the “garnet signature” in MORB. *Contributions to Mineralogy and Petrology*, 124: 185-208.

HIRSCHMANN, M.M. *et al.*, 2003. Alkalic magmas generated by partial melting of garnet pyroxenite. *Geology*, 31, 481–484.

HOFMANN, A.W., WHITE, W.M., 1982. Mantle plumes from ancient oceanic crust. *Earth Planet. Sci. Lett.* 57, 421–436.

HOFMANN, A.W., 1997. Mantle Geochemistry: The message from the oceanic volcanism. *Nature*, 385: 219-229.

HOFMANN, A.W., 2003. Sampling mantle heterogeneity through oceanic basalts: isotopes and trace elements. In: *Holland, H.D., Turekian, K.K. (Eds.), Treatise on Geochemistry*, vol. 2. Elsevier, pp. 61–101.

HOFMANN, A.W., 2014. Sampling Mantle Heterogeneity through Oceanic Basalts: Isotopes and Trace Elements. In: *Holland, H.D., Turekian, K.K. (Eds.), 3.3 – Treatise on Geochemistry*, second ed., vol. 3, pp. 67–101. <https://doi.org/10.1016/B978-0-08->

0959757.00203-5.

ITO, G.; VAN KEKEN, P.E., 2007. Hotspots and melting anomalies. *Treatise on Geophysics*, v. 7, p. 371–435.

JACKSON, M.G., DASGUPTA, R., 2008. Compositions of HIMU, EM1, and EM2 from global trends between radiogenic isotopes and major elements in ocean island basalts. *Earth Planet Sci. Lett.* 276, 175–186. <https://doi.org/10.1016/j.epsl.2008.09.023>.

JACKSON, E.D., SHAW, H.R., BARGER, K.E., 1975. Calculated geochronology and stress field orientations along the Hawaiian chain. *Earth and Planetary Science Letters*, 26: 145 – 155.

JANNEY, P.E., *et al.* 2000. Geochemical evidence from the Pukapuka volcanic ridge system for a shallow enriched mantle domain beneath the South Pacific Superswell. *Earth. Planet. Sci. Lett.* 181, 47-60.

JAPSEN, P., BONOW, J.M., GREEN, P.F., COBBOLD, P.R., CHIOSSI, D., LILLETVEIT, R., MAGNAVITA, L.P., PEDREIRA, A., 2012. Episodic burial and exhumation in NE Brazil after opening of the South Atlantic. *Bull. Geol. Soc. Am.* 124, 800–816. <https://doi.org/10.1130/B30515.1>.

JESUS, J.V.M., SANTOS, A.C., MENDES, J.C., SANTOS, W.H., REGO, C.A.Q., GERALDES, M.C., 2019. Petrogênese do Banco Davis, Cadeia Vitória-Trindade, Atlântico Sul: o Papel de Voláteis (H₂O e CO₂) na Evolução Magmática do Banco Davis. *Anu. do Inst. Geociências* 42, 237–253. https://doi.org/10.11137/2019_3_237_253.

JIANG, Qiang, *et al.*, 2021. Origin of geochemically heterogeneous mid-ocean ridge basalts from the Macquarie Ridge Complex, SW Pacific. *Lithos*, 380: 105893.

JUNG, C., *et al.*, 2006. Petrogenesis of Tertiary mafic alkaline magmas in the Hoheifel, Germany. *Journal of Petrology*, 47.8: 1637-1671.

KAMENETSKY, V.S. *et al.*, 2001. Remnants of Gondwanan continental lithosphere in oceanic upper mantle: evidence from the South Atlantic Ridge. *Geology*, 29 (3), 243–246.

KELEMEN *et al.*, 2014. One view of the geochemistry of subduction-related magmatic arcs, with an emphasis on primitive andesite and lower crust. *Treatise on Geochemistry*, 4, pp. 749-805.

KING, S.D., ANDERSON, D.L., 1998. Edge-driven convection. *Earth Planet. Sci. Lett.* 160, 289–296. [https://doi.org/10.1016/S0012-821X\(98\)00089-2](https://doi.org/10.1016/S0012-821X(98)00089-2)

KING, S.D., RITSEMA, J., 2000. African hot spot volcanism: Small – scale convection in the upper mantle beneath cratons. *Science*, 290: 1137 – 1140.

KOGISO, T., HIRSCHMANN, M.M., 2006. Partial melting experiments of bimineralec eclogite and the role of recycled mafic oceanic crust in the genesis of ocean island basalts. *Earth Planet. Sci. Lett.* 249, 188–199.

KOGISO T. *et al.*, 1997. High l (HIMU) ocean island basalts in southern Polynesia: New evidence for whole mantle scale recycling of subducted oceanic crust. *J. Geophys. Res.* 102, 8085–8103.

KONRAD, K. *et al.*, 2018. On the relative motions of long-lived Pacific mantle plumes. *Nature Communications*, 9, 854.

KORENAGA, J.; KELEMEN, P.B. 2000. Major element heterogeneity in the mantle

source of the north Atlantic igneous province. *Earth Planet. Sci. Lett.*, 184, 251-268.

- KNESEL, K.M., DE SOUZA, Z.S., VASCONCELOS, P.M., COHEN, B.E., SILVEIRA, F.V., 2011. $^{40}\text{Ar}/^{39}\text{Ar}$ Argeochronology reveals the youngest volcanism in mainland Brazil and no evidence for a plume trace on the continent. *Earth and Planetary Science Letters* 302, 38–50.
- KOPPERS, A.A.P., 2002. ArArCALC-software for $^{40}\text{Ar}/^{39}\text{Ar}$ age calculations. *Computers and Geosciences*, 28(5):605–619. [https://doi.org/10.1016/S0098-3004\(01\)00095-4](https://doi.org/10.1016/S0098-3004(01)00095-4)
- LASSITER, J.C., HAURI, E.H., 1998. Osmium-isotope variations in Hawaiian lavas: evidence for recycled oceanic lithosphere in the Hawaiian plume. *Earth and Planetary Science Letters*, v. 164, p. 483-496.
- LE BAS, M.J. & STRECKEISEN, A.L., 1991. The IUGS systematics of igneous rocks. *Journal of the Geological Society*, London. V. 148, p. 825–833.
- LE BAS, M.J. *et al.*, 1986. A chemical classification of volcanic rocks based on the total alkali-silica diagram. *Journal of Petrology*, v. 27, p. 745-750, 1986.
- LE MAITRE, R.W., 2005. *Igneous Rocks: A Classification and Glossary of Terms: Recommendations of the International Union of Geological Sciences Subcommittee on the Systematics of Igneous Rocks*. 2nd Edition. Cambridge University Press. 256p.
- LE ROEX, A. P., DICK, H. J. B., FISHER, R. L., 1989. Petrology and geochemistry of MORB from 258E to 468E along the Southwest Indian Ridge: evidence for contrasting styles of mantle enrichment. *Journal of Petrology*, 30, 947-986.
- LE ROUX, P. J. *et al.*, 2002. Mantle heterogeneity beneath the southern Mid-Atlantic Ridge: trace element evidence for contamination of ambient asthenospheric mantle. *Earth and Planetary Science Letters* 203, 479-498.
- LE ROEX, A. *et al.*, 2010. Shona and discovery Aseismic Ridge Systems, South Atlantic: trace element evidence for enriched mantle sources. *Journal of Petrology*, 51: 2089–2120.
- LE ROEX, A.P., AND LANYON, R., 1998. Isotope and trace element geochemistry of Cretaceous Damaraland lamprophyres and carbonatites, northwestern Namibia: Evidence for plume lithosphere interaction. *Journal of Petrology*, v. 39, p. 1117–1146, doi: 10.1093/petrology/39.6.1117.
- LOUBET, M., SASSI, R., DI DONATO, G., 1988. Mantle heterogeneities: a combined isotope and trace element approach and evidence for recycled continental crust materials in some OIB sources. *Earth and Planetary Science Letters*, Volume 89, Issues 3–4, Pages 299-315, ISSN 0012-821X, [https://doi.org/10.1016/0012-821X\(88\)90118-5](https://doi.org/10.1016/0012-821X(88)90118-5).
- LUSTRINO, M., 2005. How the delamination and detachment of the lower crust can influence basaltic magmatism. *Earth Science Review*, 72: 21-38.
- MALLIK, A., DASGUPTA, R., 2012. Reaction between MORB-eclogite derived melts and fertile peridotite and generation of ocean island basalts. *Earth and Planetary Science Letters* 329-330, 97-108.

MAIA, T.M. Petrologia inédita das rochas do Monte Submarino Vitória, Cadeia Vitória Trindade, Atlântico Sul, 2019. 92 p. Monography Geology Bsc. Course, Rio de Janeiro State University, Rio de Janeiro, Brazil,

MAIA, T.M., SANTOS, A.C., ROCHA-JÚNIOR, E.R.V., VALERIANO, C.M., MENDES, J.C., JECK, I.K., SANTOS, W.H., OLIVEIRA, A.L., MOHRIAK, W.U., 2021. First petrologic data for Vitória Seamount, Vitória-Trindade Ridge, South Atlantic: a contribution to the Trindade mantle plume evolution. *Journal of S. Am. Earth Sci.* v. 109, 103304. <https://doi.org/10.1016/j.jsames.2021.103304>.

MANJÓN-CABEZA CÓRDOBA, A., BALLMER, M. D., 2021. The role of edge-driven convection in the generation of volcanism – Part 1: A 2D systematic study. *Solid Earth*, 12, 613–632. <https://doi.org/10.5194/se-12-613-2021>

MARQUES, L.S., ULBRICH, M.N.C., RUBERTI, E., TASSINARI, C.G., 1999. Petrology, geochemistry and Sr-Nd isotopes of the trindade and Martin Vaz volcanic rocks (southern Atlantic Ocean). *J. Volcanol. Geoth. Res.* 93, 191–216. [https://doi.org/10.1016/S0377-0273\(99\)00111-0](https://doi.org/10.1016/S0377-0273(99)00111-0).

MARQUES, L.S., DE MIN, A., ROCHA-JÚNIOR, E.R.V., BABINSKI, M., BELLIENI, G., FIGUEIREDO, A.M.G., 2018. Elemental and Sr-Nd-Pb isotope geochemistry of the Florianópolis Dyke Swarm (Paraná Magmatic Province): Crustal contamination and mantle source constraints. *Journal of Volcanology and Geothermal Research*, 355, 149-164.

MARTINS, S., J. MATA, J. MUNHÁ, M. H. MENDES, C. MAERSCHALK, R. CALDEIRA, N. MATTIELL, 2010. Chemical and mineralogical evidence of the occurrence of mantle metasomatism by carbonate-rich melts in an oceanic environment (Santiago Island, Cape Verde). *Mineralogy and Petrology*, v. 99, n. 1–2, p. 43–65.

MATA, J., *et al.*, 1998. Elemental and isotopic (Sr, Nd, and Pb) characteristics of Madeira Island basalts: evidence for a composite HIMU-EM I plume fertilizing lithosphere. *Canadian Journal of Earth Sciences*, 35.9: 980-997.

MEISLING, K.E., COBBOLD, P.R., MOUNT, V.S., 2001. Segmentation of an obliquely rifted margin, Campos and Santos basins, southeastern Brazil. *AAPG (Am. Assoc. Pet. Geol.) Bull.* 85, 1903–1924. <https://doi.org/10.1306/8626D0A9-173B-11D7-8645000102C1865D>.

MIZUSAKI, A.M., ALVES, D.B., CONCEIÇÃO, J.C.J., 1994. Eventos magmáticos nas bacias do Espírito Santo, Mucuri e Cumuruxatiba. In: *CONGR. BRAS. GEOL.* 38, Baln. Camboriú, B. Res. Expandidos. Baln. Camboriú: SBG L., pp. 566–567.

MOHRIAK, W.U., 2005. Interpretação geológica e geofísica da Bacia do Espírito Santo e da região de Abrolhos: petrografia, datação radiométrica e visualização sísmica das rochas vulcânicas. *Bol. Geociencias Petrobras* 14, 133–142.

MOHRIAK, W.U., 2020. Genesis and evolution of the South Atlantic volcanic islands offshore Brazil, *Geo-Marine Letters*, 40:1–33. <https://doi.org/10.1007/s00367-019-00631-w>

MOHRIAK, W.U., ROSENDAHL, B.R., 2003. Transform zones in the South Atlantic rifted continental margins. *Geol. Soc. London, Spec. Publ.* 210, 211–228. <https://doi.org/10.1144/GSL.SP.2003.210.01.13>

MOORE, A., *et al.*, 2008 Controls on post-Gondwana alkaline volcanism in Southern Africa. *Earth and Planetary Science Letters*, 2008, 268.1-2: 151-164.

MORGAN, W.J., 1971. Convection plumes in the lower mantle. *Nature*, 230, 42 – 43.

MOTOKI, A., MOTOKI, K.F., MELO, D.P., 2012. Submarine morphology characterization of the Vitória-Trindade Chain and the adjacent areas, state of Espírito Santo, Brazil, based on the predicted bathymetry of the TOPO version 14.1. *Rev. Brasil. Geomorfol.* 13, 151–170. <https://doi.org/10.20502/rbg.v13i2.195>.

MÜLLER, R.D., SDROLIAS, M., GAINA, C., ROEST, W.R., 2008. Age, spreading rates, and spreading asymmetry of the world's ocean crust. *Geochemistry Geophysics Geosystems*, 9:Q04006. <https://doi.org/10.1029/2007GC001743>

NETO, C.C.A., VALERIANO, C.M. VAZ, G.S., MEDEIROS, S.R, RAGATKY, C.D. 2009. Composição isotópica do Sr no padrão NBS987 obtida por TIMS no Laboratório de Geocronologia e Isótopos Radiogênicos - LAGIR, da Faculdade de Geologia da UERJ. *Anais do XI Simpósio de Geologia do Sudeste, Sociedade Brasileira de Geologia*, p. 21.

NIU, Y.-L., *et al.*, 2002. Geochemistry of near-EPR seamounts: importance of source vs. process and the origin of enriched mantle component. *Earth and Planetary Science Letters*, v. 199, p. 327-345.

NOBLET, C., LAVENU, A., MAROCCO, R., 1996. Concept of continuum as opposed to periodic tectonism in Andes. *Tectonophysics* 255, 65–78.

O'CONNOR, J.M., DUNCAN, R.A., 1990. Evolution of the Walvis Ridge–Rio grande rise hot spot system: implications for african and South American plate motions over plumes. *J. Geophys. Res.* 95, 17475–17502. <https://doi.org/10.1029/JB095iB11p17475>.

O'CONNOR, J.M., JOKAT, W., WIJBRANS, J.R., COLLI, L., 2018. Hotspot tracks in the South Atlantic located above bands of fast flowing asthenosphere driven by waning pulsations from the African LLSVP, *Gondw. Res.*, 53, 197–208.

OLIVEIRA, A.L., SANTOS, A.C., NOGUEIRA, C.C., MAIA, T.M., GERALDES, M.C., 2021. Green core clinopyroxenes from Martin Vaz archipelago Plio-Pleistocenic alkaline rocks, south atlantic ocean, Brazil: a magma mixing and polybaric crystallization record. *J. S. Am. Earth Sci.* <https://doi.org/10.1016/j.jsames.2020.102951>, 102951.

PEATE, D.W. *et al.*, 1999. Petrogenesis and stratigraphy of the High-Ti/Y Urubici magma type in the Paraná Flood Basalt Province and implications for the nature of the 'Dupal'- type mantle in the South Atlantic Region. *J. Petrol.* 40, 451–473.

PEIXOTO, C.A., HEILBRON, M., RAGATKY, D., ARMSTRONG, R., DANTAS, E., VALERIANO, C.M., SIMONETTI, A., 2017. Tectonic evolution of the Juvenile Tonian Serra

da Prata magmatic arc in the Ribeira belt, SE Brazil: Implications for early west Gondwana amalgamation. *Precambrian Research* 302, 221–254.

PERLINGEIRO, G., VASCONCELOS, P.M., KNESEL K.M., THIEDE, D.S., CORDANI, U.G., 2013. $^{40}\text{Ar}/^{39}\text{Ar}$ geochronology of the Fernando de Noronha Archipelago and implications for the origin of alkaline volcanism in the NE Brazil. *Journal of Volcanology and Geothermal Research* 249, 140-154. <http://dx.doi.org/10.1016/j.jvolgeores.2012.08.017>

PEYVE, A.A., SKOLOTNEV, S.G., 2014. Systematic variations in the composition of volcanic rocks in tectono-magmatic seamount chains in the Brazil Basin. *Geochem. Int.* 52, 111–130. <https://doi.org/10.1134/S0016702914020062>.

PILET, S., BAKER, M.B., STOLPER, E.M., 2008. Metasomatized lithosphere and the origin of alkaline lavas. *Science*, 20:916-919. <https://doi.org/10.1126/science.1156563>

HERNANDEZ, J., SYLVESTER, P., POUJOL, M., 2005. The metasomatic alternative for ocean island basalt chemical heterogeneity. *Earth and Planetary Science Letters*, 236:148-166. <https://doi.org/10.1016/j.epsl.2005.05.00434>

BAKER, M.B., MÜNTENER, O., STOLPER, E.M., 2011. Monte Carlo Simulations of Metasomatic Enrichment in the Lithosphere and Implications for the Source of Alkaline Basalts. *Journal of Petrology*, 52:1415-1442. <https://doi.org/10.1093/petrology/egr007>

PEYVE, A. A., SKOLOTNEV, S. G., 2014. Systematic variations in the composition of volcanic rocks in tectonomagmatic seamount chains in the Brazil Basin. *Geochem. Int.* 52, 111–130.

PIRES, G.L.C., BONGIOLO, E.M., 2016. The nephelinitic–phonolitic volcanism of the Trindade Island (South Atlantic Ocean): Review of the stratigraphy, and inferences on the volcanic styles and sources of nephelinites. *Journal of South American Earth Sciences*, 72:49-62. <https://doi.org/10.1016/j.jsames.2016.07.008>

PIRES, G.L.C., BONGIOLO, E.M., GERALDES, M.C., RENAC, C., SANTOS, A.C., JOURDAN, F., NEUMANN, R., 2016. New $^{40}\text{Ar}/^{39}\text{Ar}$ ages and revised $^{40}\text{K}/^{40}\text{Ar}^*$ data from nephelinitic–phonolitic volcanic successions of the Trindade Island (South Atlantic Ocean). *J. Volcanol. Geoth. Res.* 327, 531–538. <https://doi.org/10.1016/j.jvolgeores.2016.09.020>.

QUARESMA, G.O.A., 2019. Geoquímica Isotópica Sr-Nd-Pb e Geocronologia $^{40}\text{Ar}/^{39}\text{Ar}$ do Banco Submarino Davis, Cadeia Vitória-Trindade: Possíveis Implicações com a Movimentação da Placa Sul-Americana durante o Mioceno. 121 p. *Monography Geology Bsc. Course, Rio de Janeiro State University*, Rio de Janeiro, Brazil.

REGELOUS, M., NIU, Y.L., ABOUCHAMI, W., CASTILLO, P.R., 2009. Shallow origin for South Atlantic Dupal Anomaly from lower continental crust: geochemical evidence from the Mid-Atlantic Ridge at 26 degrees S. *Lithos* 112, 57–72.

REGO, C.A.Q., QUARESMA, G.O., SANTOS, A.C., MOHRIAK, W.U., JESUS,

J.V.M., RODRIGUES, S.W.O., 2021. Davis Bank geodynamic context, South Atlantic Ocean: Insights into the Vitória-Trindade Ridge evolution. *Journal of South American Earth Sciences*, v. 112, 103620. <https://doi.org/10.1016/j.jsames.2021.103620>

REHKÄMPER, M., HOFMANN, A.W., 1997. Recycled ocean crust and sediment in Indian Ocean MORB. *Earth Planet. Sci. Lett.* 147, 93–106.

RENNE, P.R., MUNDIL, R., BALCO, G., MIN, K., LUDWIG, K.R., 2010. Joint determination of ^{40}K decay constants and $^{40}\text{Ar}^*/^{40}\text{K}$ for the Fish Canyon sanidine standard, and improved accuracy for $^{40}\text{Ar}/^{39}\text{Ar}$ geochronology. *Geochimica et Cosmochimica Acta*, 74: 5349– 5367. <https://doi.org/10.1016/j.gca.2010.06.017>

RENNE, P.R., BALCO, G., LUDWIG, K.R., MUNDIL, R., MIN, K., 2011. Response to the comment by W.H. Schwarz *et al.* on “Joint determination of K-40 decay constants and Ar- 40*/K-40 for the Fish Canyon sanidine standard, and improved accuracy for Ar- 40/Ar-39 geochronology” by Renne *et al.* (2010). *Geochimica Cosmochimica Acta*, 75:5097–5100. <https://doi.org/10.1016/j.gca.2011.06.021>

RICCOMINI, C., VELÁZQUEZ, V.F., GOMES, C.B., 2005. Tectonic controls of the enozoic and enozoic alkaline magmatism in central-southeastern Brazilian Platform. In: Comin-Chiaramonti, P., Gomes, C.B. (Eds.), *Mesozoic to Cenozoic Alkaline Magmatism in the Brazilian Platform. Edusp-Fapesp*, São Paulo, pp. 31–56.

ROCHA M.P., SCHIMMEL M., ASSUMPCÃO M., 2011. Uppermantle seismic structure beneath SE and Central Brazil from P- and S-wave regional travel-time tomography. *Geophysical Journal International*, 184:268-286.

ROCHA-JÚNIOR, E.R.V. *et al.*, 2013. Sr-Nd-Pb isotopic constraints on the nature of the mantle sources involved in the genesis of the high-Ti tholeiites from Northern Paraná Continental Flood Basalts (Brazil). *J. S. Am. Earth Sci.* 46, 9–25. <https://doi.org/10.1016/j.jsames.2013.04.004>.

ROCHA-JÚNIOR, E.R.V., MARQUES, L.S., BABINSKI, M., MACHADO, F.B., PETRONILHO, L.A., NARDY, A.J.R., 2020. A telltale signature of Archean lithospheric mantle in the Paraná continental flood basalts genesis. *Lithos*, 364-365, 105519. <https://doi.org/10.1016/j.lithos.2020.105519>

RUDNICK, R. L., FOUNTAIN, D. M., 1995. Nature and composition of the continental crust: a lower crustal perspective. *Reviews in Geophysics*, 33, 267–309.

SAGER, W.W., 2007. Divergence between paleomagnetic and hotspot model predicted polar wander for the Pacific plate with implications for hotspot fixity. In: *Plates, Plumes, and Planetary Processes (eds G.R. Foulger and D.M. Jurdy)*, Geological Society of America, Boulder, CO, pp. 335 – 358.

SALTERS, V.J.M., STRACKE, A., 2004. Composition of the depleted mantle. *G-cubed* 5, Q05B07. <https://doi.org/10.1029/2003GC000597>.

SANTOS, A.C., 2013. *Petrography, Lithogeochemistry and $^{40}\text{Ar}/^{39}\text{Ar}$ Dating of the Seamounts and Martin Vaz Islands -Vitoria-Trindade Ridge*. Dissertation. Universidade do Estado do Rio de Janeiro, Brazil.

SANTOS, A.C., GERALDES, M.C., VARGAS, T., WILLIAMS, S., 2015. *Geology of Martin Vaz, South Atlantic, Brazil*. *J. Maps* 11, 314–322. <https://doi.org/10.1080/17445647.2014.936913>.

SANTOS, A. C., 2016. *Petrology of Martin Vaz Island and Vitoria-Trindade Ridge Seamounts: Montague, Jaseur, Davis, Dogaressa and Columbia. Trace Elements, $^{40}\text{Ar}/^{39}\text{Ar}$ Dating and Sr and Nd Isotope Analysis Related to the Trindade Plume Evidence*. Ph. D. Thesis. Universidade do Estado do Rio de Janeiro, Brazil.

SANTOS, A. C., GERALDES, M.C., SIEBEL, W., MENDES, J., BONGIOLO, E., SANTOS, W.H., GARRIDO, T.C.V., RODRIGUES, S.W.O., 2018a. Pleistocene alkaline rocks of Martin Vaz volcano, South Atlantic: low-degree partial melts of a CO₂-metasomatized mantle plume. *Int. Geol. Rev.* 61, 296–313. <https://doi.org/10.1080/00206814.2018.1425921>.

SANTOS, A. C., MOHRIAK, W.U., GERALDES, M.C., SANTOS, W.H., PONTENETO, C.F., STANTON, N., 2018b. Compiled potential field data and seismic surveys across the Eastern Brazilian continental margin integrated with new magnetometric profiles and stratigraphic configuration for Trindade Island, South Atlantic, Brazil. *Int. Geol. Rev.* 61, 1728–1744. <https://doi.org/10.1080/00206814.2018.1542634>.

SANTOS, A. C., MATA, J., JOURDAN, F., RODRIGUES, S.W. DE O., MONTEIRO, L.G.P., GUEDES, E., BENEDINI, L., GERALDES, M.C., 2021. Martin Vaz island geochronology: constraint on the Trindade Mantle Plume track from the youngest and easternmost volcanic episodes. *J. S. Am. Earth Sci.* 106, 103090. <https://doi.org/10.1016/j.jsames.2020.103090>.

SAUNDERS, A.D., NORRY, M.J., TARNEY, J., 1988. Origin of MORB and chemically-depleted mantle reservoirs: Trace element constraints. *J. Petrol.* (1), 415–445 Special Volume.

SCHAEFER, B., 2016. *Radiogenic Isotope Geochemistry: A guide for Industry Professionals*. Oxford University Press, United Kingdom, pp. 196.

SHARP, W.D., RENNE, P.R., 2005. *The $^{40}\text{Ar}/^{39}\text{Ar}$ dating of core recovered by the Hawaii Scientific Drilling Project (phase 2)*, Hilo, Hawaii. *Geochemistry Geophysics Geosystems*, 6(4):Q04G17. <https://doi.org/10.1029/2004GC000846>

SIEBEL, W., BECCHIO, R., VOLKER, F., HANSEN, M.A.F., VIRAMONTE, J., TRUMBULL, R.B., HAASE, G., ZIMMER, M., 2000. Trindade and Martin Vaz islands, South Atlantic: isotopic (Sr, Nd, Pb) and trace element constraints on plume related magmatism. *J. S. Am. Earth Sci.* 13, 79–103. [https://doi.org/10.1016/S0895-9811\(00\)00015-8](https://doi.org/10.1016/S0895-9811(00)00015-8).

SKOLOTNEV, S. G., PEYVE, A. A., TURKO, N. N., 2010. New data on the structure of the Vitoria–Trindade seamount chain (western Brazil basin, South Atlantic). *Dokl. Earth Sci.* **431**, 435–440.

SKOLOTNEV, S.G., PEIVE, A.A., 2017. Composition, structure, origin, and evolution of offaxis linear volcanic structures of the Brazil Basin, South Atlantic. *Geotectonics* 51, 53–

73. <https://doi.org/10.1134/S001685211701006X>.

SKOLOTNEV, S.G. *et al.*, 2011. First data on the age of rocks from the central part of the Vitória–Trindade Ridge (Brazil basin, South Atlantic). *Dokl. Earth Sci.* 437, 316–322. <https://doi.org/10.1134/S1028334X11030093>.

SMITH, A. D., 2013. Recycling of oceanic crust and the origin of intraplate volcanism. *Australian Journal of Earth Sciences*, 60(6-7), 675-680.

SOBOLEV A. V., HOFMANN A. W., NIKOGOSIAN I. K. (2000) Recycled oceanic crust observed in ‘ghost plagioclase’ within the source of Mauna Loa lavas. *Nature*, 404, 986– 990.

SOBOLEV, A.V., HOFMANN, A.W., SOBOLEV, S.V., NIKOGOSIAN, I.K., 2005. An olivine-free mantle source of Hawaiian shield basalts. *Nature* 434, 590-597. <https://doi.org/10.1038/nature03411>

SOBOLEV, A. V., HOFMANN, A.W., KUZMIN, D.V., YAXLEY, G.M., ARNDT, N.T., CHUNG, S.L., DANYUSHEVSKY, L.V., ELLIOTT, T., FREY, F.A., GARCIA, M.O., *et al.*, 2007. The amount of recycled crust in sources of mantle-derived melts. *Science* 316, 412–417. <https://doi.org/10.1126/science.1138113>

SOBOLEV, S. V. *et al.*, 2011 Linking mantle plumes, large igneous provinces and environmental catastrophes. *Nature*, 477.7364: 312-316.

SOBREIRA, J.F.F., FRANÇA, R.L., 2006. Um modelo tectono-magmático para a região do complexo vulcânico de Abrolhos. *Bol. Geociências Petrobras* 14, 143–147.

SOBREIRA, J.F.F. SZATMARI, P., 2003. Idades Ar–Ar para as rochas ígneas do Arquipélago de Abrolhos, margem sul da Bahia. In: *IX SNET–Simpósio Nacional de Estudos Tectônicos*, Abstracts, pp. 382–383.

SOBREIRA, J.F.F.; SZATMARI, P.; MOHRIAK, W.U.; VALENTE, S.C.; YORK, D., 2004. Recorrência, em diferentes escalas, do magmatismo paleogênico no Arquipélago de Abrolhos, Complexo Vulcânico de Abrolhos. *XLII CONGRESSO BRASILEIRO DE GEOLOGIA*, 2004, Araxá, Minas Gerais. Anais. Araxá.

SOMOZA, R., GHIDELLA, M.E., 2012. Late Cretaceous to recent plate motions in western South America revisited. *Earth Planet. Sci. Lett.* 331, 152–163.

SOUZA, D.H., HACKSPACHER, P.C., SILVA, B.V., SIQUEIRA-RIBEIRO, M.C., HIRUMA, S.T., 2021. Temporal and spatial denudation trends in the continental margin of southeastern Brazil. *Journal of South American Earth Sciences*, v. 105, 102931, 0895-9811, <https://doi.org/10.1016/j.jsames.2020.102931>.

STANTON, N., GORDON, A., CARDOZO, C., KUSZNIR, N., 2021. Morphostructure, emplacement and duration of the Abrolhos Magmatic Province: A geophysical analysis of the largest post-breakup magmatism of the South-Eastern Brazilian margin. *Marine and Petroleum Geology*, V. 133, 105230. <https://doi.org/10.1016/j.marpetgeo.2021.105230>.

STANTON, N. *et al.*, 2022. The Abrolhos Magmatic Province, the largest postbreakup magmatism of the Eastern Brazilian margin: a geological, geophysical, and geochemical review. In: *Meso-Cenozoic Brazilian Offshore Magmatism*. Academic Press, p. 189-230.

STRACKE, A., HOFMANN, A. W., HART, S. R., 2005. FOZO, HIMU, and the rest of the mantle zoo, *Geochem. Geophys. Geosyst.*, 6, Q05007, 10.1029/2004GC000824.

SUN, S.S., HANSON, G.N., 1975. Origin of Ross Island basanitoids and limitations upon the heterogeneity of mantle sources for alkali basalts and nephelinites. *Contrib. Mineral. Petrol.* 52, 77-106.

SUN, S.-S., MCDONOUGH, W.F., 1989. Chemical and isotopic systematics of ocean basalts; implications for mantle composition and processes. *Geological Society*, London, Special Publications 42, 313–345.

TADURNO, J.A., 2008. Hotspots unplugged. *Scientific American*, 1: 88-93.

TADURNO, J.A., COTTRELL, R.D., 1997. Paleomagnetic evidence for motion of the Hawaiian hotspot during formation of the Emperor seamounts. *Earth and Planetary Science Letters*, 153 : 171 – 180.

TADURNO, J.A. *et al.*, 2009. The bent Hawaiian - Emperor hotspot track: Inheriting the mantle wind. *Science*, 324: 50 – 53.

TANAKA, T., TOGASHI, S., KAMIOCA, H., 2000. JNd-1: A Neodymium isotopic reference in consistency with La Jolla Neodymium. *Chemical Geology*, 168:279–281. [https://doi.org/10.1016/S0009-2541\(00\)00198-4](https://doi.org/10.1016/S0009-2541(00)00198-4)

TAYLOR, S. R., MCLENNAN, S. M., 1985. The Continental Crust: its Composition and Evolution. *Oxford: Blackwell Scientific*, 312 pp.

TEDESCHI, M., NOVO, T., PEDROSA-SOARES, A.C., DUSSIN, I.A., TASSINARI, C.G.T., SILVA, L.C., GONÇALVES, L., ALKMIM, F.F., LANA, C., FIGUEIREDO, C., DANTAS, E., MEDEIROS, S., CAMPOS, C., CORRALES, F., HEILBRON, M., 2016. The Ediacaran Rio Doce magmatic arc revisited (Araçuaí-Ribeira orogenic system, SE Brazil). *J. S. Am. Earth Sci.* 68, 186–187.

THIRLWALL, M. F., 1995. Generation of the Pb isotopic characteristics of the Iceland plume. *J. Geol. Soc. London*, 152, 991-996.

THIRLWALL, M. F., 1997. Pb isotopic and elemental evidence for OIB derivation from young HIMU mantle. *Chemical Geology*, 139.1-4: 51-74.

THOMAZ-FILHO A.; RODRIGUES A.L., 1999. O Alinhamento de Rochas Alcalinas Poços de Caldas-Cabo Frio (RJ) e sua Continuidade na Cadeia Vitória-Trindade. *Revista Brasileira de Geociências*, v. 29(2), v. 189-194.

THOMPSON, R.N., GIBSON, S.A., MITCHELL, J.G., DICKIN, A.P., LEONARDOS, O.H., BROD, J.A., GREENWOOD, J.C., 1998. Migrating cretaceous – eocene magmatism in

the Serra do mar alkaline province, SE Brazil: melts from the deflected trindade mantle plume?

J. Petrol. 39, 1493–1526. <https://doi.org/10.1093/etroj/39.8.1493>.

TOYODA, K., HORIUCHI, H., TOKONAMI, M., 1994. DUPAL anomaly of Brazilian carbonatite: geochemical correlation with hotspots in the South Atlantic and implications for the mantle source. *Earth and Planetary Science Letters*, v. 126. p. 315–331.

VALENCIO, D.A.; MENDÍA, J.E., 1974. Palaeomagnetism and K/Ar Ages of Some Igneous Rocks Of The Trindade Complex And The Valado Formation, From Trindade Island, Brazil. *Revista Brasileira de Geociências*, v. 4, p. 124-132.

VALERIANO, C.M., *et al.*, 2003. A new TIMS laboratory under construction in Rio de Janeiro, Brazil. In IV south American symposium on isotope geology, salvador. In: *Short Papers IV South American Symposium on Isotope Geology*, vol. 1, pp. 131–133.

VALERIANO, C.M VAZ, G.S., MEDEIROS, S.R., NETO, C.C.A., RAGATKY, C.D., GERALDES, M.C., 2008. The Neodymium isotope composition of the JNdi-1 oxide reference material: results from the LAGIR Laboratory, Rio de Janeiro. *Proceedings of the VI South American Symposium on Isotope Geology*, San Carlos de Bariloche – Argentina – 2008 (CD- ROM), p. 1-2.

VALERIANO, C.M, MEDEIROS, S.R., VAZ, G.S., NETO, C.C.A., 2009. Sm-Nd isotope dilution TIMS analyses of BCR-1, AGV-1 and G-2 USGS rock reference materials: first results from the LAGIR laboratory at UERJ, Rio de Janeiro. In: *Boletim de resumos expandidos do simpósio 45 anos de geocronologia no brasil*, IGc–USP, CPGeo – Centro de Pesquisas Geocronológicas, CD-ROM.

VALERIANO, C.M., MENDES, J.C., TUPINAMBÁ, M., BONGIOLO, E., HEILBRON, M., JUNHO, M.D.C.B., 2016. Cambro–Ordovician post-collisional granites of the Ribeira belt, SEBrazil: a case of terminal magmatism of a hot orogen. *J. S. Am. Earth Sci.* 68, 269–281. <https://doi.org/10.1016/j.jsames.2015.12.014>.

VANDECAR, J.C., JAMES, D.E., ASSUMPCAO, M., 1995. Seismic evidence for a fossil mantle plume beneath SouthAmerica and implications for plate driving forces. *Nature*, v. 378, p. 25–31.

VIDAL, P. H., 1992. Mantle: more HIMU in the future?. *Geochim. Cosmochim. Acta* 56, 4295-4299.

WILSON, J.T., 1963. A possible origin of the Hawaiian Islands. *Canadian Journal of Physics*, 41: 863 – 870.

WEAVER, B. L., *et al.*, 1986. Role of subducted sediment in the genesis of ocean-islandbasalts: geochemical evidence from South Atlantic Ocean islands. *Geology*, 14, 275^278.

WEAVER, B.L. *et al.*, 1987. Geochemistry of ocean island basalts from the South

Atlantic: Ascension, Bouvet, St. Helena, Gough and Tristan da Cunha. In: *Fitton JG, Upton BGJ (eds) Alkaline Igneous Rocks. Geol Soc London Spec Publ 30*, pp 253-267

WEAVER, B.L., 1990. Geochemistry of highly-undersaturated ocean island basalt suites from the South Atlantic Ocean: Fernando de Noronha and Trindade islands. *Contr. Mineral. and Petrol.* 105, 502–515. <https://doi.org/10.1007/BF00302491>

WEAVER, B., 1991. Trace element evidence for the origin of ocean-island basalt. *Geology*, v. 19, p. 123-126.

WHITE, W.M., 1985. Sources of oceanic basalt: Radiogenic Isotopic Evidence. *Geology*, 13: 115-118.

WHITE, W.M. 2015. Isotopes, DUPAL, LLSVPs, and Anekantavada. *Chemical Geology* 419, 1240 10–28.

WORKMAN, R.K., HART, S.R., 2005. Major and trace element composition of the depleted MORB mantle (DMM). *Earth and Planetary Science Letters*, 231, 53-72. <https://doi.org/10.1016/j.epsl.2004.12.005>

YANG, Z.-F., *et al.*, 2019. Using major element logratios to recognize compositional patterns of basalt: Implications for source lithological and compositional heterogeneities. *Journal of Geophysical Research: Solid Earth*, 124.4: 3458-3490.

YAXLEY, G.M., GREEN, D.H., 1998. Reactions between eclogite and peridotite: mantle refertilisation by subduction of oceanic crust. *Schweiz. Mineral. Petrogr. Mitt.* 78, 243–255.

YAXLEY, G.M., 2000. Experimental study of the phase and melting relations of homogeneous basalt + peridotite mixtures and implication for the petrogenesis of flood basalts: *Contributions to Mineralogy and Petrology*, v. 139, p. 326-338.

ZINDLER, A., HART, S.R., 1986. Chemical geodynamics. *Ann. Rev.: Earth Planet Sci. Lett.* 14, 493–571. <https://doi.org/10.1146/annurev.ea.14.050186.002425>.

ZINDLER, A., JAGOUTZ, E., GOLDSTEIN, S., 1982. Nd, Sr and Pb isotopic systematics in a three component mantle: a new perspective. *Nature*, 298: 519±523